Investigation of Free Space Optical Link Performance with Wavelength Diversity under Different Turbulence Conditions

A Thesis Submitted to

Nirma University

In Partial Fulfilment of the Requirements for

The Degree of

Doctor of Philosophy

in

Technology & Engineering

By

Dhaval Gopalchandra Shah

(11EXTPHDE72)

Electronics and Communication Engineering Department

Institute of Technology, Nirma University

Ahmedabad, Gujarat, India

November, 2017

Nirma University
Institute of Technology

CERTIFICATE

This is to certify that the thesis entitled **Investigation of Free Space Optical link performance with wavelength diversity under different turbulence conditions** has been prepared by **Mr. Dhaval G. Shah (11EXTPHDE72)** under my supervision and guidance. The thesis is his own original work completed after careful research and investigation. The work of the thesis is of the standard expected of a candidate for Ph.D. Programme in **Electronics and Communication Engineering** and I recommend that it be sent for evaluation.

Date: 14/11/2017

Signature of Guide

Forwarded through:

(i) Head, Electronics and Communication Engineering Department

(ii) Dean, Faculty of Technology and Engineering

16-11-17

(iii) Dean, Faculty of Doctoral Studies and Research

To:

Executive Registrar

Nirma University

ABSTRACT

Free Space Optical (FSO) communication is rapidly growing technology in the field of wireless communication. Higher bandwidth, licence free spectrum, high security and quick deployment are the key advantages of this technology. However, the atmospheric losses due to bad weather and atmospheric turbulence are still the challenges which prevent the growth of FSO communication at a higher rate. Wavelength diversity technique has shown the capability to overcome these challenges. In this technique, the information signal is transmitted simultaneously on a different wavelength which increases the availability of FSO link and overcomes the problem of link blockage. Apart from this, each wavelength is immune against certain atmospheric elements so the use of multiple wavelengths for transmission helps to combat the atmospheric losses. Further, different wavelengths are affected differently by same atmospheric condition which makes FSO communication robust under different atmospheric turbulence conditions.

In this thesis, wavelength diversity technique is applied to enhance the performance of FSO system under different turbulence conditions. Three different wavelengths of 1550, 1310 and 850 nm are chosen for this technique. Different turbulence conditions are realized by adopting well-defined channel model for a particular turbulence condition. K channel model has been considered to categorize strong turbulence condition and Exponentiated Weibull channel has been used to represent all turbulence scenarios. Outage probability and average Bit Error Rate (BER) are considered as a performance metrics. Simulations results are obtained using Matlab software.

The performance of FSO system under strong turbulence with wavelength diversity technique is investigated with three different combining methods: optimal combining, equal gain combining and selection combining. Mathematical expressions are derived to evaluate average BER and outage probability. The results exhibit that wavelength diversity with optimal combining method achieves better improvement compared to equal gain combining and selection combining methods. The obtained BER results are also compared with the published article in which spatial diversity technique is used to mitigate the effect of strong turbulence using same channel model. It is observed that wavelength diversity archives 2–3 dB higher improvement.

An effort has been made to identify an appropriate diversity order to improve the BER and outage probability of the system under all turbulence conditions. The effect of receiver aperture size on the results is also analyzed. 10 mm and 60 mm aperture size is considered to represent an ideal and practical FSO implementation. Different turbulence condition is characterized using Exponentiated Weibull channel and optimal combining method is considered at receiver. Numerical results achieved from the derived expression of average BER and outage probability show that increasing diversity order improves the results with both aperture size. It is observed that increasing receiver aperture size decreases the performance improvement. But, the BER requirement for modern communication is easily fulfilled with the diversity order of 3 even at 60 mm receiver aperture under all turbulence conditions.

A comparative analysis of BER results of FSO system with wavelength diversity using under different turbulence conditions is carried out. The results obtained considering Exponentiated Weibull channel for all turbulence conditions are compared with the published articles in the literature in which different turbulence conditions are represented by appropriate classical channel models. It is found that deployment of wavelength diversity archives a maximum gain when different turbulence conditions are characterized with Exponentiated Weibull channel.

Nirma University
Institute of Technology

DECLARATION

I, **Dhaval G. Shah**, registered as Research Scholar, bearing Registration No. **11EXTPHDE72** for Doctoral Programme under the **Faculty of Technology and Engineering** of Nirma University do hereby declare that I have completed the course work, pre-synopsis seminar and my research work as prescribed under R. Ph.D. 3.5.

I do hereby declare that the thesis submitted is original and is the outcome of the independent investigations / research carried out by me and contains no plagiarism. The research is leading to the discovery of new facts / techniques / correlation of scientific facts already known. (Please tick whichever is applicable). This work has not been submitted to any other University or Body in quest of a degree, diploma or any other kind of academic award.

I do hereby further declare that the text, diagrams or any other material taken from other sources (including but not limited to books, journals and web) have been acknowledged, referred and cited to the best of my knowledge and understanding.

Date: 14/11/2017

Dhaval G. Shah
(11EXTPHDE72)

I endorse the above declaration made by the student.

Date: 14/11/2017

Dr. D. K. Kothari
Guide

ACKNOWLEDGEMENT

First and foremost, I would like to express my eternal gratitude to God and my parents, whose blessings have made me what I am today.

I am always thankful to my thesis supervisor, Dr. Dilipumar Kothari, for his valuable suggestions, inspiring guidance and consistent support. I would also like to thank him for proof reading this thesis. I am also thankful to Dr. Alka Mahajan, Director, Institute of Technology, Nirma University for providing opportunity and support to carry out this research. I wish to express my sincere gratitude to the Nirma University for allowing me to join Ph.D. Programme and providing support during the course of this programme.

I am also very grateful to my research progress committee members, Dr. Anjan K. Ghosh, Vice-chancellor, Tripura University and Dr. Mihir Shah, Professor, L. D. Engineering College, Ahmedabad for their insightful suggestions and discussion. Their constructive criticism and comments help me to nurture and strengthen my research work.

I express my sincere thanks to Dr. Y. N. Trivedi, Dr. Sachin Gajjar, Prof. Akash Mecwan and Prof. B. D. Fataniya for their fruitful suggestions and encouragement. I would also like to thank all friends, colleagues and well-wisher for their direct or indirect support in the successful completion of this work.

Special thanks to my wife and kids for their motivational support and unconditional love. The time devoted to this thesis is from their accounts.

Contents

CERTIFICATE .... **ii**

DECLARATION .... **iii**

ACKNOWLEDGEMENT .... **iv**

ABSTRACT… .... **v**

List of Figures .... **x**

List of Tables .... **xii**

List of Abbreviations .... **xiii**

Chapter 1 Introduction **15**

1.1 Motivation 17

1.2 Objective 18

1.3 Contributions of Thesis 18

1.4 Organization of Thesis 20

Chapter 2 Literature Review **23**

2.1 Free Space Optical Communication 24

2.2 Classification of FSO 28

2.3 Comparison of FSO System with Existing Technologies 30

2.4 Challenges of FSO System 31

2.4.1 Building Motion 31

2.4.2 Atmospheric Losses 32

2.4.3 Atmospheric Turbulence 36

2.5 FSO Channel Models 38

2.5.1 Lognormal Channel Model 39

2.5.2 Gamma Gamma Channel Model 40

2.5.3 Negative Exponential Channel Model 42

2.5.4 K Channel Model 43

2.5.5 Exponentiated Weibull Channel Model 44
2.6 Turbulence Mitigation Techniques 45
2.6.1 Aperture Averaging 45
2.6.2 Adaptive Optics 48
2.6.3 Error Correcting Codes 50
2.6.4 Hybrid RF/FSO 52
2.6.5 Diversity Techniques 54
2.7 Comparison of Turbulence Mitigation Techniques 61
2.8 Conclusion 63
Chapter 3 Performance Evaluation of FSO system with Wavelength Diversity under Strong Turbulence Conditions 65
3.1 System Model 66
3.2 K Channel Model 67
3.3 Performance Metric of FSO Channel 69
3.3.1 Average BER 70
3.3.2 Outage Probability 70
3.4 Average BER of FSO System with Wavelength Diversity 71
3.4.1 Optimal Combining 72
3.4.2 Equal Gain Combining 73
3.4.3 Selection Combining 74
3.4.4 Results and Discussions 75
3.5 Outage Probability of FSO System with Wavelength Diversity 80
3.5.1 Optimal Combining 81
3.5.2 Selection Combining 81
3.5.3 Results and Discussions 82
3.6 Performance Comparison of Wavelength Diversity with Spatial diversity. 84
3.7 Conclusion 86

Chapter 4 Performance of FSO Link with Wavelength Diversity over Exponentiated Weibull Channel....87

4.1 Exponentiated Weibull Channel Model 88

4.2 System Model.... 89

4.3 Outage Probability 91

4.4 Average BER of the System 92

4.5 Results and Discussion.... 94

4.5.1 Outage probability with wavelength diversity.... 95

4.5.2 Average BER with Wavelength diversity.... 101

4.6 Performance of FSO system with 60 mm aperture size.... 106

4.6.1 Outage Probability at 60 mm receiver aperture 107

4.6.2 Average BER at 60 mm receiver aperture 110

4.7 Conclusion.... 114

Chapter 5 Comparative Analysis of BER performance of FSO system with wavelength diversity under different turbulence conditions 117

5.1 Performance comparison of LN and EW 118

5.2 Performance comparison of EW and Gamma-Gamma channel 122

5.3 Performance comparison of EW and K channel 126

5.4 Conclusion.... 129

Chapter 6 Conclusion and Future Scope 131

6.1 Conclusion.... 131

6.2 Future scope of work.... 133

Publications 135

References 137

List of Figures

Fig. 1.1 Prediction of the growth of FSO technology 15
Fig. 2.1 Block diagram of FSO system 25
Fig. 2.2 Different OOK schemes 26
Fig. 2.3 Pulse Position Modulation scheme 27
Fig. 2.4 Classification of FSO system 29
Fig. 2.5 Indoor WOC system..29
Fig. 2.6 Effect of fog attenuation on visibility 34
Fig. 2.7 Effect of beam wandering and scintillation 37
Fig. 2.8 Block diagram of AO system 48
Fig. 2.9 Optimal Combining Method 54
Fig. 2.10 Equal Gain Combining method...55
Fig. 2.11 Selection Combining 56
Fig. 2.12 Performance of FSO link with MISO diversity 59
Fig. 3.1 FSO system model with wavelength diversity...66
Fig. 3.2 BER performance of SISO-FSO system at different wavelength 77
Fig. 3.3 BER performance of FSO system link with SC scheme. 77
Fig. 3.4 BER performance of FSO system link with EGC method...........................78
Fig. 3.5 BER performance of FSO system link with OC method 78
Fig. 3.6 Performance Comparison of OC, EGC and SC scheme with W=2 at 2 km .80
Fig. 3.7 Outage probability of FSO system using SC method 83
Fig. 3.8 Outage probability of FSO system using OC method.................................83
Fig. 3.9 Comparison of wavelength and spatial diversity using OC at 2 km distance 85
Fig. 4.1 Outage probability versus normalized average electrical SNR at 1.5 km.....96
Fig. 4.2 Outage probability versus normalized average electrical SNR at 2.5 km.....96
Fig. 4.3 Outage probability with different diversity order under moderate turbulence 97
Fig. 4.4 Outage probability with different diversity order under strong turbulence ..98

Fig. 4.5 Outage probability with different diversity order under moderate turbulence 99
Fig. 4.6 Outage probability with different diversity order under strong turbulence.. 99
Fig. 4.7 Average electrical SNR versus average BER for link length of 1.5 km 101
Fig. 4.8 Average electrical SNR versus average BER for link length of 2.5 km 102
Fig. 4.9 Average BER with different diversity order under moderate turbulence... 102
Fig. 4.10 Average BER with different diversity order under strong turbulence 103
Fig. 4.11 Average BER at 2.5 km with different diversity order under strong turbulence 104
Fig. 4.12 Average BER at 2.5 km with different diversity order under strong turbulence 104
Fig. 4.13 Outage probability at the length of 1.5 km with 60 mm receiver aperture107
Fig. 4.14 Outage probability at the length of 2.5 km with 60 mm receiver aperture108
Fig. 4.15 Average BER for link length of 1.5 km with 60 mm aperture size.......... 110
Fig. 4.16 Average BER for link length of 2.5 km with 60 mm aperture size.......... 111
Fig. 5.1 BER Performance comparison of LN and EW with wavelength diversity 119
Fig. 5.2 BER Performance comparison of LN and EW under weak turbulence 119
Fig. 5.3 Performance comparison of LN and EW under moderate turbulence 121
Fig. 5.4 Performance comparison of LN and EW under moderate turbulence 121
Fig. 5.5 Performance compassion of GG and EW for moderate turbulence condition 124
Fig. 5.6 Performance compassion of GG and EW for strong turbulence condition 124
Fig. 5.7 Performance compassion at 2 km under moderate turbulence condition... 125
Fig. 5.8 Performance compassion at 2 km under strong turbulence condition........ 125
Fig. 5.9 Performance compassion using K and EW at 2 km 128
Fig. 5.10 Performance compassion using K and EW at 3 km 128

List of Tables

Table 2.1 Performance comparison of OOK and PPM modulation format 27
Table 2.2 Comparison of FSO and RF system 30
Table 2.3 Various factor causing building motion 32
Table 2.4 International visibility code for different weather conditions. 33
Table 2.5 Summary of different turbulence mitigation techniques 62
Table 3.1 Required SNR at the BER of 10^{-4} for different combining methods 79
Table 3.2 Outage probability of FSO system at SNR of 30 dB 84
Table 4.1 Outage probability of FSO system at SNR of 20 dB 100
Table 4.2 Average BER of FSO system with different diversity order at different distances 105
Table 4.3 Outage probability of FSO system with 60 mm aperture at SNR of 20 dB 108
Table 4.4 Outage probability of FSO system at SNR of 30 dB 109
Table 4.5 Average BER with 60 mm aperture at SNR of 20 dB.............................112
Table 4.6 Average BER of FSO system with 60mm aperture diameter at 30 dB SNR 113
Table 5.1 BER performance comparison between LN and EW under weak turbulence 120
Table 5.2 BER performance comparison between LN and EW under moderate turbulence...122
Table 5.3 Performance comparison between Gamma-Gamma and EW 126
Table 5.4 BER Performance comparison between K and EW 127
Table 5.5 Required SNR for the BER of 10^{-4}...129

List of Abbreviations

AO	Adaptive Optics
ATP	Automatic Tracking and Pointing
AWGN	Additive White Gaussian Noise
BER	Bit Error Rate
CAGR	Compound Annual Growth Rate
CSI	Channel State Information
EGC	Equal Gain Combining
ESA	European Space Agency
EW	Exponentiated Weibull
FOC	Fiber Optical Communication
FSO	Free Space Optical
GaAs	Gallium Arsenide
GG	Gamma Gamma
He-Ne	Helium-Neon
LASER	Light Amplification by Stimulated Emission and Radiation
LDPC	Low-Density Parity Check
LED	Light Emitting Diode
LOS	Line of Sight
MANET	Mobile Ad-hoc NETwork
MISO	Multiple Input Single Output
MLCD	Mars Laser Communication Demonstration
NASA	National Aeronautics and Space Administration
NE	Negative Exponential
OC	Optimal Combining
OOK	On-Off Keying
OVSF	Orthogonal Variable Spreading Factor
PAM	Pulse Amplitude Modulation
PDF	Probability Density Function

PPM	Pulse Position Modulation
QAM	Quadrature Amplitude Modulation
RF	Radio Frequency
RS	Reed-Solomon
RZ	Return-to-zero
SC	Selection Combining
SILEX	Semiconductor-laser Inter-satellite Link Experiment
SIMO	Single Input Multiple Output
SISO	Single Input Single Output
SNR	Signal to Noise Ratio
WDM	Wavelength Division Multiplexing
WOC	Wireless Optical Communication
WS	Wavefront Sensor

Chapter 1

Introduction

Wireless communication is of great interest due to endless demand for high data rate communication devices. A plethora of wireless communication standards have saturated the Radio Frequency (RF) spectrum. An alternative to RF communication is an essential requirement of modern communication. Free Space Optical (FSO) communication is evolving as an alternative to RF. It is rapidly growing technology in the field of wireless communication.

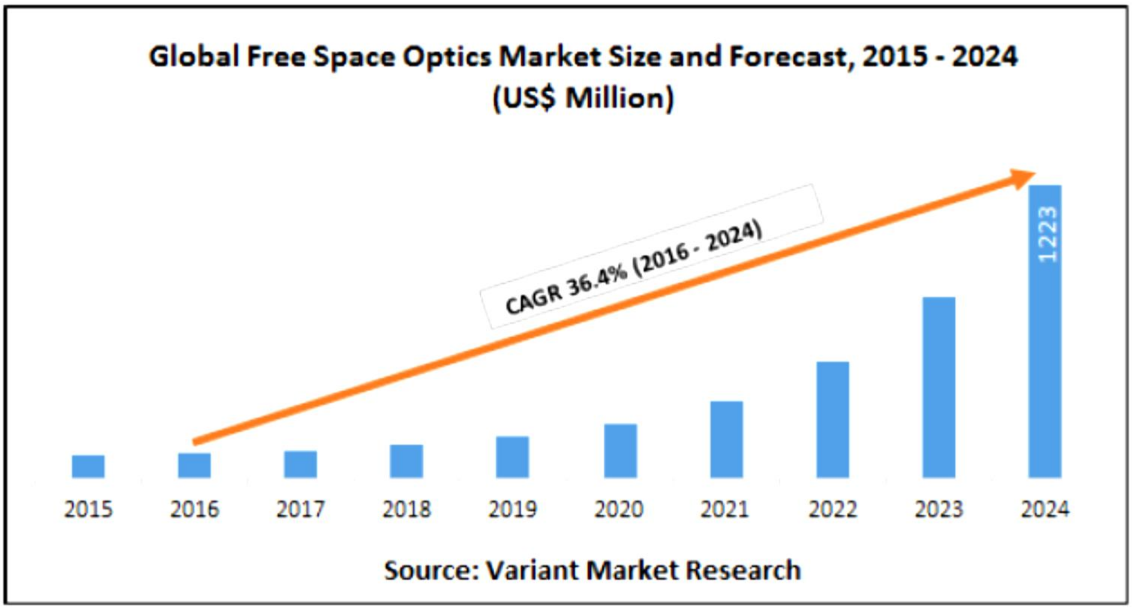

Fig. 1.1 Prediction of the growth of FSO technology
Source: Variant Market Research: Global Free Space Optics Market size and Forecast 2015–2024 Report

Fig. 1.1 shows the forecast of FSO market size in the decade 2015-2024, reported by Variant Market Research. It clearly indicates an exponential rise in the usage of FSO technology in the field of wireless communication.

FSO is Line of Sight (LOS) communication technology. It uses light propagation to transmit information from source to destination through free space as an unguided channel. Use of optical carrier allows higher bandwidth and license-free spectrum. Interception of the optical signal is very difficult, which results in high security in the communication. Higher bandwidth, high security, license-free spectrum, ease of deployment and less power consumption compared to Radio Frequency (RF) transmission makes FSO more suitable for the high-speed broadband networks (Chan, 2006) (Wasiczko, 2005). Unlike FOC system, it does not require any digging or permission for the use of transmission medium. This reduces the setup time and installation cost too. Moreover, FSO system can be deployed at places where laying down the fiber is very difficult.

Though FSO has tremendous potential to compete with existing communication technologies, the growth of FSO technology is hampered by various parameters like building motion, atmospheric losses due to weather (due to rain, fog, haze, etc.) and atmospheric turbulence. These parameters reduce the link deployment distance or interrupt the communication. The problem due to building motion on which transceiver is deployed can be overcome by either automatic beam tracking system or large beam divergence. Atmospheric losses due to bad weather condition can be compensated by operating FSO at a higher wavelength. However, performance degradation due to atmospheric turbulence is still challenging problem. Atmospheric turbulence causes random fluctuation in the intensity and phase of the received signal at the receiver. This directly affects the quality of received signal and reduces the deployable link distance. It can occur even in clear weather condition for any duration of day and night. So, atmospheric turbulence is considered a major challenge to FSO system, which is addressed in this thesis.

1.1 Motivation

There are different turbulence mitigation techniques like aperture averaging, adaptive optics, error correction coding, hybrid Radio Frequency (RF)/FSO technique and different diversity techniques. Each of these has their own merits and demerits. Aperture averaging mitigates turbulence effect by increasing receiver aperture size. Increasing receiver aperture size also increases background noise on the received signal. Apart from this, it demands very large size of receiver aperture to mitigate strong turbulence condition and fails to improve the performance of FSO under weak turbulence condition (Wasiczko, 2005). Adaptive optics technique corrects the distorted wavefront of the received signal in real time, but distorted wavefront measurement sensor performance is very poor under strong turbulence (P. Barbier, 1998). So, this method is not appropriate under strong turbulence condition. On the other hand, use of error-correcting codes improve the performance of the system under all turbulence conditions but it demands large memory to store long data stream and also adds latencies to the output. Hybrid RF/FSO is another technique to combat worst weather and atmospheric condition. In this method, the signal is transmitted over RF under bad weather condition. However, it is a very costly solution as it requires to integrate two different systems. Further, frequent switching among these systems results in the underutilization of channel bandwidth. Diversity technique is also capable to mitigate the effect of different turbulence conditions. In this technique, multiple copies of the signal are transmitted either at a different time, wavelength or using multiple transmitter/receiver or both which is known as time diversity, wavelength diversity and spatial diversity, respectively. Use of time diversity to improve the performance of FSO under different turbulence condition drastically reduces the data rate (Nistazakis, 2012). Whereas, spatial diversity technique requires more than 5 pairs of transceivers to improve performance under strong turbulence condition (Tsiftsis, 2009). Each of the above-mentioned techniques either has certain limitations or adds significant cost by demanding additional circuitry.

Wavelength diversity is considered as a promising solution in this situation. In this technique, multiple copies of information are sent on different wavelength at the same time. Transmission of the information signal on multiple wavelengths at the same time also increase the availability of FSO link and solve the problem of temporary blockage of the link as well. Basically, wavelength diversity is taking advantage of the fact that each wavelength is immune to certain atmospheric particles. The combination of different wavelengths in the deployment of wavelength diversity will make FSO system robust in all weather conditions. This motivates to apply wavelength diversity technique to improve the performance of FSO under different turbulence conditions.

1.2 Objective

The main objective of this thesis is to investigate the performance improvement of FSO system under different turbulence condition using wavelength diversity with an adequate diversity order. This has been achieved by addressing following objectives.

1. To study the different challenges of FSO system and identify a suitable technique to mitigate different atmospheric turbulence effect.
2. To derive the mathematical expression of outage probability and average Bit Error Rate (BER) for FSO system with wavelength diversity under strong turbulence condition with different combining techniques at receiver.
3. To investigate the performance improvement of wavelength diversity based FSO system under moderate and strong turbulence condition and identify an adequate diversity order for the same.
4. To compare the obtained results with the published article to identify an appropriate channel model that represents all turbulence condition and achieves significant performance improvement with wavelength diversity.

1.3 Contributions of Thesis

The major contributions in this thesis are mainly divided into four parts.

- Study on different challenges of FSO system with a possible solution is carried out. Atmospheric turbulence is identified as a major challenge for terrestrial FSO link. The channel between source and destination under turbulence condition is represented by the suitable channel model. A study of different channel models for different turbulence conditions is performed. A detailed literature review on turbulence mitigation techniques is carried out and identified wavelength diversity technique to mitigate the effect of different atmospheric turbulence condition.

- The performance of FSO system with wavelength diversity under strong turbulence condition using K channel is investigated. The source information is transmitted onto three carrier wavelengths. The signals at receiver side are combined using three different methods: Optimal Combining (OC), Equal Gain Combining (EGC) and Selection Combining (SC). Average BER and outage probability are considered to evaluate the performance of wavelength diversity based FSO system. Mathematical expressions are derived to obtain average BER for all the three combining schemes (OC, EGC and SC). Comparative analysis is carried out for the results obtained from all three schemes. Further, outage probability of the system is investigated by deriving an approximated closed-form mathematical expression considering OC and SC method at receiver. A comparison of BER results obtained with wavelength diversity and spatial diversity technique is performed. It also justifies the use of wavelength diversity technique.

- The obtained results under strong turbulence condition using K channel show that required SNR is more than 30 dB to achieve the BER in the range of 10^{-6} which is the need of modern communication systems for the data rates in the range of 1-100 Mbps (Goldsmith, 2005). Considering this fact, the performance of FSO system with wavelength diversity is investigated using Exponentiated Weibull (EW) channel model for moderate and strong turbulence conditions. It is achieved by deriving mathematical expressions of outage probability and average BER using OC method at receiver. The effect of receiver aperture size on the performance of the system is also examined. 10 mm and 60 mm receiver aperture sizes are considered for the same. Numerical results are obtained with both the receiver aperture size at different link distances varying from 1 km to 3 km at a regular interval of 0.5 km under both the turbulence conditions for different diversity levels (starting from no diversity case to diversity of the order of 6). It reveals that diversity order of 3 is sufficient for practical FSO applications.

- The performance of FSO system with wavelength diversity under weak turbulence condition, represented by EW channel is investigated. The obtained results are compared with the published article in which weak turbulence is presented with the classical Lognormal channel model. Similarly, a comparison is also presented for moderate to strong turbulence condition. In this case, BER results obtained with wavelength diversity considering EW model and Gamma-Gamma model for moderate and strong turbulence is compared. Finally, BER performance obtained with wavelength diversity under strong turbulence using K channel is compared with results obtained considering EW channel. This work shows that EW is more suitable to represent different turbulence condition than other channel models to gain the maximum advantage of wavelength diversity technique.

1.4 Organization of Thesis

The rest of the thesis is organized as follows.

Chapter 2 presents the working and classification of Free Space Optical (FSO) system. A comparison of FSO system with existing technologies is carried out. Various challenges of FSO system are presented and possible solutions are discussed. An atmospheric turbulence is found as a major challenge. FSO channel under atmospheric turbulence is described with the help of an appropriate channel model. A study of different channel models which categorizes FSO channel under different turbulence condition is done. Different atmospheric turbulence mitigation techniques have been reviewed and found that wavelength diversity technique is most suitable to encounter all turbulence conditions.

FSO system model with wavelength diversity is presented in chapter 3. The performance of this system model under strong turbulence condition using K channel is investigated. Applying wavelength diversity demands a proper signal combining method at the receiver side. To identify a proper combining technique for maximum improvement, mathematical expression of average BER for the different combining techniques (OC, EGC and SC) is derived. The BER performance obtained with different combining techniques is compared and reported. An outage probability of system is considered as the other parameter to judge performance. An approximated closed form of mathematical expression is also derived to evaluate outage probability considering OC and SC method at receiver and results are presented for the same. Further, the performance obtained with wavelength diversity is also compared with the published article in the literature on strong turbulence effect mitigation by spatial diversity method.

The performance of FSO system with wavelength diversity under moderate and strong turbulence condition using Exponentiated Weibull (EW) channel is investigated and reported in chapter 4. It is found in the terms of average BER and outage probability. Mathematical expressions for both are derived considering OC method at the receiver side. The results are obtained based on these expressions for the higher diversity order up to 6. This helps to identify an appropriate diversity order for performance improvement of FSO system under different turbulence condition. An effect of receiver aperture size on the performance of FSO system with wavelength diversity is also examined and reported in this chapter.

Chapter 5 presents a comparative analysis of BER performance of wavelength diversity based FSO system under different turbulence condition, characterized by EW channel model with different well-known classical models for a particular turbulence condition. The performance of FSO system with wavelength diversity under weak turbulence using EW is compared with the results reported in the published article in the literature, considering Lognormal channel model for weak turbulence. Similarly, BER comparison is also carried out for moderate and strong turbulence scenario. In this comparison, turbulence conditions are characterized using EW channel and Gamma-Gamma channel. Finally, BER performance obtained with wavelength diversity considering EW channel and K channel for strong turbulence condition is compared and discussed.

Lastly, the conclusion of this thesis is presented in chapter 6. The points are identified for future research based on this work and reported in this chapter.

Chapter 2

Literature Review

FSO communication is becoming a popular technology for all types of data transmission in wireless mode. It uses light as a carrier between transmitter and receiver for communication in full duplex mode. Use of light for communication was started around 800 BC by ancients Greeks and Romans for signaling purpose through fire beacons. Similarly, French naval navigators were communicating through optical telegraph in 1790-1794. The first experimental setup of FSO communication was carried out by Alexander Graham Bell in 1880. In this setup, voice signal was transmitted over a 200 m distance by modulating sunlight on foil diaphragm (Killinger, 2002). This prototype is called as photo-phone. After the invention of efficient light sources such as Light Emitting Diode (LED) and Light Amplification by Stimulated Emission and Radiation (LASER), FSO technology has captured a lot of attention from researcher and industries. The researchers of MIT Lincolns Laboratory have used GaAs (Gallium Arsenide) based LED to broadcast television signal over a distance of about 48 km in 1962 (Goodwin, 1970). Around 1970, Nippon Electric Company (NEC) of Japan has established first commercial full-duplex LASER link using He-Ne (Helium-Neon) LASER over the distance of 14 km between Yokohama and Tamagawa (Goodwin, 1970). After this successful experiment, the possibility of FSO application has been explored in the different fields. National Aeronautics and Space Administration (NASA) has shown the application of FSO in their Mars Laser Communication Demonstration (MLCD) program (Bemard L. Edwards, 2004). Similarly, European Space Agency (ESA) has also performed Semiconductor-laser Inter-satellite Link Experiment (SILEX) in the deep space (G. Fletcher, 1991). FSO link between satellites in the space near earth is also implemented at the data rates of 10 Gbps in the past decade. (Hemmati, 2006), (A. Jooshesh, 2012). The application of FSO is also explored for military communication (Juan C. Juarez, 2006). Nowadays FSO technology has drawn a lot of attention for last mile applications. As the use of the optical carrier for information transmission provides license-free spectrum and higher bandwidth. Secure and quick deployment of information within network makes FSO as an alternative option to RF communication.

This chapter presents the working and classification of FSO system. Various challenges faced in the implementation of terrestrial FSO link is also discussed with possible solutions. Atmospheric turbulence has been identified as a major challenge to FSO system so, the literature review on the different turbulence mitigation techniques is carried out and discussed in this chapter.

2.1 Free Space Optical Communication

Free Space Optical (FSO) communication is rapidly growing technology in the field of wireless communication. It is basically Line of Sight (LOS) communication technology. It uses light propagation to transmit information from source to destination through free space as an unguided channel. The block diagram of FSO system is shown in Fig. 2.1. FSO system consists of transmitter, receiver and free space channel. The working principle of FSO is similar to Fiber Optical Communication (FOC), only the difference is in the transmission medium. In FSO information is transmitted through unguided free space. The transmitter section consists of a modulator, a driver circuit, optical source, and collimator. The incoming message or signal is modulated by the modulator. Different types of binary and multilevel modulation format are supported by FSO. On-Off Keying (OOK) and Pulse Position Modulation (PPM) are considered as binary level format and Pulse Amplitude Modulation (PAM) and Quadrature Amplitude Modulation (QAM) come under multilevel format category. However, selection of modulation format depends on the bandwidth and power requirement of transmission and desired speed of FSO application. Normally, QAM and PPM are bandwidth efficient modulation schemes, but both the schemes reduce signal power level significantly. This makes them unsuitable for high background noise conditions

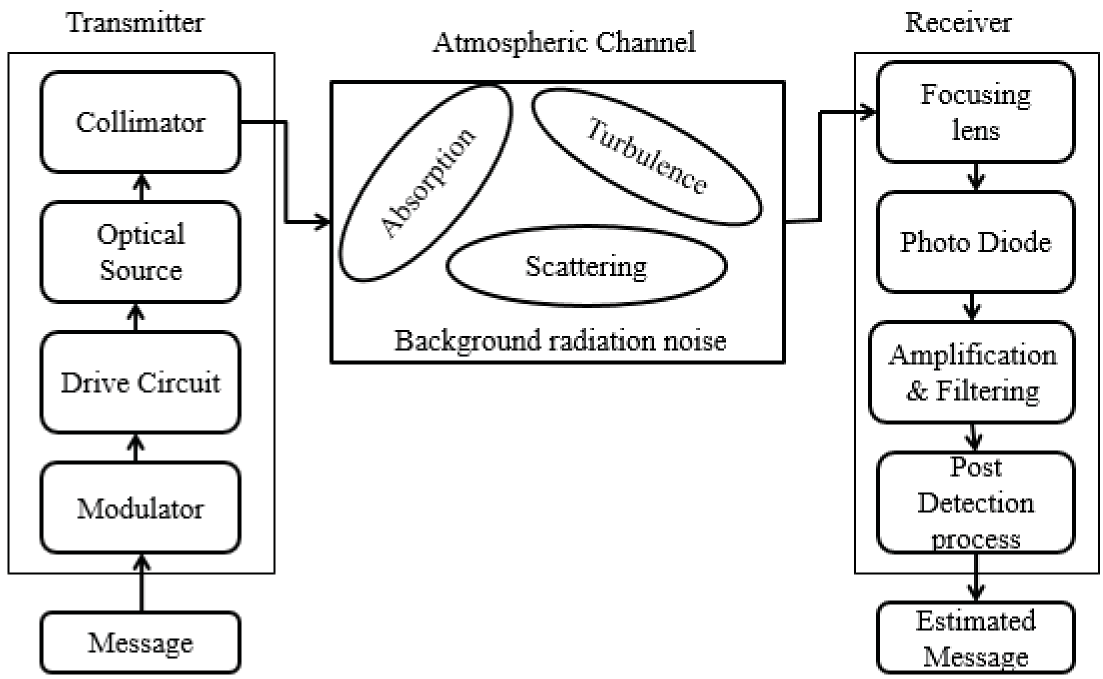

Fig. 2.1 Block diagram of FSO system

(Hranilovic, 1999), (Gagliardi, 1976). Binary-level modulation schemes are widely accepted for FSO communication due to simplicity and high power efficiency. In OOK modulation, data is transmitted with two different voltage levels ('1' is transmitted with a pulse and '0' is transmitted with no pulse) and threshold detection is applied at receiver to detect signal level. The bit rate for OOK is denoted as

$$R_b = 1/\, T_b \tag{2.1}$$

where, T_b is the bit duration and it is directly related to the rate at which the source can be switched on and off. The normalized transmit pulse shape for OOK is given by

$$P(t) = \begin{Bmatrix} 1, & for\ t \in (0, T_b\,) \\ 0, & elsewhere \end{Bmatrix} \tag{2.2}$$

Return-to-zero (RZ) and Manchester coding are the variants of OOK. In RZ OOK, the signal returns to zero level in each pulse. The bits '1' and '0' are represented with the transition of high-to-low and low-to-high, respectively in Manchester coding. This transition occurs at a midpoint of the pulse period. Figure 2.2 shows different variants of OOK scheme.

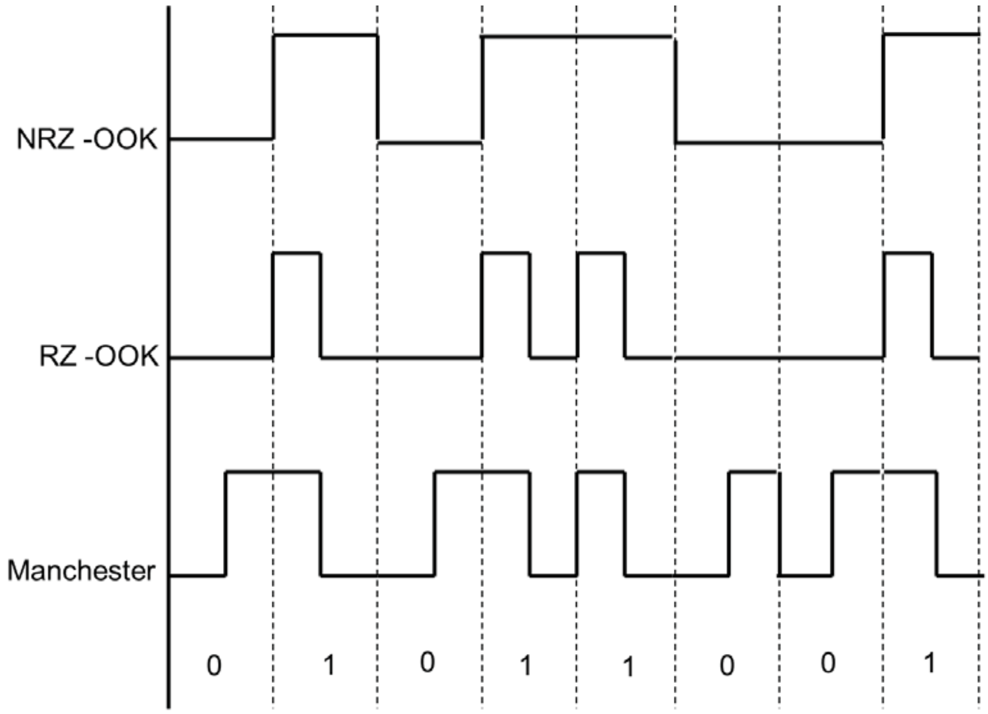

Fig. 2.2 Different OOK schemes

PPM is one of the most commonly used optical block encoding schemes, where an input word is converted into the position of a rectangular pulse within a frame. In this scheme, bits are transmitted in blocks instead of one at a time as shown in Fig 2.3. Optical block encoding is achieved by converting each word of one bit into one of $L = 2^l$ optical fields for transmission. The frame with duration T_f is divided into L slots and only one of these slots contains a pulse. This scheme can also be denoted as L-PPM, in order to emphasize the choice of L. The transmit pulse shape for L-PPM is given by

$$P(t) = \left\{ \begin{matrix} 1, for\ t\ \epsilon \left[\frac{(m-1)T_f}{L}, \frac{mT_f}{L}\right] \\ 0, elsewhere \end{matrix} \right\} \quad (2.3)$$

Since L possible pulse positions code for $\log_2 L$ bits of information, the bit rate is given by

$$R_b = \log_2 L / T_f \quad (2.4)$$

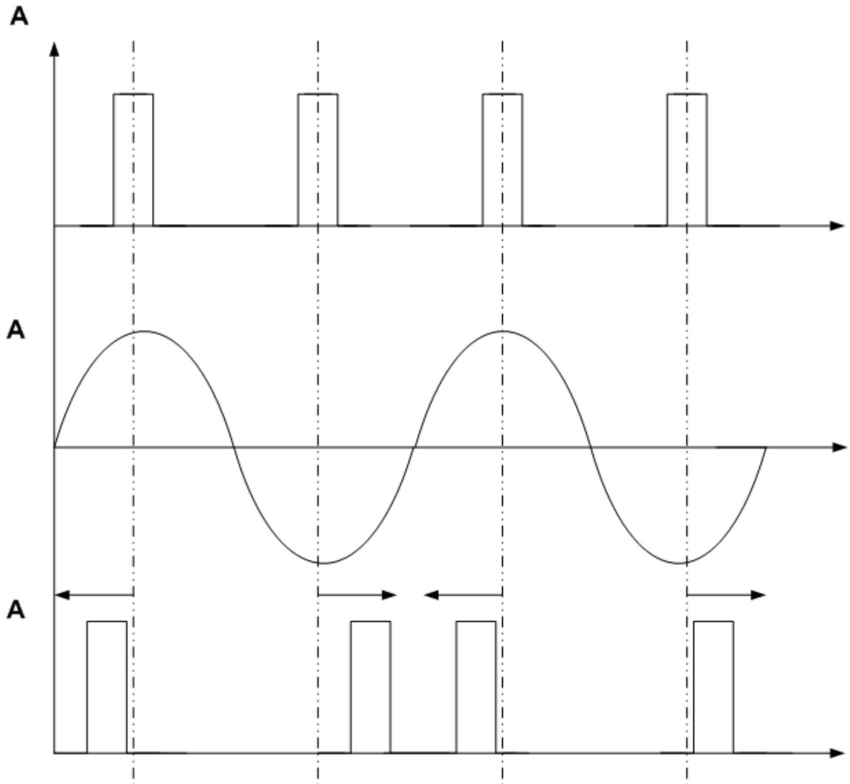

Fig. 2.3 Pulse Position Modulation scheme

A comparison of OOK and PPM based on bandwidth and power requirement is shown in Table 2.1. It is clear that PPM scheme requires less power than OOK. But, in the case of bandwidth requirement, OOK wins the race. However, due to implementation simplicity, OOK modulation is commonly preferred in FSO communication. The same scheme is considered in this thesis.

Table 2.1 Performance comparison of OOK and PPM modulation format (Trisno, 2006)

Modulation Scheme	Power Requirement	Bandwidth Requirement
OOK	P_0	R_b
RZ-OOK	P_0 - 3	$2R_b$
Manchester coding	P_0	$2R_b$
L-PPM	P_0 - 5log10 [(L/2)log2L]	$LR_b/\log_2 L$

After passing through modulator block, the modulated signal is given to the driver circuit. The function of the driver circuit is to set the proper bias voltage and current for an optical source for light emission as per information signal i.e “1 or 0”. It also provides the current to drive the optical source into saturation whenever the input bit is “1”. Normally, LED or LASER diode is used as an optical source. An additional circuitry such as temperature monitoring and coolers are also incorporated in the circuit to maintain proper cooling. The emitted signal from an optical source is transmitted in the free space directly or through the collimator. A collimator is a special collection of lenses use to reduce the beam divergence of the LASER. Finally, the signal transmitted towards aligned receiver block.

At receiver, the incoming signal is concentrated on photodiode via focusing lens. Photodiode converts the incoming light signal into electrical signal. Then, the converted signal is given to amplifier and filter section. Transimpedence amplifier is used as an amplifier, which converts the incoming current signal into output voltage form. After proper filtering and pulse shaping, it is given to post detection block to detect the incoming signal as “1” or “0”. In FSO, communication between two devices is performed via light without wire, so it is also called as Wireless Optical Communication (WOC). The classification of FSO is given in the next section.

2.2 Classification of FSO

The classification of FSO system is shown in Fig. 2.4. It is mainly classified into two categories: Indoor system and Outdoor system. In the indoor system, mostly LED is used as light source, therefore it is also considered as visible light communication. It is further classified into three categories, namely: Directed LOS, Non-directed LOS, and Diffused link. Fig. 2.5 shows the block diagram of different types of indoor Wireless Optical Communication (OWC) systems. In Directed LOS system, transmitter and receiver are aligned on the same axis which is not required in the case of Non-directed LOS. In the Non-directed LOS system field of view angle is larger than Directed LOS system. Diffused link system, the transmitter emits the optical power with the wider angle towards the surface of the room and receiver receives the optical power reflected from the same surface. These types of system overcome the alignment issue, which occurs in the Directed LOS system.

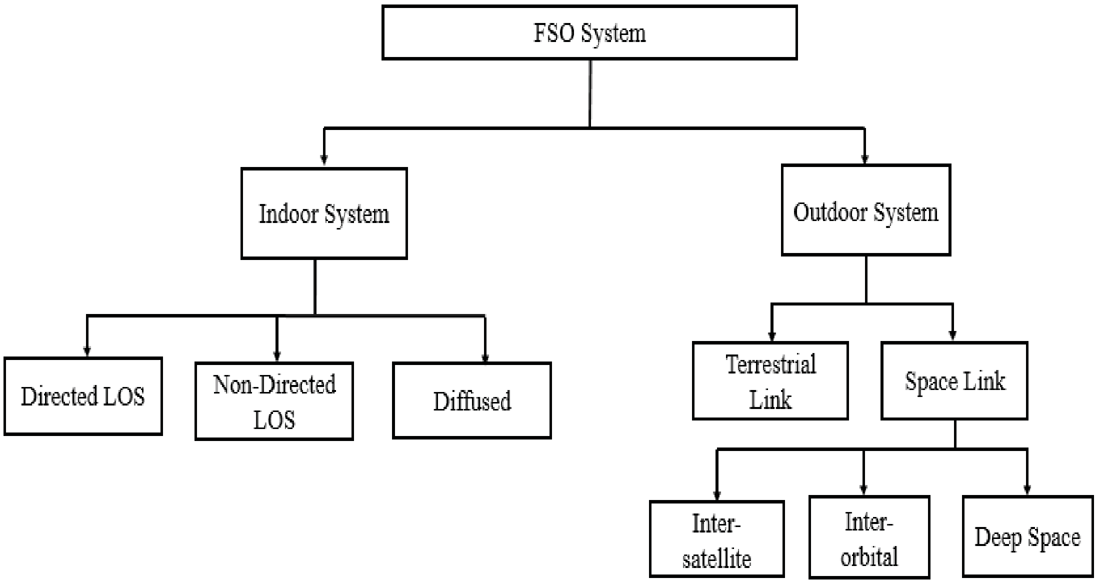

Fig. 2.4 Classification of FSO system

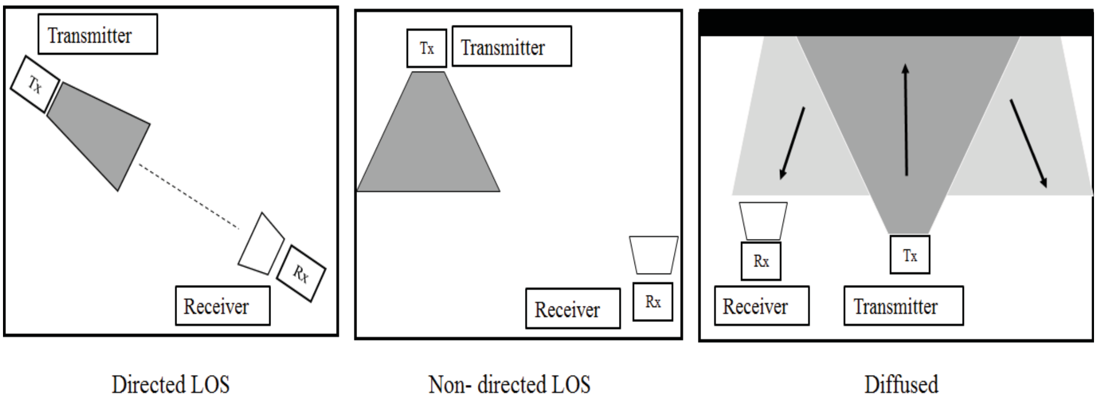

Fig. 2.5 Indoor WOC system

The outdoor system uses LASER diode to transmit signal in the free space and it is considered as FSO system. The outdoor system is further classified as terrestrial link and space link. The terrestrial link is normally used for building-to-building, mountain-to-mountain and the places where transmitter and receiver are placed on the same horizontal plane. Whereas, in the space link type, the link is designed for ground-to-satellite, satellite-to-ground, satellite-to-satellite. The communication link can also be designed between two satellite and orbit in the space link system. In this thesis, work is presented for terrestrial FSO link.

2.3 Comparison of FSO System with Existing Technologies

Currently, FOC and RF systems are adopted across the world for all types of communication. The FSO system has an equal potential in the communication field. It can replace existing technologies (RF and FOC) fully/partially depending upon the application. Implementation of FSO link does not require any digging or permission for the use of transmission medium, unlike FOC system. This reduces the setup time and installation cost too. Moreover, It can be deployed at places where laying down of fiber is very difficult. The performance of FSO system in the clear weather (attenuation loss of 0.5 dB/km) is equal to the FOC system for the short distance (Kim, 2001). FSO system also provides tremendous advantages over RF system too. A comparison between FSO and RF system is shown in Table 2.2.

Table 2.2 Comparison of FSO and RF system

Parameter	FSO	RF
Modulation Bandwidth	THz	GHz
Beam Divergence	Narrow	Wider
Directivity	High	Low
License requirement	No	Yes
Security level	High	Moderate

- Modulation Bandwidth: The optical carrier frequencies are normally in the range of 20 – 300 Thz (W. Hameed, 2010), which is quite higher compared to RF system.

- Beam Divergence: It is inversely proportional to aperture diameter and directly proportional to the wavelength of the signal. Thus, beam spreading of RF carrier is wider than the optical carrier. This results in lower intensity signal at the receiver for transmitted power in RF system. Whereas, the intensity of signal increases with narrow beam divergence in FSO system.

- Directivity: FSO is point-to-point communication and also has narrow beam divergence, which leads to high directivity compared to RF.

- License Requirement: Spectrum license is mandatory in RF system and it increases overall cost and setup time of RF system. While FSO uses the optical carrier and till date, no licensing is required to use an optical carrier. It allows the deployment of FSO system faster and cheaper compared to the RF system.

- Security Level: Tapping of the optical signal is not possible. Thus, FSO system becomes highly secure compared to RF.

These advantages of FSO come with certain challenges. FSO system demands accurate beam tracking and alignment. Moreover, the performance of FSO system highly depends on the atmospheric conditions.

2.4 Challenges of FSO System

FSO system has to overcome certain challenges to realize the above-mentioned advantages. The major impairments are building motion, atmospheric losses and atmospheric turbulence. Each of these degrades the performance of terrestrial FSO link.

2.4.1 Building Motion

An alignment between transmitter and receiver is a primary requirement for FSO communication. The transceiver is set either on a rooftop or on the top floor of a building near a window in the city area for the terrestrial link in the city. Building motion causes misalignment between transmitter and receiver, which may result either in poor quality of the signal or complete link failure at the receiver. The constant movement due to various factors like thermal expansion, wind or vibration due to heavy machinery causes building motion. Table 2.3 shows the various factors and their impact on building motion. This effect can be compensated by using either Automatic Tracking and Pointing (ATP) system or large beam divergence and field view. Each of these solutions come with some limitations. ATP system allows great link margin with an additional complexity and cost. Whereas large beam divergence reduces the link margin but it is cheaper than ATP.

Table 2.3 Various factor causing building motion (Schuster, 2002)

Factors	Effect of building	Scale	Frequency
Thermal expansion	Tip/Tilt	High	Once per day
Wind	Sway	Medium	Once every several seconds
Equipment (e.g., HVAC), door slamming, etc.	Vibration	Low	Many times per second

2.4.2 Atmospheric Losses

Absorption and scattering of the optical signal is the main reason of atmospheric losses. Both of these effects are highly wavelength dependent. Absorption in the FSO occurs mostly due to water molecules, carbon dioxide and ozone (Long, 1963), (Langer, 1957). Scattering occurs due to the presence of various particles (dust, smoke, raindrops, fog, and snow) in the atmosphere. Based on the particle size, scattering can be categorized in three ways: Rayleigh, Mie and Non-selective. When the particle size is smaller than the incident wavelength, it creates Rayleigh scattering. Air molecules and haze are mainly responsible for Rayleigh scattering (Willebrand, 2002). At higher wavelength (greater than 1μm), this scattering can be neglected but at shorter wavelength, the impact of Rayleigh scattering is noticeable. Mie scattering occurs when the particle size is comparable to the incident wavelength. Fog and aerosol particles are the main contributors in Mie scattering (Eardley, 1996). Mie scattering is more prominent near-IR wavelength range. If the particle size is larger than the incident wavelength, it results into non-selective scattering. In the non-selective scattering, attenuation coefficient does not depend on the wavelength. This happens in the case of rain and snow. These types of scattering are characterized by the geometrical optical model (Mahalati, 2012), (Wallace, 1977).

The effect of absorption and scattering on optical signal is described with the help of Beer – Lambert 's law. According to this law (M.Bass, 2010), the intensity of optical signal at point x and time t' in the atmosphere can be expressed approximately as

$$I(\lambda, t', x) = I(\lambda, t, 0)e^{-\int_0^x K(\lambda)N(x',t)dx'} \tag{2.5}$$

where, $I(\lambda, t, 0)$ represents intensity of transmitter, $K(\lambda)$ and $N(x', t)$ represents total attenuation and space time distribution of spices in atmosphere, respectively. Total attenuation $K(\lambda)$ represents attenuation due to absorption and different type of scattering.

Table 2.4 International visibility code for different weather conditions. (Lightpointe, 2009)

Weather conditions	Precipitation		Amount (mm/hr)	Visibility (range)	dB Loss/km	Deployment Distance (m)
Dense Fog				0m - 50m	-271.65	122m
Thick Fog				200m	-59.57	490m
Moderate Fog	Snow			500m	-20.99	1087m
Light Fog	Snow	Cloudburst	100	770m 1 km	-12.65 -9.26	1565m 1493m
Thing Fog	Snow	Heavy rain	25	1.9 km 2 km	-4.22 -3.96	3238m 3369m
Haze	Snow	Medium rain	12.5	2.8 km 4 km	-2.58 -1.62	4331m 5566m
Light Haze	Snow	Light rain	2.5	5.9 km 10km	-0.96 -0.44	7146m 9670m
Clear	Snow	Drizzle	0.25	18.1km 20 km	-0.24 -0.22	11468m 11743m
Very clear				23 km 50 km	-0.19 -0.06	12112m 13771m

Absorption and scattering affect the visibility between transmitter and receiver, which reduce the overall FSO link range. Table 2.4 shows the international visibility code for different weather conditions. Fog, rain and snow are the main contributors to absorption and scattering in the FSO system.

2.4.2.1 Fog

Fog is a contributor in both, absorption and scattering. Water vapor is the main reason for absorption in the fog. There is a predefined absorption window of water vapor (Zuev, 2012) and according to that, absorption due to water vapor is very less at 1550 nm. The particle size of fog is same as the incident wavelength, which causes the scattering of the signal. The scattering due to fog is calculated by using Kruse formula (Wainright, 2005).

$$\alpha = \frac{3.91}{v}\left(\frac{\lambda}{550nm}\right)^{-q} \tag{2.6}$$

where, α represent scattering coefficient, V stands for visibility in km, λ is incident wavelength and $q = 0.585V^{1/3}$ for $V < 6$km, which represents the size distribution of scattering particle. Fig. 2.6 shows the effect of fog attenuation on the visibility over different wavelength.

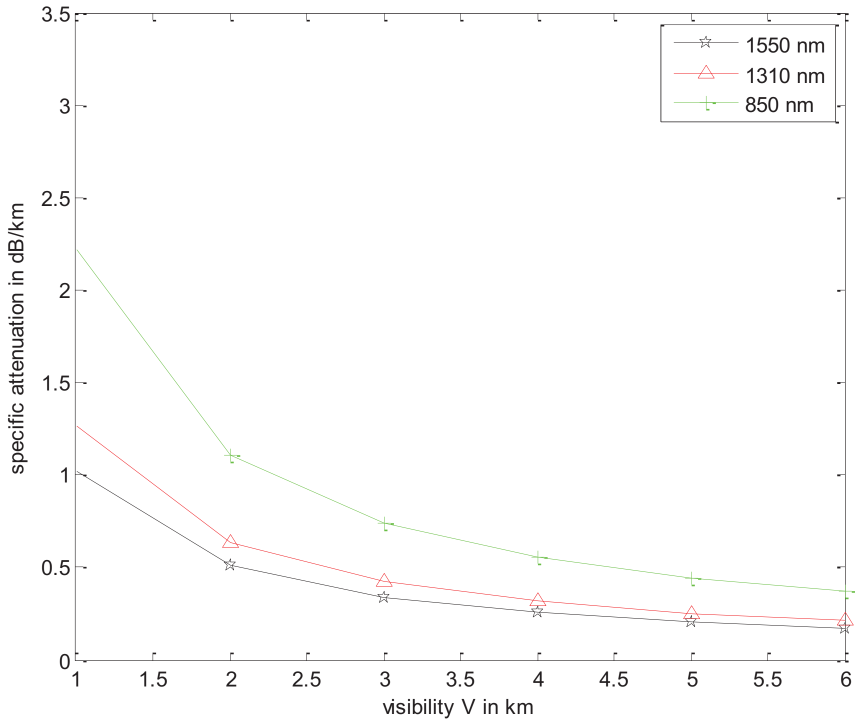

Fig. 2.6 Effect of fog attenuation on visibility

From Fig. 2.6, it is clear that at higher wavelength effect of attenuation is less compared to the lower wavelength. This insists the use of 1550 nm wavelength under fog condition. Although, authors (Wainright, 2005) have shown that the performance of 850 nm and 1550 nm is similar when the visibility is around 500 m due to fog. But, the performance of FSO is not good with the wavelength having a range in between 1000 nm-1310 nm under same conditions. This indicates that the signal transmission on multiple wavelengths will help to improve the performance of FSO link under fog condition.

2.4.2.2 Rain

The effect of rain on the FSO link is less severe than fog as raindrops are significantly larger than incident wavelength. Rain attenuation caused by rain rate (R), which is function of distance (d) and it can be expressed as (ITU, 2007)

$$\alpha_{rain} = m_1 R^{m_2} \tag{2.7}$$

where, R represents rain rate in mm/hr. m_1 and m_2 are the model parameters and their value depends on rain drop size and temperature. The attenuation loss due to rain is around 10 dB/km and 1 dB/km for heavy rain (25mm/hr) and light rain (2.5 mm/hr), respectively (A.Z Suriza, 2013), (Crane, 1997). It is also established that use of 1550 nm wavelength in FSO link is most suitable to combat the rain attenuations. (Hilal A. Fadhil, 2013).

2.4.2.3 Snow

Snow also affects the FSO link distance. The attenuation loss due to snow is higher than rain and lesser than fog, as the particle size lies in the intermediate range (higher than rain particle and smaller than fog particle). Snow attenuation can be classified as either Dry snow or wet snow. The total attenuation due to snow is calculated by (Vavoulas, 2012)

$$\alpha_{snow} = dA^{w} \tag{2.8}$$

where, A represents snow rate (mm/hr), The value of d and w in the dry and wet snow is given in (Vavoulas, 2012). For dry snow: $d = 5.42 \text{ X } 10^{-5} + 5.49$ and $w = 1.38$ and d $= 1.02 \text{ X } 10^{-4} + 3.78$ and $w = 0.72$ for wet snow condition.

The effect of rain and fog on FSO link is analyzed through simulations and experiment. In (Dhaval Shah, 2014), Simulations are performed to optimize FSO link distance in the rainy conditions of Ahmedabad. Wavelength Division Multiplexing (WDM) based FSO link is designed for 2.5 Gbps data rate at 1550nm wavelength. It is found that heavy rain reduces the link distance drastically. The effect of rain and fog mitigation by combined diversity is examined (Dhaval Shah, 2015). In this work, information signal is transmitted at the same time on 850 nm and 1550 nm towards the receiver. It is observed that transmission of a signal on these wavelengths enhances the performance and link availability during rain and fog conditions.

An experiment is carried out to analyze the impact of rain condition and other parameters (beam divergence, distance and input power) on FSO link (Dhaval Shah, 2016). Link is established in the campus of Nirma University (between Main parking and K-block) for the distance of about 750m. Practical results are verified with the simulation results which is performed in Optsim 7. From this experimental study, it is revealed that operating link with higher wavelength and narrow beam divergence helps to increase link distance. Further, the impact of light rain is very less on the deployed link. Simulation results show that use of higher wavelength gives better results under different weather conditions. An operation of implemented link degrades at a certain instance in clear weather conditions due to atmospheric turbulence. The effect of atmospheric turbulence on FSO link is explained in the next section.

2.4.3 Atmospheric Turbulence

Atmospheric turbulence is the major challenge for terrestrial FSO link. It is defined as the fluctuation in the refractive index due to variation in the temperature and pressure of the atmosphere. A variation in the temperature and pressure creates small air pockets, also called as eddies. Each of these has different size and different refractive index. These pockets work as a prism or lens for an optical signal and create interference to the propagating optical signal. This interference causes random fluctuation in the intensity and phase of the received signal at the receiver. Based on the eddy size, atmospheric turbulence effects are mainly classified into two categories: Beam wandering and Scintillation.

Beam wandering occurs due to larger turbulence eddies. The signal passing through larger turbulence eddies divert from its propagation path and may result in the link failure. The effect of beam wandering and scintillation on the transmitting signal is shown in Fig. 2.7. The displacement of the beam due to beam wandering is dependent on link distance, operating wavelength and transmitter beam size (H. Kaushal, 2011).

When the eddies size is smaller or equivalent to the size of the beam, the passing signal is diffracted and takes a different path to reach the receiver end. This causes a random irradiance fluctuation of transmitting beam and degrades the signal quality at the receiver. The intensity fluctuation of the received signal is known as scintillation. The combined effect of beam wander and scintillation deteriorates the signal quality of received signal and overall, it hampers the performance of FSO system.

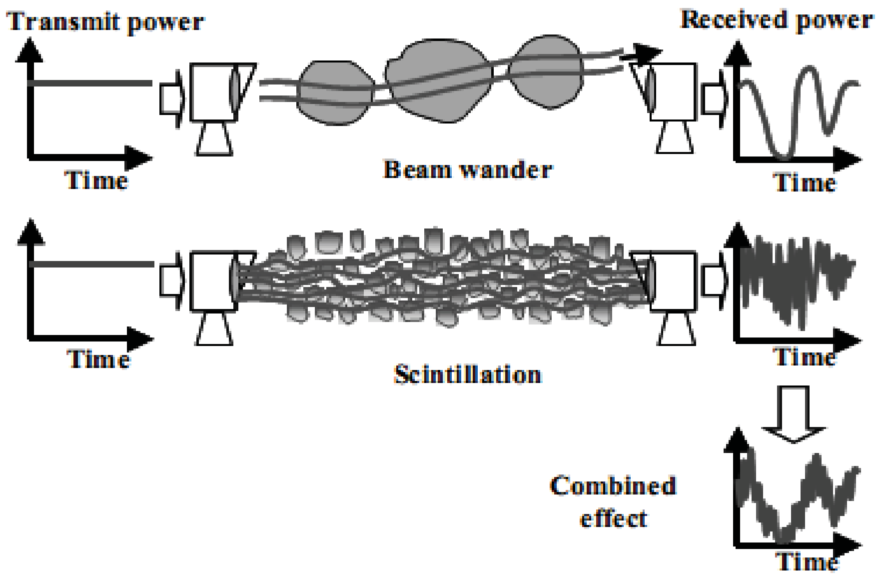

Fig. 2.7 Effect of beam wandering and scintillation (Kamugisha Kazaura, 2006)

The amount of intensity fluctuation is measured in terms of scintillation index. It is also referred as a normalized variance of intensity fluctuation, σ_I^2. It is calculated as in (Andrews, 2001), (Andrews, 2005)

$$\sigma_I^2 = \frac{<I^2> - <I>^2}{<I>^2} \tag{2.9}$$

where, I is the received intensity at any point on detector and the angular bracket (< >) indicates an ensemble average. Scintillation index value helps to categorize turbulence strength. It is very less in the case of weak turbulence, ($\sigma_I^2 < 0.3$) and for strong turbulence is more than 1 (Henniger, 2010). The scintillation index value for horizontal path under weak turbulence is also calculated from Rytov variance (β_0) and it is obtained as (Henniger, 2010)

$$\beta_0 = 0.49 C_n^2 K^{7/6} L^{11/6} \tag{2.10}$$

where, $K = \frac{2\pi}{\lambda}$ (optical wavenumber), L represents the link distance and C_n^2 is the refractive index structure parameter, which also gives the measure of turbulence strength in $m^{-2/3}$. It strongly depends on height, time of day and geographical location (E. S. Oh, 2004). There are numerous models of C_n^2 available to approximate turbulence strength (Kaushal, 2017). From the study of these models, it is observed that the value of C_n^2 is almost constant for horizontal link above the ground. The typical value of C_n^2 for the weak and strong turbulence is 10^{-17} $m^{-2/3}$ and 10^{-13} $m^{-2/3}$, respectively.

Among the above-mentioned impairments to FSO system, atmospheric turbulence is a major challenge, as it can occur even in clear weather condition. FSO channel under different turbulence conditions can be represented by selecting proper channel model as per turbulence strength. FSO channel models for different turbulence conditions are discussed in the next section.

2.5 FSO Channel Models

In FSO system, the transmitter transmits a signal along a horizontal path towards a receiver which is at the LOS with the transmitter. The received signal after passing through atmosphere with Additive White Gaussian Noise (AWGN) is expressed as

$$y = \eta I x + n \qquad (2.11)$$

where, y is the output, η is the effective photo-current conversion ratio of the receiver, I is the normalized irradiance (statistical average $E[I] = 1$) received at the receiver, x is the modulated signal and n is AWGN with mean 0 and variance $N_0/2$. The definition of irradiance varies as per turbulence strength. There are different channel models available to describe the different turbulence regime. Most widely used channel models like; Lognormal, Gamma-Gamma, Negative Exponential (NE), K and Exponentiated Weibull (EW) are discussed in this section.

2.5.1 Lognormal Channel Model

The lognormal channel is widely used and acceptable channel model for weak turbulence condition. The Probability Density Function (PDF) of this channel model is derived using a first-order Rytov approximation. According to that, the irradiance of an optical wave traveling through turbulence is obtained by

$$\mathrm{I} = \langle \mathrm{I} \rangle \exp 2\Upsilon_1 \tag{2.12}$$

where $\Upsilon_1 = \frac{1}{2}(\phi_1 + \phi_1^*)$ and ϕ_1 represents the first-order log-amplitude of the field and phase perturbation, respectively as per Rytov approximation. The log-amplitude Υ_1 follows a Gaussian distribution and the irradiance is normalized ($\langle \mathrm{I} \rangle = 1$). Taking the transformation of variables $\Upsilon_1 = \frac{1}{2}\ln \mathrm{I}$, the PDF of irradiance I can be calculated as

$$\mathrm{f_I(I)} = \mathrm{f}_{\Upsilon_1}(\Upsilon_1)\frac{d\Upsilon_1}{d\mathrm{I}}\bigg|_{\Upsilon_1 = \ln \mathrm{I}} \tag{2.13}$$

$$\mathrm{f_I(I)} = \frac{1}{2\mathrm{I}\sqrt{2\pi\sigma_{\Upsilon 1}^2}} \exp\left[-\frac{\left(\frac{1}{2}\ln \mathrm{I} - \langle \Upsilon_1 \rangle\right)^2}{2\sigma_{\Upsilon 1}^2}\right] \tag{2.14}$$

Eq. 2.14 denotes a lognormal distribution and the variance of Υ_1 can be expressed in terms of log-irradiance variance as (Barrios Porras, 2013)

$$\sigma_{\ln I}^2 = 4\sigma_{\Upsilon 1}^2 \tag{2.15}$$

Now, considering the expected value of Eq. (2.12)

$$\langle \mathrm{I} \rangle = \langle \mathrm{I} \rangle \langle \exp(2\Upsilon_1) \rangle = \langle \mathrm{I} \rangle \exp[2(\langle \Upsilon_1 \rangle + \sigma_{\Upsilon 1}^2)] \tag{2.16}$$

The equality condition satisfies only if the argument within the exponential part is 0. Then,

$$\langle \Upsilon_1 \rangle = -\sigma_{\Upsilon 1}^2 \tag{2.17}$$

Putting the Eq. (2.15) and (2.17) into Eq. (2.14), the final Power Density Function (PDF) of the lognormal channel is obtained as

$$f_I(I) = \frac{1}{I\sqrt{2\pi\sigma_{\ln I}^2}} \exp\left[-\frac{\left(\ln I + \frac{1}{2}\sigma_{\ln I}^2\right)^2}{2\sigma_{\ln I}^2}\right] \tag{2.18}$$

Authors (H. Moradi, 2010) have opted this model to analyze the Bit Error Rate (BER) of FSO link. They have derived closed-form equation to obtain BER under different fading intensity with the assumption that perfect Channel State Information (CSI) is available at the receiver. Average BER of FSO link under weak turbulence using same channel model without perfect CSI at receiver is reported in (Dhaval Shah, 2012)

At higher turbulence strength, various scattering effects must be considered during channel estimation. These scattering effects have a great impact on the tail region of PDF and this channel underestimates the behavior in the tail region of PDF (Uysal, 2006). As detection and fading probability are mainly focused on the tail region of the PDF, lognormal distribution fails in strong turbulence scenario.

2.5.2 Gamma Gamma Channel Model

Gamma-Gamma channel model is applicable for weak and strong turbulence scenario. This model is defined based on modified Rytov theory (L. C. Andrew, 1999), (Andrews, 2000), (Al-Habash, 2001). According to that, an optical channel is defined as the product of two independent complex perturbations due to small and large-scale turbulent eddies. i.e. (I) = $X*Y$ where, X and Y represent fluctuation due to large and small scale turbulent eddies, respectively and both are considered as independent and identically distributed gamma random variables. In this case, the PDF of X and Y is obtained as

$$f_X(x) = \frac{\alpha(\alpha x)^{\alpha-1}}{\Gamma(\alpha)} \exp(-\alpha x) \tag{2.19}$$

$$f_Y(y) = \frac{\beta(\beta y)^{\beta-1}}{\Gamma(\beta)} \exp(-\beta y) \tag{2.20}$$

The conditional PDF of the irradiance is calculated as

$$f_I(I|x) = f_Y(y) \left.\frac{dy}{dI}\right|_{y=\frac{I}{x}} \tag{2.21}$$

$$f_{\mathrm{I}}(I|x) = \frac{\beta}{x\Gamma(\beta)}\left(\frac{\beta I}{x}\right)^{\beta-1} \exp\left(-\frac{\beta I}{x}\right) \tag{2.22}$$

It is assumed that *Y* modulates *X*. Now, the unconditional PDF of irradiance is obtained by

$$f_I(I) = \int_0^\infty f_{\mathrm{I}}(I|x)\, f_X(x) dx \tag{2.23}$$

This leads to

$$f_I(I) = \frac{(\alpha\beta I)^{\beta-1}}{\Gamma(\alpha)\Gamma(\beta) I}\int_0^\infty t^{(\alpha-\beta-1)} \exp\left(-t + \frac{\alpha\beta I}{t}\right) dt \tag{2.24}$$

here t = αx, this integral is related to modified Bessel function of the second kind [(I. Gradshteyn, 2007), Eq. (8.432.6)]. So, the final PDF of Gamma-Gamma is

$$f(I) = \frac{2(\alpha\beta)^{(\alpha+\beta)/2}}{\Gamma(\alpha)\Gamma(\beta)} I^{\frac{\alpha+\beta}{2}-1}\, \mathrm{K}_{\alpha-\beta}\left(2\sqrt{\alpha\beta I}\right),\ I > 0 \tag{2.25}$$

here, $K_a(.)$ represents second-order modified Bessel function. α and β are the numbers scatter due to large and small eddies in the free space. The value of α and β are calculated as (Al-Habash, 2001)

$$\alpha = \left[\exp\left(\frac{0.49\beta_0^2}{(1+0.18d^2+0.56\beta_0^{12/5})^{7/6}}\right) - 1\right]^{-1} \tag{2.26}$$

$$\beta = \left[exp\left(\frac{0.51\beta_0^2}{(1+0.9d^2+0.62d^2\beta_0^{12/5})^{5/6}}\right) - 1\right]^{-1} \tag{2.27}$$

here, $d = (kD^2/4L)^{\frac{1}{2}}$ and $\beta_0^2 = 0.5C_n^2 k^{\frac{7}{6}} L^{\frac{11}{6}}$, where L and D represents link distance and receiver aperture diameter. $k = \frac{2\pi}{\lambda}$, signifies the optical wavenumber, where, λ represents operational wavelength of the link. C_n^2 is the refractive index structure parameter, the value of this parameter is taken as per turbulence strength. This model is more suitable for physical FSO link performance comparison as α and β can be directly related with the physical link parameters (i.e. link length, receiver aperture size, operation wavelength). Authors (Gappmair, 2009) and (Uysal, 2006) have used this model for error rate performance analysis of coded FSO link.

2.5.3 Negative Exponential Channel Model

NE channel model can be used to define channel characteristic under strong turbulence regime. The PDF of NE is derived considering a circular complex Gaussian random variable

$$U = Y_1 + Y_2 = Y\exp(-i\theta)\,,\;\; where\; i^2 = -1 \tag{2.28}$$

And Y_1 and Y_2 are considered as independent and follow Gaussian process with mean 0 and variance σ^2. The joint PDF of Y and θ is obtained as

$$f(y,\theta) = yf(y_1,y_2) = yf(ycos\theta\,, ysin\theta) = yf(ycos\theta)f(ysin\theta) \tag{2.29}$$

As, Y_1 and Y_2 are independent, the equality between them is given as

$$f(y_1,y_2) = \frac{1}{2\pi\sigma^2}\exp\left(-\frac{y_1^2+y_2^2}{2\sigma^2}\right) \quad \text{where, } y_1^2 + y_2^2 = y^2 \tag{2.30}$$

From Eq. (2.29) we get,

$$f(y,\theta) = \frac{y}{2\pi\sigma^2}\exp\left(\frac{y^2}{2\sigma^2}\right) \quad , y \geq 0,\; 0 \leq \theta < 2\pi \tag{2.31}$$

Now, the PDF can be determined as the marginal distributions of $f(y,\theta)$) , so,

$$f_y(y) = \int_0^{2\pi} f(y,\theta)d\theta = \frac{y}{\sigma^2}\exp\left(-\frac{y^2}{2\sigma^2}\right) \tag{2.32}$$

Eq. (2.32) can be identified as Rayleigh distribution, which follows a uniform distribution in the interval [0, 2π) (Parikh, 2011) (Dhaval Shah, 2014).

$$f_\phi(\theta) = \int_0^{\infty} f(y,\theta)dy = \frac{1}{2\pi} \tag{2.33}$$

Now, considering the transformation of variable $I = Y^2$,

$$f_I(I) = f_Y(y)\frac{dy}{dI}\bigg|_{y=\sqrt{I}}$$

$$f_I(I) = \frac{1}{2\sigma^2}\exp\left(-\frac{I}{2\sigma^2}\right) \tag{2.34}$$

By replacing $2\sigma^2 = \mu$, the final PDF of NE channel model is obtained as

$$f(I) = \frac{1}{\mu}\exp(-\frac{I}{\mu}) \tag{2.35}$$

where, μ represent mean radiance. Here scintillation index is in vicinity of 1. In the literature (Popoola, 2003) and (Nistazakis, 2011), author have analyzed the performance of FSO link under strong turbulence using NE model.

2.5.4 K Channel Model

K distribution is widely accepted for the application under strong turbulence condition (Al-Habash, 2001). Initially, K distribution was applied to model non-Rayleigh eco (E.Jakeman, 1976). Later on, authors (E.Jakeman, 1978) (Jakeman, 1980) have proved that this distribution offers excellent agreement with various experimental data that includes scattering due to strong turbulence condition. The PDF of K channel is derived with the help of conditional NE channel model. According to that,

$$f_{(I|\mu)}(I|\mu) = \frac{1}{\mu}\exp(-\frac{I}{\mu}) \tag{2.36}$$

here, μ represents mean of irradiance and that follows Gamma distribution.

$$f_{(\mu)}(\mu) = \frac{\alpha^{\alpha}\,\mu^{\alpha-1}}{\Gamma(\alpha)}\exp(-\,\alpha\mu), \mu > 0 \tag{2.37}$$

where, Γ(.) represents Gamma function and α gives the effective number of discrete scatter in the channel. The irradiance with unconditional distribution is obtained as (Parikh, 2011)

$$f_I(I) = \int_0^{\infty} f_{(I|\mu)}(I|\mu) f_{(\mu)}(\mu) dI \tag{2.38}$$

Putting Eq. (2.13) and Eq. (2.24) into Eq. (2.25), the final PDF of K channel is calculated as

$$f(I) = \frac{2(\alpha)^{(\alpha+1)/2}}{\Gamma(\alpha)} I^{\frac{\alpha-1}{2}}\, \mathrm{K}_{\alpha-1}\big(2\sqrt{\alpha I}\big),\ I > 0 \tag{2.39}$$

where, I is the normalized irradiance and K_{v} (.) is the v^{th} order modified Bessel function of the second kind. As $\alpha \to \infty$, Eq. 2.39 approaches to NE channel model. In (H. G. Sandalidis, 2008), authors have opted this model to represent strong turbulence scenario and obtained BER of FSO link with pointing errors for the distance of more than 1 km. (Kiasaleh, 2006) and (Uysal M., 2004) have also applied this model to characterize strong turbulence and analyzed the FSO link performance.

2.5.5 Exponentiated Weibull Channel Model

EW channel model is a newly introduced model to characterize all turbulence condition. It is enhanced version of Weibull channel model which is used for fading channel measurement in the wireless communication field (Alouini, 2001), (Lupupa, 2009). The PDF of Weibull distribution is

$$f_I(I) = \frac{\beta}{\eta}\left(\frac{I}{\eta}\right)^{\beta-1} exp\left[-\left(\frac{I}{\eta}\right)^{\beta}\right] \tag{2.40}$$

where, $\beta > 0$ is shape parameter and $\eta > 0$ represents scale parameter. η depends on β and it is related to the mean value of the irradiance. For the cases of $\beta = 1$and $\beta = 2$, Eq. (2.40) reduces to the Negative exponential and Rayleigh PDF, respectively.

This model is only applicable for stationary conditions, where channel statistic remains constant over the observation time period. This limitation is addressed by Mudholkar and Srivastava (Mudholkar, 1993) by adding an additional shape parameter to the Weibull distribution and proposed a new model which is called as Exponentiated Weibull (EW) distribution. The PDF of EW is given by (Barrios Porras, 2013)

$$f_I(I) = \frac{\alpha\beta}{\eta}\left(\frac{I}{\eta}\right)^{\beta-1} exp\left[-\left(\frac{I}{\eta}\right)^{\beta}\right]\left\{1 - exp\left[-\left(\frac{I}{\eta}\right)^{\beta}\right]\right\}^{\alpha-1} \tag{2.41}$$

where, $\beta > 0$ and $\alpha > 0$ are shape parameters, and $\eta > 0$ is a scale parameter, which is related to the mean value of the irradiance. If ($\alpha = 1$), then Eq. (2.41) represents the Weibull distribution and for the cases of ($\alpha = 1$, $\beta = 2$), and ($\alpha = 1$, $\beta = 1$), Eq. (2.41) represents Rayleigh and the Negative exponential distribution, respectively.

Barrios and Dios (Barrios, 2013) have used this EW distribution to model the distribution of the irradiance in FSO link. They have also suggested that EW distribution can be used to categorize fading in all turbulence regime for the FSO link.

FSO channel under turbulence condition can be characterized using any of these channel models as per turbulence strength. In this thesis, K channel and EW channel models have been used to define strong turbulence and different turbulence condition, respectively. Once, FSO channel under turbulence condition is defined, different turbulence mitigation techniques can be applied to compensate different turbulence effect.

2.6 Turbulence Mitigation Techniques

Atmospheric turbulence severely affects the performance of FSO system. There are various techniques available to mitigate this effect, namely aperture averaging, adaptive optics, error correcting codes, hybrid RF/FSO and different diversity techniques. Each of these has certain advantages and limitations. This section presents a detailed study of these techniques.

2.6.1 Aperture Averaging

In FSO communication, received signal quality is degraded due to turbulence in the free space. The effect of turbulence, which is mainly due to scintillation, can be compensated by increasing receiver aperture size. This phenomenon is called as Aperture averaging. Large receiver aperture averages the received fluctuation, which leads to less signal fluctuation compared to point receiver. The reduction in the received fluctuation due to aperture averaging is measured by the parameter, called as aperture averaging factor, A. Aperture averaging factor (A) is described as ratio of variance of the received signal fluctuation with large aperture diameter D_E to that with a point receiver D_P. i.e.

$$A = \frac{\sigma_I^2\ (D_E)}{\sigma_I^2\ (D_P)} \tag{2.42}$$

There are numerous approximations available to define aperture averaging factor. Initially, Fried (Fried, 1973) had derived the approximate formula of the averaging factor under weak turbulence. Based on this preliminary work, authors (Churnside, 1991) have derived the approximate expression of aperture averaging factor for plane and spherical wave under strong and weak turbulence conditions. However, the result obtained based on those approximations are far from the practical results by a factor of 2, especially when aperture diameter size is same as the inner scale of turbulence. Andrew (Andrews, 1992) has provided an accurate approximation for aperture averaging factor for both spherical and plane wave under weak turbulence conditions. According to that, the approximate value of aperture averaging factor under weak turbulence for plane wave and the spherical wave is given by Eq. (2.39) and Eq. (2.40), respectively.

$$A_{plane} = \left[1 + 1.062\left(\frac{KD_E^2}{4L}\right)\right]^{-7/6} \tag{2.43}$$

$$A_{spherical} = \left[1 + 0.333\left(\frac{KD_E^2}{4L}\right)^{5/6}\right]^{-7/6} \tag{2.44}$$

where, L represents link length, $K = 2\pi/\lambda$, defines optical wavenumber and D_E represents aperture size. An experimental study on different aperture averaging factor approximation under weak turbulence for different aperture size ranging from 1 cm to 16 cm is presented in (Wasiczko, 2005).

Normally, Plane wave and spherical wave model are suitable for space-to-ground and ground-to-space optical links with a point source, respectively. Whereas, Gaussian beam model provides a good approximation for the horizontal (terrestrial) link (Majumdar, 2008). However, Gaussian beam statistical properties are close to the point source properties (Yuksel, 2005). So, plane wave and spherical wave approximation are also valid for the terrestrial link. Authors (Yuksel, 2005) have performed an experiment to obtain a value for aperture averaging factor with aperture size from 1 cm to 16 cm under moderate turbulence condition for FSO link of 832 m. Their results also demonstrate that increasing aperture size reduces the intensity fluctuation of the signal.

Aperture averaging method is applied in various literature to reduce turbulence effect. In literature (G. L. Bastin, 2005), authors have applied this method to analyze the BER performance of FSO link. They have performed the experiment at Kennedy Space Center- NASA with the help of commercially available transceiver, made by FSONA Company. The FSO link was set up for the distance of 1 km with operating wavelength of 1550 nm. A consistent improvement in the BER is observed with an increase in the size of receiver aperture. The receiver aperture size was varied from 1 inch to 8 inches.

BER of 10^{-3} was obtained with receiver aperture of 2 inches. Almost 90 dB improvement in the BER was observed with an aperture of 8 inches compared to 2-inch aperture size.

Cheng et. al. (Cheng, 2015) have investigated the effect of aperture averaging on the error performance of FSO link under weak turbulence for the marine environment. The analysis was carried out considering Gaussian-beam wave. The results are reported for different receiver aperture size (2 cm, 4 cm, and 6 cm). Increasing aperture size improves the BER performance under weak turbulence marine time condition. For 10^{-5} BER, the improvement in the BER of 10 dB with 6 cm aperture size compared to 2 cm. They have also evaluated receiver aperture averaged irradiance scintillation index under weak turbulence for terrestrial and marine time and found that the larger aperture reduces the atmospheric turbulence in both the case.

The impact of this method under different turbulence regime is investigated in (M.A. Khalighi, 2009). An Effect of a plane wave, spherical wave and Gaussian beam propagation on the aperture averaging factor under moderate and strong turbulence condition is also analyzed. In all propagation models, as receiver aperture size increases, aperture average factor reduces. The impact of aperture averaging was same for the plane wave and Gaussian wave propagation and better than spherical wave under moderate turbulence condition at particular aperture size. Whereas, higher aperture averaging gain is observed for Gaussian beam propagation with larger receiver size under strong turbulence condition. They have also investigated BER performance in all turbulence condition with 5 mm, 10mm, 20 mm, 50 mm, 100mm and 200 mm receiver aperture size. Aperture averaging performs better in strong turbulence condition compared to weak and moderate turbulence conditions. The improvement of 53 dB in SNR for BER of 10^{-5} is observed with 10 mm aperture size compared to point receiver (0 mm) under strong turbulence. These trends continue with higher aperture size as well. At very large aperture size (200 mm), the observed gain in SNR is about 75 dB with the same BER. In the case of moderate turbulence, the improvement in the SNR is 20 dB and 54 dB at BER of 10^{-5} with the aperture size of 5 mm and 200 mm, respectively, compared to point receiver. BER performance improvement is also observed under weak turbulence as well with this method, but it is far lesser than other two turbulence scenarios. It is only 0.33 dB with 50 mm aperture size compared to point receiver for the BER of 10^{-5}.

Though aperture averaging method mitigates turbulence effect, this advantage comes with larger receiver aperture, which also increases the background noise. For strong turbulence condition, effective aperture receiver size should be larger than 10 cm (Wasiczko, 2005). There is no significant improvement observed by this method under weak turbulence regime. So, this method is not applicable to improve the performance of FSO system under all turbulence conditions.

2.6.2 Adaptive Optics

Adaptive optics (AO) is another method to mitigate turbulence effect. AO correct the received distorted wavefront in real time to reduce the fluctuation of the received signal. AO systems measure the distortions in a wavefront and compensate it in real time with a device that corrects those errors with the help of a deformable mirror or liquid crystal array. Fig. 2.8 shows the working of AO system.

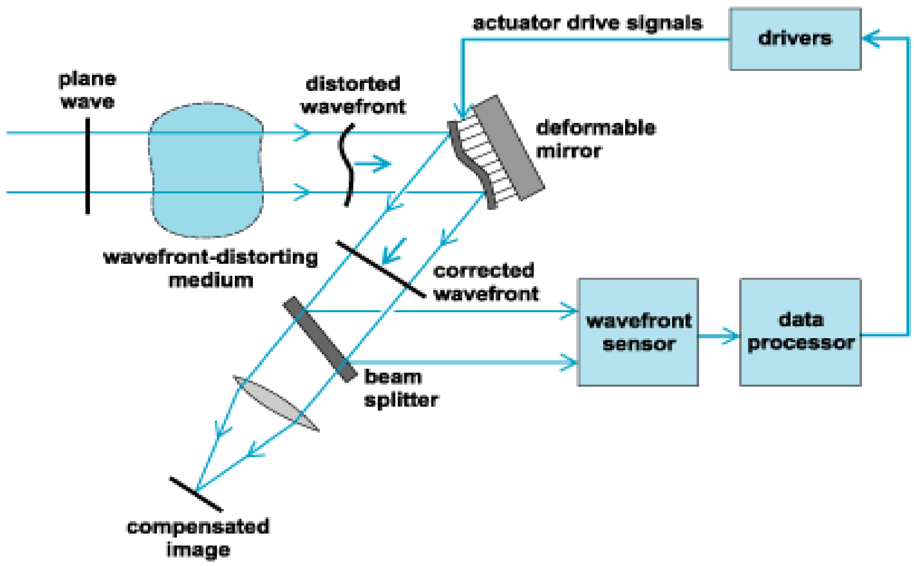

Fig. 2.8 Block diagram of AO system (Grumman, 2017)
Source:http://www.northropgrumman.com/BusinessVentures/AOAXinetics/IntelligentOptics/Technology/Pages/AdaptiveOpticalSystem.aspx

The transmitted signal is incident on the deformable mirror after passing through the atmosphere. The deformable mirror reflects the distorted wavefront on the beam splitter, which splits the signal and passes that portion of the signal to Wavefront Sensor (WS). The function of WS is to measure the phase of an optical wavefront. Based on the value of WS, driver circuit generates the actuator driving signal, which is fed to wavefront actuator to compensate phase fluctuation. This closed-loop control system performs the phase conjugation by distorting the wavefront of the light beam without disturbing the intensity profile. This real-time correction of the transmitted beam is also known as precompensation.

There are numerous ways to correct wavefront in real time. In (Vorontsov, 1997), authors have performed wavefront correction using parallel stochastic perturbation method. They have corrected phase distortion with the help of 127-element liquid crystal phase modulators. Their approach reduces the time requirement of the adaptive control process. However, it is observed that this method failed to achieve proper wavefront corrections.

The performance of FSO link under all turbulence (weak to strong) condition incorporating AO has been investigated by Barbier (P. Barbier, 1998). They have used commercially available Shack-Hartmann (SH) wavefront sensor for the measurement of the phase of the wavefront. Scintillation reduction of propagating signal was analyzed using Monte-Carlo simulations. They have also examined the effect of a dynamic range of the wavefront sensor, limited adaptive optics aperture size, and link length on the performance improvement obtained with AO. There is no significant improvement is observed with the aperture size of 4 cm under different turbulence conditions. It is observed that acceptable aperture size is 15 cm to obtain typical BER in the range of 10^{-9}. The performance improvement with AO is negligible at shorter link distance (1 km). However, AO increases the average intensity of signal by a factor of 6 over a 5 km path under weak turbulence. But it fails to give good improvement under strong turbulence at the same distance compared to weak turbulence condition.

Schwartz et. al. (Schwartz, 2009) have investigated an AO system approach to mitigate the effect of atmospheric turbulence with numerical simulations. The results are presented for different turbulence conditions at the link length of 10 km with different wavefront correction methods, namely; iterative, non-iterative and phase correction method. In the iterative method (also known as optimal correction method), wavefront correction is obtained by phase conjugation. Whereas, non-iterative correction method uses SH sensor to measure the phase of the wavefront. In the optimal correction method, a significant correction is obtained with an aperture size of 30 cm in different turbulence condition with an operating wavelength of 1550 nm. Wavefront correction by this method required two deformable mirror sets to correct phase and amplitude both. This adds cost and complexity of the system. In the second method, it is observed that SH wavefront sensor is not robust and the performance of it decreases in the strong turbulence condition. On the other hand, phase correction method demands frequently update of the deformable mirror during the lifetime of atmospheric turbulent cells.

The addition of AO in FSO link improves the performance of FSO link under weak and moderate turbulence. However, deployment of AO does not improve performance significantly under strong turbulence condition. Apart from this, commercially available SH wavefront sensor performance is very poor as well under strong turbulence condition. Incorporation of AO in FSO system increase cost drastically. Moreover, the improvement obtained by AO is not feasible with the smaller size of the aperture.

2.6.3 Error Correcting Codes

The performance of FSO link under atmospheric turbulence condition can be improved by applying different error controlling codes such as Reed-Solomon (RS) codes, Turbo codes, convolution codes, Low-Density Parity Check (LDPC) code and Trellis codes. Use of these codes adds redundant information on the transmitting signal. At the receiver side, decoding algorithm is applied to decode the generated code from the received signal. So, the error occurs during communication due to fading can be detected and corrected. An error performance of error-correcting codes under fading conditions is presented in (Hagenauer, 1987), (J. A. Anguita, 2005) and (Alzubi, 2014). These studies show that improvement provided by RS code and Convolution code is adequate for weak turbulence condition. Whereas LDPC and Turbo codes are more preferred under strong turbulence conditions.

In (S. S. Muhammad, 2007), authors have investigated the performance of terrestrial FSO link with RS coded PPM. They have investigated the performance of FSO link under ambient noise and moderate fog condition with and without RS (255,127) coding techniques with different levels of PPM (16-PPM and 256-PPM). It is observed that application of RS code improves receiver sensitivity by 6 dB at BER of 10^{-6} for both the level of PPM. A similar improvement is observed under moderate fog conditions. However, RS coding fails in the case where fog attenuation is higher than 10 dB.

The performance of FSO link with different coding techniques under weak and strong turbulence is examined and reported by Xu (F. Xu, 2008). RS, Turbo, Convolution and Concatenated Convolution and RS (CCRS) code are considered for the performance evaluation. Results are presented for all coding techniques with and without time diversity. The improvement of 1 dB in SNR with RS coding compared to without the use of coding technique at BER of 10^{-5} is observed under weak turbulence. The same is about 3.5 dB for the other three schemes compared to that of no coding technique. The presented results for the strong turbulence case show that these coding techniques are not improving the performance of FSO link. This also indicates that only coding technique is not sufficient under strong turbulence scenario. The noticeable improvement in the performance is observed with the time diversity scheme. It is observed that Turbo coding with time diversity achieves the highest improvement under strong turbulence scenario. It improves the SNR by 31 dB and 47.5 dB for the diversity order of 2 and 4, respectively at BER of 10^{-5}. The consideration of time diversity with coding techniques also marginally improves the performance under weak turbulence. Convolution code has shown the highest performance improvement of 5.2 dB compared to that of no coding with time diversity of the order of 2. It is noteworthy to mention that improvement obtained by time diversity with coding techniques demands large memory for error correcting coding techniques at receiver and also adds a delay in the data detection.

An error correction of turbulence affected FSO link with LDPC coding is performed by Anguita (J. A. Anguita, 2005). In this article, turbulence effect was simulated with Gamma-Gamma channel model and comparison of the performance of LDPC with RS code is presented. The codeword lengths of LDPC codes were of 2025 and 4320 bits at a code rate of 0.91 and 0.75, respectively. A comparison is given with two RS codes; RS (255,239) and RS (255,191) with the rate of 0.94 and 0.75, respectively. The presented results have shown that LDPC provides an outstanding improvement of 20 dB compared to without coding method. It is also observed that LDPC provides great improvement in the performance over RS coding under strong and weak turbulence conditions. The maximum gain achieved in SNR is 12 dB and 14 dB with the LDPC code rate of 0.91 and 0.75, respectively compared to RS code under strong turbulence condition. The same is reported as 7.5 dB and 9 dB under weak turbulence condition. This enhancement comes with an additional encoder at the transmitter and a decoder at a receiver side.

The performance comparison of uncoded FSO link with different coding techniques is presented in (D. Shah, 2017). In this paper, the author has examined the performance of FSO link under strong turbulence with convolution coding, Orthogonal Variable Spreading Factor (OVSF) coding and the combination of both codings. Strong turbulence condition is represented by NE channel model. These results again show that applying error controlling code improves the performance of FSO link. A maximum improvement in SNR of 13 dB is observed with the combination of OVSF and convolution coding. The performance gain is achieved by applying only convolution code is 2 dB higher than the case of OVSF code.

It is evident from the literature that application of error control coding techniques improves the performance of FSO link. But, this improvement comes with some stringent requirements. Normally, the coherence time of FSO is about 10 ms (F. Xu, 2008), this demands large memory to store long data stream. This makes receiver design more complex and adds latencies. Another option of interleaving transmitted data with coding scheme requires an additional section of encoder and decoder.

2.6.4 Hybrid RF/FSO

Atmospheric turbulence and different weather conditions badly affect the FSO link performance. These conditions sometimes cause link failure as well. Among different weather conditions, the effect of fog is more prominent on the FSO link performance. On the other hand, the performance of RF links badly suffer under rain condition. The pairing of FSO link with RF link compensates the effect of rain and fog both. It is known as hybrid RF/FSO link. It improves link availability under all weather conditions. FSO link transmits the information during rain condition, while RF link can be used for transmission during fog condition. So the pairing of both will overcome each other's weaknesses and give better performance under both the conditions.

The concept of Hybrid RF/FSO gains a lot of attention in the field of Mobile Ad-hoc NETwork (MANET) (D. K. Kumar, 2013), (Derenick, 2005). The performance of MANET is limited due to available limits in per-node throughput for radio frequency (RF) based communications. This limitation is easily overcome by Hybrid RF/FSO link. In (Derenick, 2005), authors have implemented hybrid RF/FSO based MANET. This network consists of 100 Mbps optical link and 802 .11g based RF transceiver. Feasibility of Hybrid RF/FSO is realized by routing real-time video information through this network. The mathematical expression of availability and capacity of FSO/RF ad-hoc mesh network considering different turbulence scenarios is presented in (Moradi, 2010). A closed-form expression for system capacity assuming Gamma-Gamma and lognormal fading conditions is reported in this work.

In (Wu, 2007), authors have evaluated the availability of hybrid RF/FSO link from ground-to-air. It is observed that FSO link fails in cloudy conditions. Use of hybrid RF/FSO link provides great improvement in this condition due to immunity of RF signal under cloudy interference. Another experimental study on hybrid RF/FSO link availability is performed by Kim (Kim, 2001). In which, a comparison of availability of FSO and hybrid RF/FSO link is carried out. It is observed that hybrid RF/FSO link availability is 99.999% compared to FSO link for distance more than 140 m.

Hybrid RF/FSO link provides robust solution under adverse weather conditions, but the channel bandwidth utilization is inefficient (H. Moradi, 2010). Apart from this, the continuous switching between FSO and RF may completely fail the system. Moreover, incorporation of the two systems drastically increases design complexity of the system.

2.6.5 Diversity Techniques

Diversity techniques are another solution to combat atmospheric turbulence. In this method, multiple copies of the information signal are transmitted by either using different time, wavelength or multiple antennas. If the same information signal is transmitted at different time stamp then it is called as time diversity. Multiple transmission of a signal on different wavelength is known as wavelength diversity. Use of multiple antenna to transmit signal is known as spatial diversity. An idea behind multiple transmission of the same information signal is that an atmospheric turbulence is random in nature and its impact will be different on multiple copies of the information signal. When all multiple copies of information signal combined using any combining method, the overall signal quality will be improved. OC, EGC and SC are commonly used combining methods at receiver in the diversity technique.

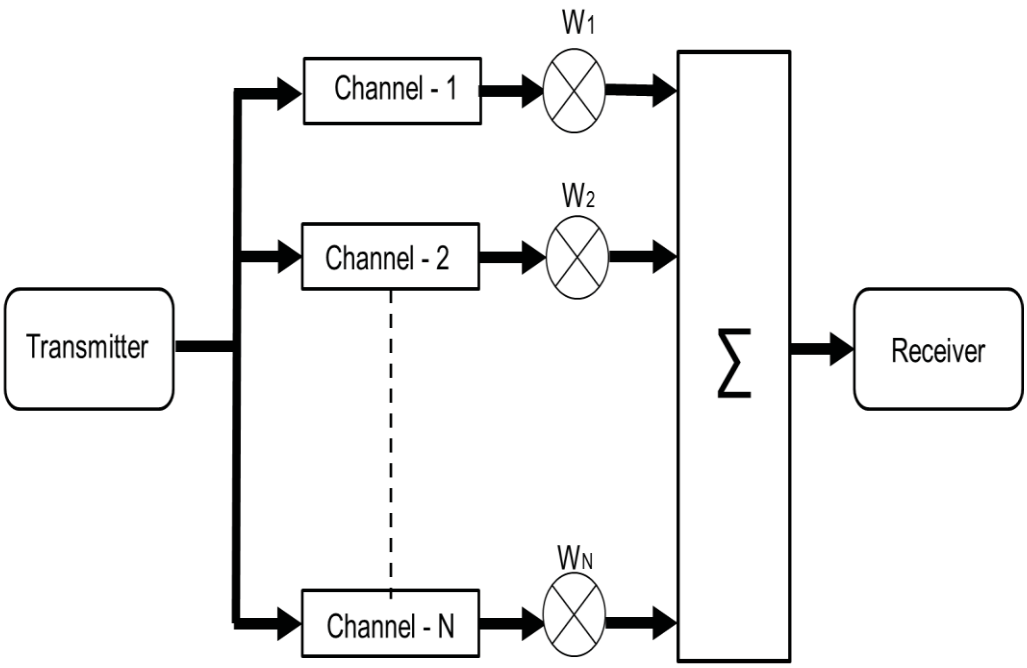

Fig. 2.9 Optimal Combining Method

In OC method, all the signals from the different channel are weighted and co-phased before applying to summing circuit as shown in Fig. 2.7. The value of weighting factor for the respective signal is selected so it can maximize the SNR value and reduces the error probability at the output. Then, the signal is applied to summing circuit. This method is also known as Maximum Ratio Combining (MRC) in the wireless communication field.

The working of EGC method is shown in Fig. 2.10. Unlike OC, it does not apply weighting to incoming signals. This makes EGC less complex than OC. All incoming signals are directly applied to the summing circuit and final output is applied to the receiver. As all incoming signals are directly combined, it also increases the probability of noise addition in the final signal. Therefore, the performance of this method is slightly lesser than OC.

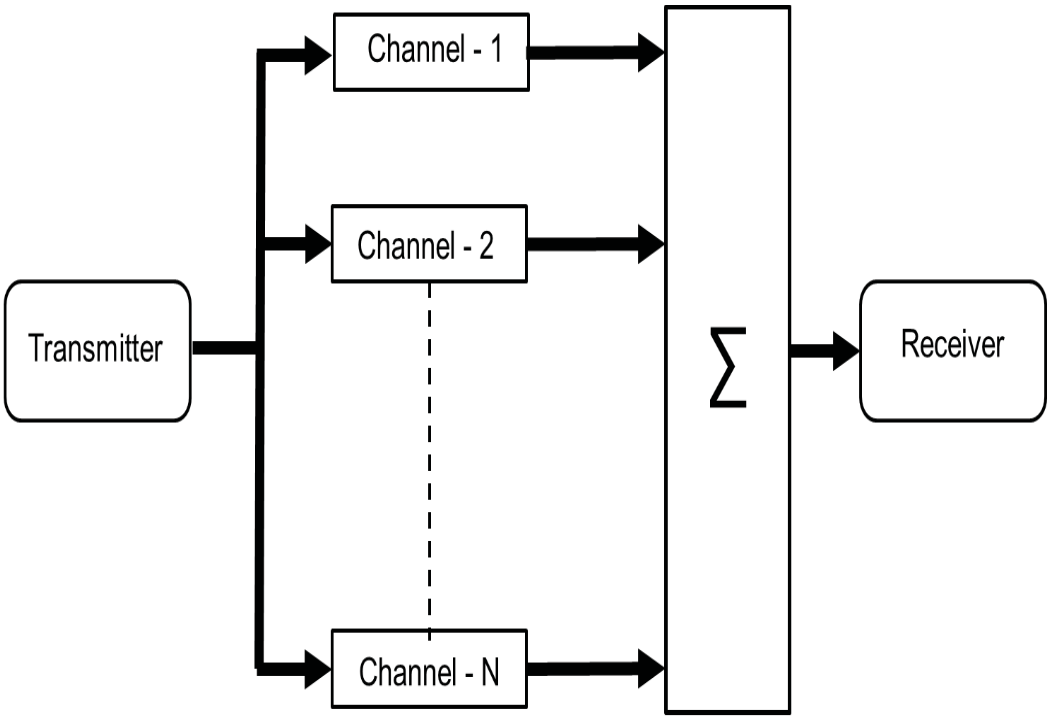

Fig. 2.10 Equal Gain Combining method

The working of SC method is shown in Fig. 2.11. In this method, the channel with maximum SNR will be selected out of all available channels. However, to identify channel with maximum SNR within the very short time interval is very challenging. Selection of highest SNR channel is similar to the selection of the channel with highest received power where average noise power is same for all the available channel. This makes a selection of highest SNR channel feasible.

Each of these combining methods has their own advantages and disadvantages. Selection of combining method for diversity techniques depend on the application and environment in which it will be deployed. Use of these methods has been reported in the literature with different diversity techniques.

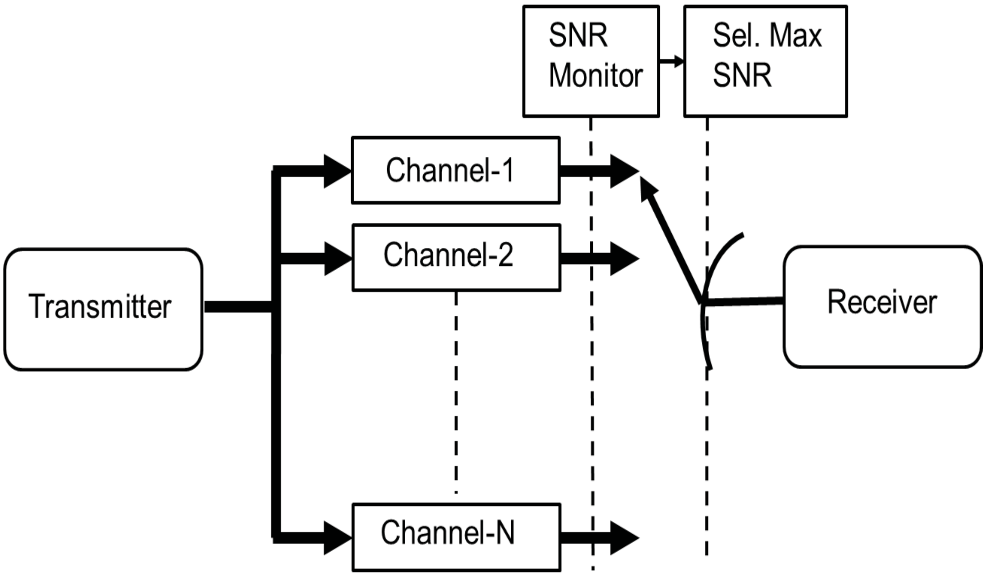

Fig. 2.11 Selection Combining

2.6.5.1 Time diversity

In (Nistazakis, 2013), authors have applied time diversity techniques to improve the performance of Single FSO system under strong turbulence condition. Strong turbulence condition is modeled with help of NE channel model. This FSO system model transmits M copies of the same signal in M different time interval. Outage Probability and BER have been considered for performance analysis and their closed-form mathematical expression have been presented. It is observed that as time diversity order increases the performance gets better. Results are presented for the diversity order of 1, 3, 5, 7, and 9. In the case of outage probability, consistent improvement of 20 dB is observed as diversity order increases. The maximum improvement of 80 dB is observed with a diversity order of 9 compared to no diversity case. A similar improvement is also observed in the case of BER with time diversity. Deployment of diversity has shown the improvement in BER performance. For the BER of 10^{-4}, required SNR is observed around 19 dB observed with a diversity order of 9. The observed SNR is 23 dB, 30 dB and 42 dB for the diversity order of 3, 5 and 7, respectively for the BER of 10^{-4}. Results have shown significant improvement in the outage probability and BER with time diversity. On the other hand, a drastic reduction in the maximum effective bit rate is observed with time diversity.

Deployment of time diversity on FSO system under moderate to strong turbulence condition is reported by Nistazakis (Nistazakis, 2012). Turbulence condition is characterized using Gamma-Gamma channel model. Results are demonstrated for the link distance of 1 km and 2 km with a diversity order of 1 to 5 with the step of 2. Presented system was operating at 1550 nm wavelength with receiver aperture diameter of 10 mm. Outage probability has been considered for performance analysis of FSO system. A maximum of 50 dB improvement in the outage probability is observed with diversity order 5 compared to no diversity case under moderate turbulence condition for both the link length of 2 km. At a shorter distance of 1 km, the observed improvement is two times under moderate turbulence scenario compared to turbulence condition. A consistent improvement of 30 dB is observed in the outage probability under strong turbulence at distance of 1 km as diversity order increases from no diversity case. The similar result is observed at the distance of 2 km. The steady improvement of 20 dB is observed in the outage as diversity order goes from 1 to 5 in the step of 2.

Both of the above literature show that time diversity improves the performance of FSO system, but it significantly reduces the data rate of deployed FSO system. Apart from this, time diversity demands same signal's multiple copies need to be transmitted in a different time interval, which demands large memory. The performance of this scheme can be further improved by using it in conjunction with different error control coding (F. Xu, 2008). However, this solution introduces long delay latencies and requires a huge amount of memory to store data. Apart from this, using of coding technique with time diversity may demand additional circuitry of interleavers, encoder and decoder.

2.6.5.2 Spatial Diversity

Spatial diversity in the FSO can be realized with multiple antennas either on the transmitter side, receiver side or at both the places. Transmission of information through multiple antenna overcomes the disadvantage of temporary blockage of FSO signal and it is also helpful to mitigate atmospheric turbulence effects.

Initially, this concept for FSO was realized by Ibrahim (Ibrahim, 1996). The performance of FSO link has been analyzed with multiple antennas at the receiver side. SC and EGC used at the receiver to combine different incoming signal. Highest improvement in Carrier-to-noise ratio (CNR) is observed for selection combining method. The observed improvement in the availability is of 7% with two branches (M=2) diversity compared to no diversity case (M=1) at particular threshold value with SC method. An optimum spacing between two diversity channels is also identified in this work. Presented results show that few centimeter spacing between two channels is sufficient. For example, the spacing between two detectors should be in between 7 cm to 50 cm for the link range of 10 km. This estimation of spacing between two detectors makes implementation of spatial diversity feasible in the FSO.

Spatial diversity with multiple antenna at receiver and transmitter to mitigate turbulence effect is investigated in (Shin, 2002). Derivation of outage probability of system with OC and EGC method is presented. Results are demonstrated for low-to-moderate turbulence condition in form of power gain analysis. Turbulence condition is realized with lognormal channel model. Results have shown that received power gain increases with the higher number of channel compared to single channel system. It is observed that obtained power gain is higher in moderate turbulence condition compared to lower turbulence condition. A comparison of power gain with OC and EGC methods is also presented. It is also observed that performance of OC and EGC is quite similar except in the deep fading case. In the deep fading case performance of OC is slightly better than EGC. Results have shown that higher number of the channel increases power gain of the system but, it increases background noise in proportion to a number of channels. This overcomes the advantage of power gain with a higher number of channel. Authors have also found that performance improvement by spatial diversity with very less number of channel is possible only under clear to moderate atmospheric turbulence condition.

A performance analysis of FSO link with spatial diversity under strong turbulence is performed by Tsiftsis (Tsiftsis, 2009). Strong turbulence scenario is realized by using

K channel model. Spatial diversity applied at both the end, which is also referred as Multiple Input Multiple Output (MIMO). An approximated closed form equation of average BER is derived for Single Input Multiple Output (SIMO) case. The performance analysis of FSO system with Multiple Input Single Output (MISO) is also demonstrated. Presented results again validate the use of spatial diversity to increase the performance of FSO link under strong turbulence condition. Fig. 2.12 shows the result of the BER performance of FSO link with MISO case. This graph is plotted for α = 4 using [(Tsiftsis, 2009), Eq. 21, with no of receiver = 1]. Where α represents an effective number of scattering in the K distribution.

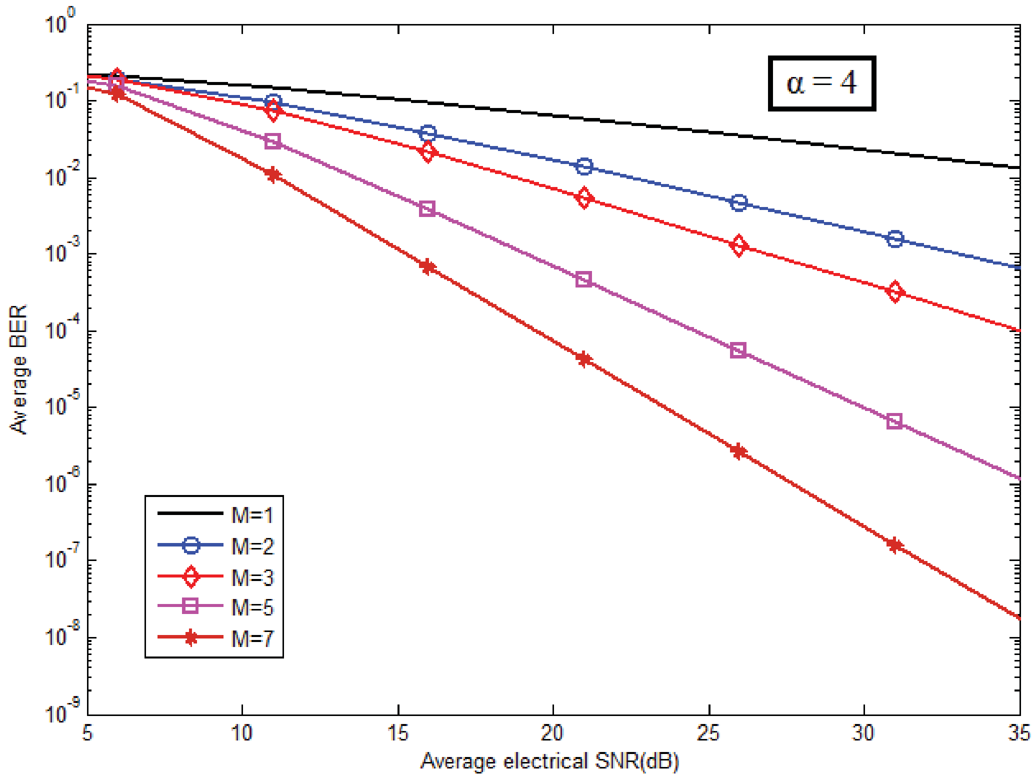

Fig. 2.12 Performance of FSO link with MISO diversity

From Fig. 2.12, it is evident that as a number of transmitting antenna increases the BER performance of the system is also improved. A major improvement in the BER performance is observed with higher diversity order (M= 5 and M=7). The observed improvement in the BER is 40 dB and 50 dB at SNR of 26 dB for diversity order of 5 and 7, respectively compared to M =1 (no diversity case). A marginal improvement of 10-12 dB is observed in the case of the diversity order of 2 and 3. Still, the achieved

BER is in the range of 10^{-2} to 10^{-3} at SNR of 26 dB. Similar results were observed for the higher value of α.These results also indicate that significant improvement in the BER performance is obtained with diversity order more than 5 in the case of MISO. So, the performance improvement is achieved with higher diversity order overwhelms by very high cost and complexity of the system.

From the above mention literature, it is very clear that spatial diversity improves the performance of FSO system in all turbulence conditions, from weak to strong. However, significant improvement in the performance observed with high diversity order (more than 5) in the case of strong and moderate turbulence condition. Deployment of FSO system with higher spatial diversity may not feasible in all geographical conditions. This also adds complexity and cost to the system.

2.6.5.3 Wavelength Diversity

Wavelength diversity has been seen as an attractive option to mitigate turbulence effect. In this method, information is transmitted on more than one wavelength at the same time. Transmission of the information signal on multiple wavelengths at the same time also increases the availability of FSO link. Basically, wavelength diversity is taking advantage of fact that each wavelength is immune to certain atmospheric particle. The combination of that wavelength in the deployment of diversity will make FSO system robust in all atmospheric conditions.

A preliminary investigation on the feasibility of wavelength diversity for the performance improvement of FSO system is presented in (Giggenbach, 2006). Theoretical and numerical analysis of the wavelength diversity effect on FSO system is reported. 840 nm and 1550 nm wavelengths were chosen for wavelength diversity. Their analysis has confirmed the feasibility of wavelength diversity during day and night time both. An attractive outcome of this study is that transmission of multiple wavelengths from the single terminal is feasible.

An investigation of wavelength diversity to improve the FSO link performance under fog condition is performed by Wainright (Wainright, 2005). The entire study was performed under lab conditions with simulation software - PcModWin by on Tar

Corporation. 850 nm, 1000 nm and 1550 nm wavelengths were considered for wavelength diversity. Their simulation results have shown significant improvement in the performance FSO under fog condition.

The performance evaluation of FSO system with wavelength diversity under weak turbulence is examined in (V.Xarcha, 2012). Weak turbulence scenario is realized by lognormal channel model and three wavelengths (850 nm, 1310 nm and 1550 nm) were considered for wavelength diversity. OC method was used to combine signal of a different wavelength at receiver. The performance of FSO is analyzed in term of outage probability and average BER. Results are presented for the link length of 1 km and 1.5 km. It is observed that increasing diversity order has gained significant improvement in the performance of FSO system at both the distance. An improvement of around 40 dB in the outage probability and 50 dB in average BER at SNR of 15 dB is observed at the distance of 1 km with diversity order of 3, compared to no diversity case. The similar was observed of about 30 dB at 1.5 distance for outage probability and average BER.

From the above research, it is clear that wavelength diversity has tremendous potential to improve the performance of FSO system. It also capable of improving performance even in fog condition, which has drawn a lot of attention towards implementation of wavelength diversity based FSO system. An existing research has addressed the performance improvement of FSO system under weak turbulence, moderate turbulence and fog conditions. This gives an opportunity to investigate and analyze the performance of FSO link under strong turbulence condition. Moreover, optimum wavelength diversity order for performance improvement is also unidentified.

2.7 Comparison of Turbulence Mitigation Techniques

Deployment of wavelength diversity for the performance improvement of FSO system has more advantage than other mitigation techniques. Use of multiple wavelengths to transmit information signal makes this scheme more attractive and robust to overcome adverse effect of atmospheric conditions. Moreover, it does not require large aperture size like in the case of aperture averaging. Further, it also does not require large memory and large latency, which is must in the case of time diversity. This technique has potential to improve the performance of FSO system under all atmospheric turbulence without any incorporation of another method, unlike AO. Apart from this, AO almost fails to improve the performance under strong turbulence scenario. Similarly, there is no significant improvement observed by aperture averaging under weak turbulence condition. Spatial diversity can also be considered as a viable option to overcome adverse turbulence effect. But it requires at least more than 5 sets of transceivers for the significant improvement in the performance of FSO. This comparison reveals that wavelength diversity is a prime applicant to mitigate turbulence effect in FSO system. The summary of different turbulence condition is shown in Table 2.5.

Table 2.5 Summary of different turbulence mitigation techniques

Mitigation Technique	**Advantages**	**Disadvantages**
Aperture Averaging	• Single pair of transceiver is required	• Large size of receiver aperture is required, which adds more background noise • Performance is not impressive under weak turbulence condition
Adaptive Optics	• Real-time distorted wavefront measurement • Real-time wavefront error correction	• Performance of wavefront measurement sensor is very poor under strong turbulence • Demands large aperture receiver • High implementation cost
Error Correcting Coding	• Single pair of transceiver is required • Applicable to all turbulence conditions	• Large memory require • Large interleave, encoder and decoder require • Add latency
Hybrid RF/FSO	• The robust solution for fog and rain condition. • Avoid temporary link blockage	• Inefficient utilization of channel bandwidth • Continuous switching may bring system down • Highly complex and costly solution
Time diversity	• Single pair of transceiver is required	• Lower effective bit rate • Long delay latencies

	• Applicable in all-weather conditions	• Require large memory and additional circuitry
Spatial diversity	• Avoid temporary link blockage • Acceptable performance in different turbulence conditions.	• More than 5 transceiver pairs required for improvement in strong turbulence. • Highly complex and costly
Wavelength Diversity	• Use of different wavelength gives immunity under different weather conditions like rain, fog, etc. • Capable of improving performance in different turbulence conditions	• Complex transmitter design • Increase cost and complexity moderately compare to other mitigation techniques.

2.8 Conclusion

In this chapter, working and classification of FSO system are discussed. A comparison of FSO system with existing technology is presented. Various challenges of FSO with the possible solutions are reported. It is found that atmospheric turbulence is a major challenge to FSO system, as it can occur even in clear weather condition. The performance of FSO is badly hampered under atmospheric turbulence condition. So, various turbulence mitigation techniques are discussed with their advantages and limitations. After the detailed study of the different turbulence mitigation techniques, wavelength diversity is identified to improve the performance of FSO system under different atmospheric turbulence condition. Further, use of this method to improve the performance of FSO system under weak to moderate turbulence conditions is only reported till date. The performance improvement of FSO system under strong turbulence using this method is not investigated yet as per my best knowledge. Also, an adequate diversity order to improve the performance of FSO under different turbulence condition is still an open problem. Both of these issues are addressed in this thesis.

Chapter 3

Performance Evaluation of FSO system with Wavelength Diversity under Strong Turbulence Conditions

Atmospheric turbulence is a major threat to the FSO system. It causes random fluctuation in the phase and intensity of signal passing through free space which degrades the quality of received signal. This situation occurs even in clear weather condition. Therefore, it is necessary to encounter this challenge. The strength of atmospheric turbulence varies from weak to strong. Preliminary investigation on the performance of FSO system under weak turbulence with wavelength diversity is already reported. But, the impact of wavelength diversity on the working of FSO link under strong turbulence is still needed to be examined. In this chapter, the performance of FSO system under strong turbulence with wavelength diversity is explored. The FSO channel under strong turbulence condition is characterized using K channel model. The performance is evaluated in terms of Average BER and outage probability. In this work, source information transmitted onto three carrier wavelengths are combined using three different methods: OC, EGC and SC. Mathematical expressions are derived for the calculation of the BER for all the three combining schemes. The obtained average BER results of these combining methods at the different link distance are also compared. Further, an outage probability of FSO system with wavelength diversity is analyzed by deriving an approximated closed-form mathematical expression considering OC and SC method at receiver. Finally, the average BER results of this system are compared with the published article on spatial diversity.

3.1 System Model

FSO system model with wavelength diversity is shown in Fig. 3.1. In this model, the composite transmitter transmits same information signal on different wavelengths towards different receivers. Each of the receivers is capable of receiving signal of a particular wavelength only. The signal received by the different receiver is combined with a proper combining method in the combining section. OC, EGC and SC are the available signals combining methods in the field of wireless communication. After applying any of these methods, the signal is given for the post-detection process. It is established that transmission of multiple wavelengths from one terminal is feasible (Giggenbach, 2006) and spacing of few centimeters between receivers gives independent fading to each received signal (K. P. Peppas, 2012), (Ibrahim, 1996). These facts justify the feasibility of this system model.

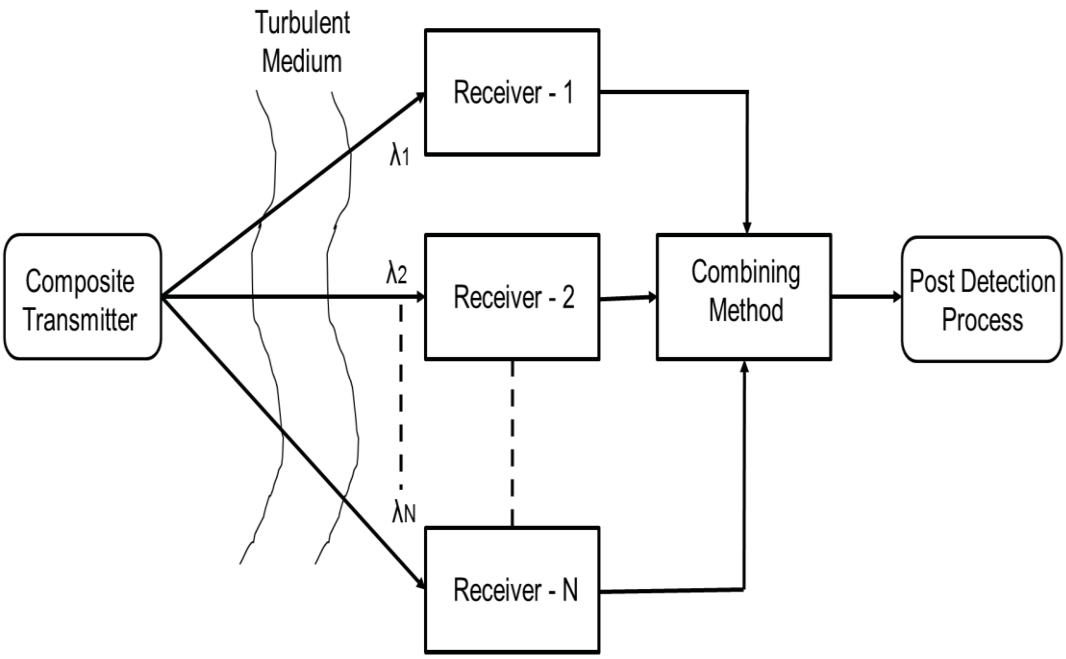

Fig. 3.1 FSO system model with wavelength diversity

Considering this model, the expression of the FSO channel model with wavelength diversity is written as

$$y_w = h_w x + n = \eta_w x I_w + n, \ w = 1, \dots, W \tag{3.1}$$

where, y_w is the output signal at each of W^{th} receivers, $h_w = \eta_w I_w$ is the intensity gain, η_w represents the conversion ratio of the photon to electric current of each receiver, x represents the modulated bit. For this case, OOK modulation has been considered. So, the value of x could be '0' or '1'. Here, n represents the Additive White Gaussian Noise (AWGN) with zero mean and variance $N_0/2$ and I_w is the normalized irradiance ($E[I_w] = 1$) seen at each receiver. The value of irradiance is estimated by considering an adequate channel model as per turbulence strength. K channel is found most suitable to represent strong turbulence condition.

3.2 K Channel Model

In strong turbulence condition, scintillation index is 1 and the value of log intensity variance is varied between 3 and 4. K-Channel model is a well-accepted model to represent this turbulence condition. It is a product of Exponential model and Gamma model. The PDF for K channel model is derived in chapter 2 which is given as

$$f(I) = \frac{2(\alpha)^{(\alpha+1)/2}}{\Gamma(\alpha)} I^{\frac{\alpha-1}{2}} \mathrm{K}_{\alpha-1}\left(2\sqrt{\alpha I}\right),\ I > 0 \tag{3.2}$$

where, α is channel parameter related to the effective number of discrete scatters, I is the normalized irradiance (i.e. $E[I] = 1$), $\Gamma(.)$ is the well-known Gamma function and $\mathrm{K}_v(.)$ is the v^{th} order modified Bessel function of the second kind. When $\alpha \to \infty$, Eq. (3.2) approaches the negative exponential (NE) distribution.

The PDF of the normalized irradiance of K channel after applying wavelength diversity is expressed as

$$f_{I_w}(I_w) = \frac{2(a_w)^{(a_w+1)/2}}{\Gamma(a_w)} I_w^{\frac{a_w-1}{2}} K_{a_w-1}\left(2\sqrt{a_w I_w}\right),\ I_w > 0 \tag{3.3}$$

where, a_w and I_w are the channel parameters related to the effective number of discrete scatters and normalized irradiance with respect to w^{th} wavelength channel. $K_v(.)$, modified Bessel function is written in terms of the Meijer G-function ((Prudnikov, 1988), Eq. (8.4.23.1)).

$$K_v(x) = \frac{1}{2} G_{0,2}^{2,0}\left(\frac{x^2}{4} \middle| \begin{matrix} - \\ \frac{v}{2}, \frac{-v}{2} \end{matrix}\right) \tag{3.4}$$

The Cumulative Density Function (CDF) of $I_w$can be easily derived by

$$F_{I_w}(I_w) = \int_0^\infty f_{I_w}(I_w) dI_w \tag{3.5}$$

After the integration, the final CDF is written as

$$F_{I_w}(I_w) = \int_0^\infty \frac{2(a_w)^{(a_w+1)/2}}{\Gamma(a_w)} I_w^{\frac{a_w-1}{2}} K_{a_w-1}\left(2\sqrt{a_w I_w}\right) dI_w \tag{3.6}$$

The second-order modified Bessel function $K_v(.)$ in terms of the Meijer G-function is written as (Wolfram, 2016) $K_v(x) = \frac{1}{2} G_{0,2}^{2,0}\left(\frac{x^2}{4}\middle|_{\frac{v}{2},\frac{-v}{2}}^{-}\right)$ Here, $v = a_w - 1$ and $x = 2\sqrt{a_w I_w}$. So, $\frac{v}{2} = \frac{a_w-1}{2}$, $\frac{-v}{2} = \frac{-(a_w-1)}{2}$ and $\frac{x^2}{4} = a_w I_w$. Based on this, $F_{I_w}(I_w)$ is written as

$$F_{I_w}(I_w) = \int_0^\infty \frac{2(a_w)^{\frac{(a_w+1)}{2}} (I_w)^{\frac{(a_w+1)}{2}-1}}{\Gamma(a_w)} \left[\frac{1}{2} G_{0,2}^{2,0}\left(a_w I_w \middle|_{\frac{a_w-1}{2},\frac{-(a_w-1)}{2}}^{-}\right)\right] dI_w$$

Which is rearranged as

$$F_{I_w}(I_w) = \int_0^\infty \frac{(a_w I_w)^{(a_w+1)/2}}{\Gamma(a_w)} I_w^{0-1} G_{0,2}^{2,0}\left(a_w I_w \middle|_{\frac{a_w-1}{2},\frac{-(a_w-1)}{2}}^{-}\right) dI_w \tag{3.7}$$

Eq. (3.7) is further simplified by applying variable separation method as shown in Eq. (3.8)

$$Z^t G_{p,q}^{m,n}\left(Z\middle|_{b_1,\ldots,b_m,\, b_{m+1},\ldots,b_q}^{a_1,\ldots,a_n,\, a_{n+1},\ldots,a_p}\right) = G_{p,q}^{m,n}\left(Z\middle|_{b_1+t,\ldots,b_m+t,\, b_{m+1}+t,\ldots,b_q+t}^{a_1+t,\ldots,a_n+t,\, a_{n+1}+t,\ldots,a_p+t}\right) \tag{3.8}$$

Applying variable separation method to Eq. (3.7) (where, $Z = a_w I_w$ and $t = (a_w + 1)/2$), the resultant equation is written as

$$F_{I_w}(I_w) = \int_0^\infty \frac{I_w^{0-1}}{\Gamma(a_w)} G_{0,2}^{2,0}\left(a_w I_w \middle|_{\frac{a_w-1}{2}+\frac{(a_w+1)}{2},\ \frac{-(a_w-1)}{2}+\frac{(a_w+1)}{2}}^{-}\right) dI_w \tag{3.9}$$

which is further expressed in the simplified form as

$$F_{I_w}(I_w) = \int_0^\infty \frac{I_w^{0-1}}{\Gamma(a_w)} G_{0,2}^{2,0}\left(a_w I_w \middle|_{a_w,1}^{1}\right) dI_w \tag{3.10}$$

The integration of single Meijer-G function can be performed as (Wolfram, 2016)

$$\int_0^\infty Z^{x-1} G_{p,q}^{m,n}\left(Z\middle|_{b_1,\ldots,b_m,\, b_{m+1},\ldots,b_q}^{a_1,\ldots,a_n,\, a_{n+1},\ldots,a_p}\right) = G_{p+1,q+1}^{m,n+1}\left(Z\middle|_{b_1+x,\ \ldots,\ b_m+x,\ 0,\ b_{n+1}+x,\ \ldots,\ b_q+x}^{1,\ a_1+x,\ \ldots,\ a_n+x,\ a_{n+1}+x,\ \ldots,\ a_p+x}\right)$$

here, $x = 0$, Applying integration on Eq. (3.10), the CDF of K channel with wavelength diversity is derived as

$$F_{I_w}(I_w) = \frac{1}{\Gamma(a_w)} G_{0+1,2+1}^{2,0+1}\left(a_w I_w \middle|_{a_w+0,1+0,0}^{1}\right) \tag{3.11}$$

Finally, the CDF of K channel with wavelength diversity is written as

$$F_{I_w}(I_w) = \frac{1}{\Gamma(a_w)} G_{1,3}^{2,1}\left(a_w I_w \middle|_{a_w,1,0}^{1}\right) \tag{3.12}$$

Now, the scintillation index (*SI*) is calculated by using

$$SI \triangleq \frac{E[I_w{}^2]-E^2[I_w]}{E^2[I_w]} = \frac{a_w+2}{a_w} \tag{3.13}$$

where $E[.]$ gives the expected value of the enclosed. Since *SI* depends on the parameter a_w, it can be seen that the turbulence is stronger for lower values of a_w and gets weaker as a_w increases. The instantaneous electrical SNR can be defined as $\gamma_w = \frac{(\eta_w I_w)^2}{N_0}$ and the average electrical SNR is defined as, $\mu_w = \frac{(\eta_w E[I_w])^2}{N_0}$. Here, $E[I_w] = 1$, since I_w is normalized. After a power transformation of the random variable $I_w = \sqrt{\frac{\gamma_w}{\mu_w}}$, the PDF for the instantaneous electrical SNR, γ_w is derived as

$$f_{\gamma_w}(\gamma_w) = \frac{(a_w)^{\frac{a_w+1}{2}}(\gamma_l)^{\frac{a_w-3}{4}}}{\Gamma(a_w)(\mu_w)^{\frac{a_w+1}{4}}} \mathrm{K}_{a_w-1}\left(2\sqrt{a_w\sqrt{\frac{\gamma_w}{\mu_w}}}\right), \ \gamma_w > 0 \tag{3.14}$$

And the corresponding CDF of the instantaneous electrical SNR γ_w is

$$F_{\gamma_w}(\gamma_w) = \frac{1}{\Gamma(a_w)} G_{1,3}^{2,1}\left(a_w\sqrt{\frac{\gamma_w}{\mu_w}} \middle|_{a_w,1,0}^{1}\right) \tag{3.15}$$

3.3 Performance Metric of FSO Channel

The performance analysis of FSO system is investigated by finding average BER and outage probability of the FSO link. Both of these parameters help to decide availability and reliability of FSO link. This section discusses the method to find out both the parameters.

3.3.1 Average BER

The BER of FSO systems with on-off keying (OOK) modulation, in the presence of AWGN, can be estimated from the following expression

$$P_e = p(0)P(e|0) + p(1)P(e|1) \tag{3.16}$$

here, $p(0)$ and $p(1)$ is being the probabilities of transmitting the bit "0" and "1", respectively. On the other hand, $P(e|0)$ and $P(e|1)$ represent the conditional bit-error probabilities for the transmitted bit. Assuming that the problem is symmetric, i.e. $p(0)$ = $p(1)$ = 0.5, and $P(e|0)$ = $P(e|1)$, the BER is estimated as a function of I, as

$$P(I) = P(e|1, I) + P(e|0, I) = P\left(n > \frac{\eta I}{2}\right) = P\left(n > \frac{-\eta I}{2}\right) = Q\left(\frac{\eta I}{\sqrt{2N_0}}\right) \tag{3.17}$$

where, Q(.) is the Gaussian Q-function defined as $Q(x) = \left(\frac{1}{\sqrt{2N_0}}\right)\int_x^{\infty} exp\left(\frac{t^2}{2}\right)dt$ and it is related to the complimentary error function $erfc(.)$ by $erfc(x) = 2Q(\sqrt{2}x)$. The average BER P_{av} , is derived by averaging Eq. (3.17) over I

$$P_{av} = \int_0^{+\infty} P(I)\,f(I)dI = \frac{1}{2}\int_0^{+\infty} erfc\left(\frac{(\eta I)}{2\sqrt{No}}\right)f(I)dI \tag{3.18}$$

3.3.2 Outage Probability

Outage probability of the system defines the availability of the channel. This is particularly a significant metric for any wireless link since it represents the probability that the instantaneous SNR at the receiver's input falls below a critical threshold, γ_{th}, which corresponds to the receiver's sensitivity limit (Nistazakis, 2013). Outage probability of the system is expressed as

$$P_{out} = \mathrm{P}_r(\gamma \leq \gamma_{th}) = F_\gamma(\gamma_{th}) \tag{3.19}$$

In the next section, Mathematical expressions of both average BER and outage probability are derived considering wavelength diversity for FSO link under strong turbulence condition.

3.4 Average BER of FSO System with Wavelength Diversity

This section presents the mathematical derivation of Average BER with and without diversity scenario. Firstly, the average BER for Single Input Single Output (SISO) link with no diversity case is derived. Following a similar approach, the average BER considering wavelength diversity is derived. For the wavelength diversity case, the expression of average BER is obtained considering OC, EGC and SC.

The average BER for SISO link of the FSO system, P_{av} is obtained by averaging Eq. (3.18) over I, i.e.

$$P_{av} = \int_0^{+\infty} P(I) f_I(I) dI = \int_0^{+\infty} Q\left(\frac{\eta I}{\sqrt{2N_0}}\right) f_I(I) dI = \int_0^{+\infty} f_I(I)\left[\frac{1}{2} erfc\left(\frac{\eta I}{2\sqrt{N_0}}\right)\right] dI \tag{3.19}$$

After placing the PDF of K channel model in Eq. (3.19), the average BER for SISO link of the FSO system is written as

$$P_{av} = \int_0^{+\infty} \frac{2(\alpha)^{(\alpha+1)/2}}{\Gamma(\alpha)} I^{\frac{\alpha-1}{2}} \mathrm{K}_{\alpha-1}\left(2\sqrt{\alpha I}\right)\left[\frac{1}{2} erfc\left(\frac{\eta I}{2\sqrt{N_0}}\right)\right] dI \tag{3.20}$$

The above integral can be expressed by the second kind of, v_{th} order modified Bessel function, $K_v(.)$ and complimentary error function $erfc(.)$ as Meijer G-functions ($erfc\left(\sqrt{x}\right) = \frac{1}{\sqrt{\pi}} G_{1,2}^{2,0}\left(x|_{0,1/2}^{1}\right)$). Thus, (3.20) is expressed as

$$P_{av} = \int_0^{\infty} \frac{(\alpha I)^{(\alpha+1)/2}}{\Gamma(\alpha)} I^{0-1} G_{0,2}^{2,0}\left(\alpha I|_{\frac{\alpha-1}{2}, \frac{-(\alpha-1)}{2}}^{-}\right) \times \frac{1}{2}\left[\frac{1}{\sqrt{\pi}} G_{1,2}^{2,0}\left(\frac{(\eta I)^2}{4N_0}|_{0,1/2}^{1}\right)\right] dI \tag{3.21}$$

Applying variable separation method (as per Eq. (3.8)), the Eq. (3.21) is rewritten as

$$P_{av} = \int_0^{\infty} \frac{I^{0-1}}{2\sqrt{\pi}\Gamma(a)} G_{0,2}^{2,0}\left(aI|_{a,}{}^{1}{}_{1}\right) G_{1,2}^{2,0}\left(\frac{(\eta I)^2}{4N_0}|_{0,1/2}^{1}\right) dI \tag{3.21}$$

Eq. (3.21) is rearranged as

$$P_{av} = \int_0^{\infty} \frac{I^{0-1}}{2\sqrt{\pi}\Gamma(a)} \left[G_{0,2}^{2,0}\left(aI|_{a,}{}^{1}{}_{1}\right)\right]\left[G_{1,2}^{2,0}\left(\frac{(\eta)^2}{4N_0} I^{\frac{2}{1}}|_{0,1/2}^{1}\right)\right] dI \tag{3.22}$$

After integration, the final expression of average BER for FSO link without diversity is written as

$$P_{av} = \frac{(2)^{(a-2)}}{\sqrt{\pi^3}\Gamma(a)} G_{5,2}^{2,4}\left(\frac{4\eta^2}{N_0 a^2} \middle| \begin{matrix} \frac{1-a}{2}, \frac{2-a}{2}, 0, \frac{1}{2}, 1 \\ 0, \frac{1}{2} \end{matrix}\right) \tag{3.23}$$

In terms of the average electrical SNR of the SISO system μ, (3.23) is expressed as

$$P_{av} = \frac{(2)^{(a-2)}}{\sqrt{\pi^3}\Gamma(a)} G_{5,2}^{2,4}\left(\frac{4\mu}{a^2} \middle| \begin{matrix} \frac{1-a}{2}, \frac{2-a}{2}, 0, \frac{1}{2}, 1 \\ 0, \frac{1}{2} \end{matrix}\right) \tag{3.24}$$

For the wavelength diversity case, the average BER of proposed FSO system model is derived by considering one transmitter and W receivers, which is clearly comparable to a single input multiple outputs (SIMO) optical communication system. In this case, the optimum decision metric for OOK will be given by

$$P(\vec{y}|off, I_w) \underset{on}{\overset{off}{\lesseqgtr}} P(\vec{y}|on, I_w) \tag{3.25}$$

where, $\vec{y} = (y_1, y_2, \dots, y_W)$ is the vector signal with W components arriving at the receivers of the wavelength diversity FSO system.

Considering this system model, the mathematical expression for the average BER of wavelength diversity based FSO system is derived using OC, EGC and SC method for combining different signals at the receiver end. The working of these methods is discussed in chapter 2.

3.4.1 Optimal Combining

In the OC method, different diversity branch signals are co-phased and weighted as per their signal strength prior to the combination. Considering this, the BER of the FSO link with wavelength diversity is written as

$$P_{W,OC} = \int_{\vec{I}} f_{\vec{I}}(\vec{I})\, Q\left(\frac{1}{\sqrt{2WN_0}}\sqrt{\sum_{w=1}^{W}(\eta_w I_w)^2}\right) d\vec{I} \tag{3.26}$$

where, $\vec{I} = (I_1, I_2, \dots, I_W)$ is the vector representation of the irradiance of W receivers. In order to integrate (3.26), an approximation for the Q-function is taken ((Wolfram, 2016), Eq. (14)) i.e. $Q(x) \approx \frac{1}{12} exp\left(\frac{-x^2}{2}\right) + \frac{1}{4} exp\left(\frac{-2x^2}{3}\right)$. Substituting this approximation in Eq. (3.26), The BER expression of FSO system with OC method is obtained as

$$P_{W,OC} \approx \frac{1}{12}\prod_{w=1}^{W}\int_0^\infty f_{I_w}(I_w)exp\left(\frac{-(\eta_w I_w)^2}{4WN_0}\right)dI_w + \frac{1}{4}\prod_{w=1}^{W}\int_0^\infty f_{I_w}(I_w)exp\left(\frac{-(\eta_w I_w)^2}{3WN_0}\right)dI_w \quad (3.27)$$

Eq. (3.27) is expressed as an exponential function and represented in the form of Meijer G-function (Wolfram, 2016), $e^{-x} = G_{0,1}^{1,0}(x|\,^{-}_{0})$ to obtain close form of it. After integration, the obtained closed equation for Eq. (3.27) is written as

$$P_{W,OC} = \frac{1}{12}\prod_{w=1}^{W}\left[\frac{2^{(a_w-1)}}{\pi\Gamma(a_w)}G_{4,1}^{1,4}\left(\frac{4{\eta_w}^2}{(a_w)^2 WN_0}\Big|\,^{\frac{1-a_w}{2},\frac{2-a_w}{2},0,\frac{1}{2}}_{0}\right)\right] + \frac{1}{4}\prod_{w=1}^{W}\left[\frac{2^{(a_w-1)}}{\pi\Gamma(a_w)}G_{4,1}^{1,4}\left(\frac{16{\eta_w}^2}{3(a_w)^2 WN_0}\Big|\,^{\frac{1-a_w}{2},\frac{2-a_w}{2},0,\frac{1}{2}}_{0}\right)\right] \quad (3.28)$$

For the average electrical SNR $\mu_w = \frac{(\eta_w E[I_w])^2}{N_0}$, Eq.(3.28) is rewritten as

$$P_{W,OC} = \frac{1}{12}\prod_{w=1}^{W}\left[\frac{2^{(a_w-1)}}{\pi\Gamma(a_w)}G_{4,1}^{1,4}\left(\frac{4\mu_w}{(a_w)^2 W}\Big|\,^{\frac{1-a_w}{2},\frac{2-a_w}{2},0,\frac{1}{2}}_{0}\right)\right] + \frac{1}{4}\prod_{w=1}^{W}\left[\frac{2^{(a_w-1)}}{\pi\Gamma(a_w)}G_{4,1}^{1,4}\left(\frac{16\mu_w}{3(a_w)^2 W}\Big|\,^{\frac{1-a_w}{2},\frac{2-a_w}{2},0,\frac{1}{2}}_{0}\right)\right] \quad (3.29)$$

where, a_w defines the number of discrete scatter of the w_{th} channel and μ_w signifies the average electrical SNR of the w_{th} channel.

3.4.2 Equal Gain Combining

The EGC method is similar to OC with an exception to neglect the weighting circuits. The average BER of the FSO system with W different channel for the case of EGC is expressed as

$$P_W^{EGC} = \int_{\vec{I}} f_{\vec{I}}(\vec{I})\,Q\left(\frac{\sum_{w=1}^{W}\eta_w I_w}{W\sqrt{2N_0}}\right)d\vec{I} \quad (3.30)$$

where, $\vec{I} = (I_1, I_2, \dots, I_W)$ is the vector representation of the irradiance of W receivers. An integration of Eq. (3.30) is obtained by Q function approximation. An approximation of Q function is considered using similar approach as in case of OC (i.e. $Q(x) \approx \frac{1}{12} exp\left(\frac{-x^2}{2}\right) + \frac{1}{4} exp\left(\frac{-2x^2}{3}\right)$). Putting this approximation in Eq. (3.29), the BER expression of FSO system with EGC method at receiver is obtained as

$$P_{W,EGC} \approx \frac{1}{12} \prod_{w=1}^{W} \int_0^{\infty} f_{I_w}(I_w) exp\left(\frac{-(\eta_w I_w)^2}{4W^2 N_0}\right) dI_w \; + \frac{1}{4} \prod_{w=1}^{W} \int_0^{\infty} f_{I_w}(I_w) exp\left(\frac{-(\eta_w I_w)^2}{3W^2 N_0}\right) dI_w \tag{3.31}$$

Representing Eq. (3.31) in exponential form with the Meijer G-function (Wolfram, 2016), $e^{-x} = G_{0,1}^{1,0}(x|\,{}^{-}_{0})$ and performing integration on it, the obtained closed form expression for the average BER considering EGC method is expressed as

$$P_{W,EGC} = \frac{1}{12} \prod_{w=1}^{W} \left[\frac{2^{(a_w-1)}}{\pi\Gamma(a_w)} G_{4,1}^{1,4}\left(\frac{4\eta_w{}^2}{(a_w)^2 W^2 N_0} \,\middle|\, {}^{\frac{1-a_w}{2}, \frac{2-a_w}{2}, 0, \frac{1}{2}}_{0}\right)\right] + \frac{1}{4} \prod_{w=1}^{W} \left[\frac{2^{(a_w-1)}}{\pi\Gamma(a_w)} G_{4,1}^{1,4}\left(\frac{16\eta_w{}^2}{3(a_w)^2 W^2 N_0} \,\middle|\, {}^{\frac{1-a_w}{2}, \frac{2-a_w}{2}, 0, \frac{1}{2}}_{0}\right)\right] \tag{3.32}$$

Finally, Eq. (3.32) is represented in form of average electrical SNR as

$$P_{W,EGC} = \frac{1}{12} \prod_{w=1}^{W} \left[\frac{2^{(a_w-1)}}{\pi\Gamma(a_w)} G_{4,1}^{1,4}\left(\frac{4\mu_w}{(a_w)^2 W^2} \,\middle|\, {}^{\frac{1-a_w}{2}, \frac{2-a_w}{2}, 0, \frac{1}{2}}_{0}\right)\right] + \frac{1}{4} \prod_{w=1}^{W} \left[\frac{2^{(a_w-1)}}{\pi\Gamma(a_w)} G_{4,1}^{1,4}\left(\frac{16\mu_w}{3(a_w)^2 W^2} \,\middle|\, {}^{\frac{1-a_w}{2}, \frac{2-a_w}{2}, 0, \frac{1}{2}}_{0}\right)\right] \tag{3.33}$$

3.4.3 Selection Combining

The general form of selection combining is to monitor all the diversity branches and select the one which has the highest SNR. Therefore, the selection of irradiance and average electrical SNR are made according to

$$I_{SC} = max(I_1, I_2, \ldots, I_w) \tag{3.34}$$

And,

$$\mu_{SC} = max(\mu_1, \mu_2, \ldots, \mu_w) \tag{3.35}$$

The average BER of the FSO system for the case of SC can be obtained as

$$P_{W,SC} = \int_0^\infty f_{I_{SC}}(I_{SC})\, Q\left(\frac{\eta_{SC} I_{SC}}{\sqrt{2WN_0}}\right) dI_{SC} \tag{3.36}$$

where, $f_{I_{SC}}(I_{SC})$ is the PDF of the highest value of the irradiance. The closed form of BER expression in this case is obtained by adopting similar approach as mentioned in the above cases. Applying the similar approach, the closed form expression of the average BER considering SC method in terms of μ_{SC} is written as

$$P_{W,SC} = \frac{1}{12}\prod_{w=1}^{W}\left[\frac{2^{(a_w-1)}}{\pi\Gamma(a_w)} G_{4,1}^{1,4}\left(\frac{4\mu_{SC}}{(a_w)^2 W}\,\middle|\, \begin{matrix}\frac{1-a_w}{2},\frac{2-a_w}{2},0,\frac{1}{2}\\ 0\end{matrix}\right)\right]$$
$$+\frac{1}{4}\prod_{w=1}^{W}\left[\frac{2^{(a_w-1)}}{\pi\Gamma(a_w)} G_{4,1}^{1,4}\left(\frac{16\mu_{SC}}{3(a_w)^2 W}\,\middle|\, \begin{matrix}\frac{1-a_w}{2},\frac{2-a_w}{2},0,\frac{1}{2}\\ 0\end{matrix}\right)\right] \tag{3.37}$$

where, μ_{SC} is the maximum average SNR achieved by the system for the irradiance I_{SC}.

3.4.4 Results and Discussions

The numerical results of average BER of FSO system with wavelength diversity under strong turbulence are presented in this section. For strong turbulence, the refractive index structure parameter $C_n^2 = 2 \times 10^{-13} m^{-2/3}$ is chosen. To apply the wavelength diversity, three wavelengths are chosen as : $\lambda_1 = 1550\ nm$, $\lambda_2 = 1310$ nm, and $\lambda_3 = 850$ nm. The selection of these wavelengths is based on the fact that these wavelengths suffer less attenuation in the atmosphere and components on these wavelengths are readily available in the market (Kaushal, 2017). The BER performance of FSO system using each of these wavelength for diversity less scenario is also presented. The receiver aperture diameter D is kept fixed at 0.01m. The sensitivity threshold and electrical SNR for all the W receivers are considered as identical, i.e., $\mu_1 = \mu_2 = \cdots = \mu_W = \mu$ and $\gamma_{th,1} = \gamma_{th,2} = \cdots = \gamma_{th,W} = \gamma_{th}$. The BER performance of FSO system with different combining techniques at receiver is evaluated for the distance of 2 km and 3 km. The results of all the three combining methods are also compared and discussed.

The BER results of FSO system with a single transceiver operating at different wavelength using Eq. (3.24) is presented in Fig. 3.2 It is apparent from Fig. 3.2 that the performance of FSO link with 1550 nm under strong turbulence is better than other two wavelengths (i.e. 850 nm and 1310 nm). However, the improvement in the BER is achieved with 1550 nm comes at higher values of average electrical SNR (more than 50 dB for BER of 10^{-3}). This reveals that the obtained performance of SISO-FSO link even with a higher wavelength under strong turbulence is not suitable for any practical application. This justifies the need for wavelength diversity also.

The graphs of average BER without and with wavelength diversity using SC, EGC and OC are plotted in Fig. 3.3, Fig. 3.4 and Fig. 3.5, respectively. In these graphs, W = 1, represents without diversity case with an operational wavelength of 1550 nm while W=2 and 3 signify the wavelength diversity order of 2 and 3 respectively. For the diversity of the order of 2, 1550 nm and 1310 nm wavelengths are chosen. The information is transmitted at 1550 nm, 1310 nm and 850 nm in the case of diversity of the order of 3.

Fig. 3.3 illustrate the BER performance of wavelength diversity based FSO system with SC combining method. This graph is plotted from Eq. (3.37). The achieved results show that the use of wavelength diversity improves the performance of FSO system under strong turbulence. The required maximum SNR is 55 dB and 68 dB at distance of 2 km and 3 km, respectively for the BER of 10^{-4} under no diversity case. As diversity order increases the required SNR for the targeted BER is decreases. The decrement of 14 dB in the required SNR is observed for the BER of 10^{-4} at the distance of 2 km with diversity order 3 compared to no diversity case. The same was 19 dB for the distance of 3 km.

Fig. 3.4 represents the performance of wavelength diversity based FSO system with EGC method at the receiver side. It is obtained using Eq. (3.33). The required maximum SNR is 38 dB and 47.5 dB to obtain the BER of 10^{-4} at the distance of 2 km and 3 km, respectively for diversity less case under strong turbulence. The observed

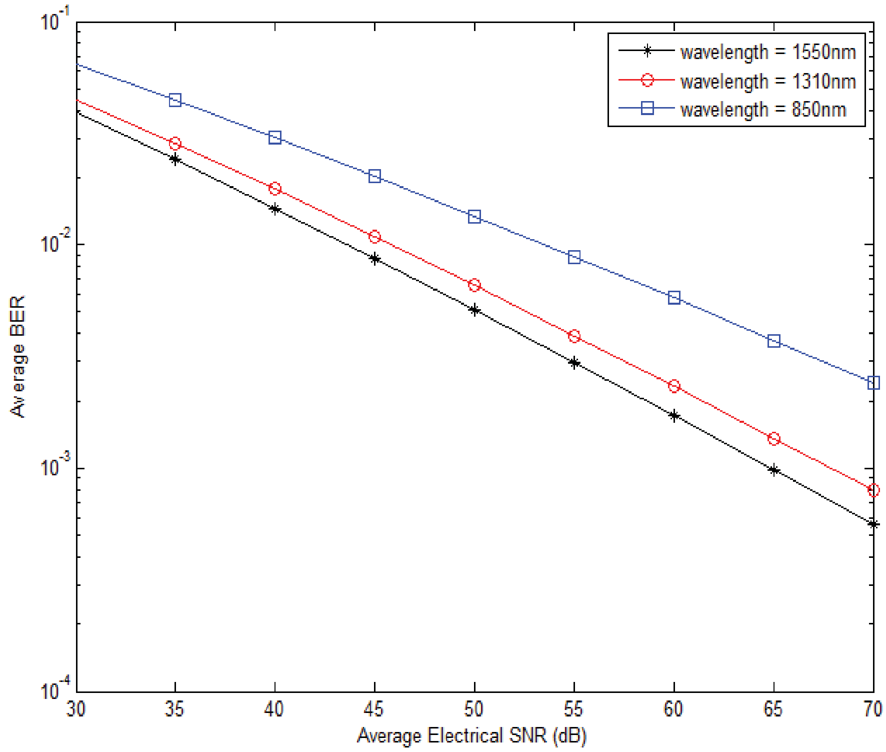

Fig. 3.2 BER performance of SISO-FSO system at different wavelength

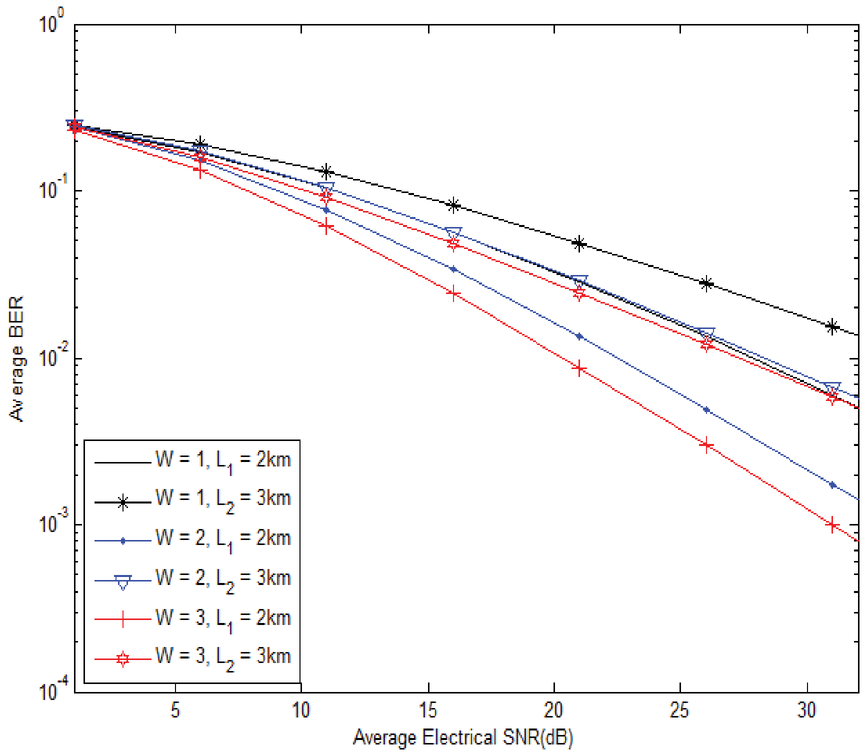

Fig. 3.3 BER performance of FSO system link with SC scheme.

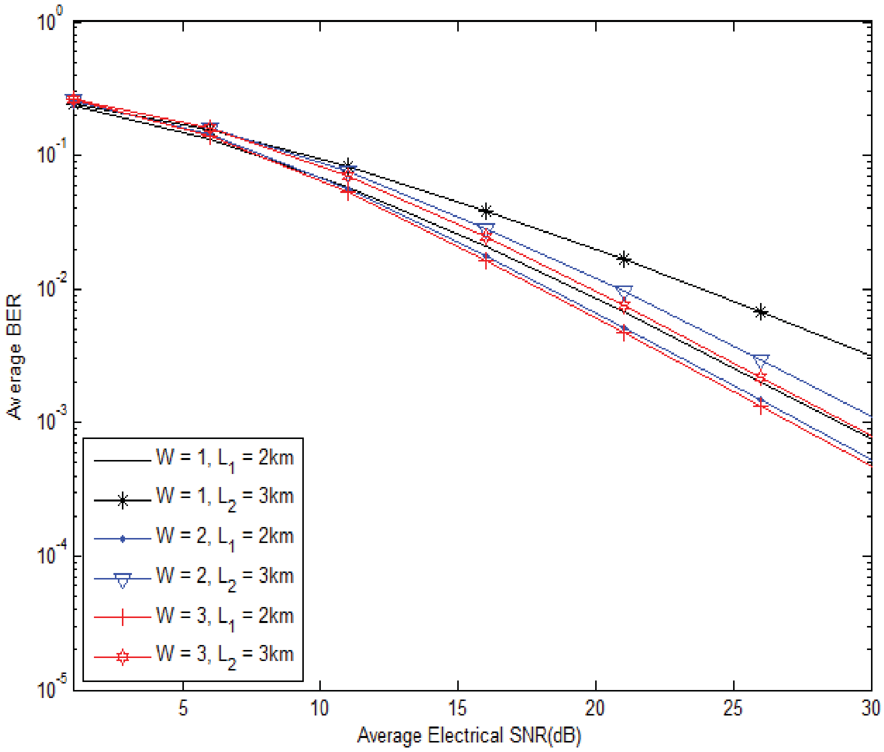

Fig. 3.4 BER performance of FSO system link with EGC method

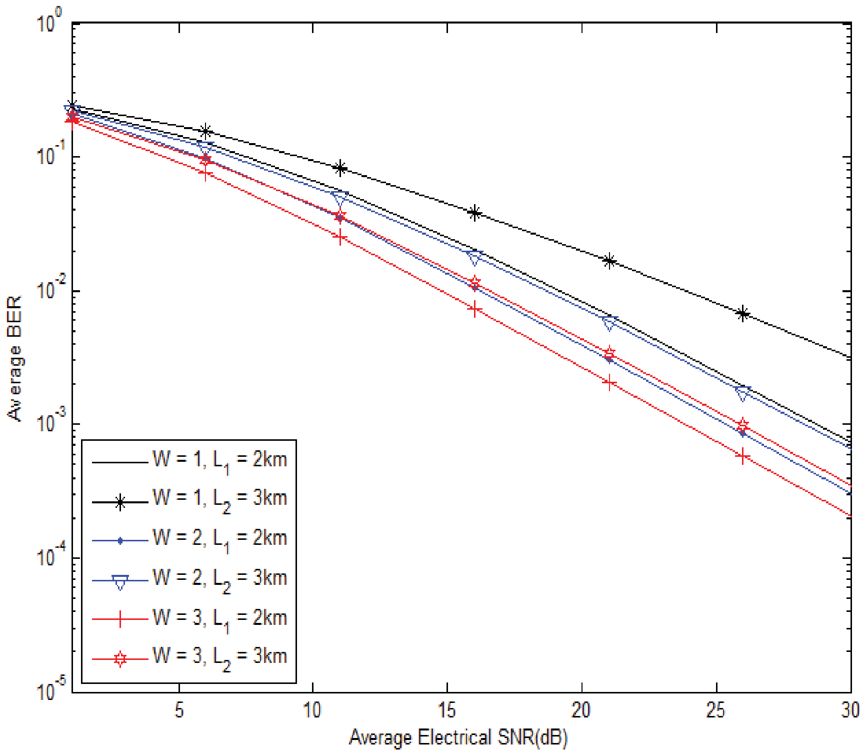

Fig. 3.5 BER performance of FSO system link with OC method

maximum improvement in the SNR for the same BER is 2 dB and 9 dB at distance of 2 km and 3 km, respectively with diversity order 3 compared to no diversity case.

The performance of FSO system considering OC method at receiver is illustrated in Fig. 3.5. These results are determined by Eq. (3.29). The results of OC method is quite similar to EGC method under no diversity case. The SNR of 38 dB is required to get BER of 10^{-4} at the distance of 2 km in without diversity case. The same is of 47.5 dB at the distance of 3 km. The observed maximum improvement in the SNR for the targeted BER is of 5 dB and 12.5 dB at the distance of 2 km and 3 km, respectively. The detailed results of required SNR at the BER of 10^{-4} for all the methods are given in Table 3.1.

Table 3.1 Required SNR at the BER of 10^{-4} for different combining methods

Diversity order	Combining Methods					
	OC		EGC		SC	
	L = 2 km	L = 3 km	L = 2 km	L = 3 km	L = 2 km	L = 3 km
W=1	38 dB	47.5 dB	38 dB	47.5 dB	55 dB	68 dB
W=2	34 dB	37.5 dB	36 dB	39.5 dB	46 dB	57 dB
W=3	33 dB	35 dB	36 dB	38.2 dB	41 dB	49 dB

The achieved results show improvement in the performance of FSO system after applying wavelength diversity in all three schemes. The results also show that the maximum improvement is obtained at a higher distance of 3 km for all the combining methods. A maximum improvement is observed in the case of SC but the required SNR is still very high to consider for any practical application. On the other hand, OC demands less SNR for targeted BER compared to other two techniques.

A performance comparison of all three techniques with a diversity order of 2 at 2 km distance is plotted in Fig. 3.6. It is evident that the OC technique provides the best performance as compared to other techniques. The difference in SNR with respect to the average BER remains almost constant for OC and EGC. The observed difference is around 2 dB. The performance of the SC is poorer compared to other two techniques. This trend continues even at higher distance and diversity order as well.

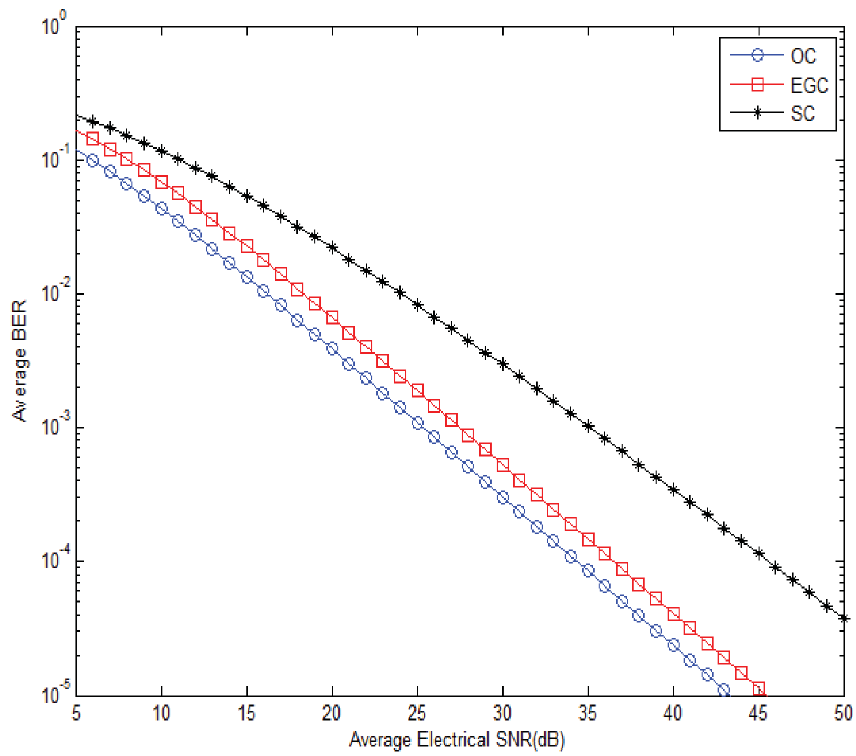

Fig. 3.6 Performance Comparison of OC, EGC and SC scheme with W=2 at 2 km

3.5 Outage Probability of FSO System with Wavelength Diversity

The outage probability of the system is the point after which noise dominates over signal. This provides probability at which the spontaneous SNR falls below the threshold SNR, γ_{th} which is related to the receiver's input sensitivity limit. Using the PDF of K channel with wavelength diversity (Eq. (3.3)) and a basic outage probability expression (Eq. (3.17)), closed form expression of outage probability for FSO system with wavelength diversity has been derived. As the performance of OC and EGC is quite similar, the results are only obtained with OC and SC methods. The mathematical expressions are derived for the same.

3.5.1 Optimal Combining

The outage probability of FSO system with wavelength diversity using optimal combining at receiver is given by

$$P_{out,oc} = \mathrm{P}_r(\gamma_w \leq \gamma_{th,w}) = F_{\gamma_w}(\gamma_{th,w}), \; w = 1, \ldots, W \tag{3.38}$$

Assuming that $P_{out,oc}$ is autonomous for different wavelengths. Then, the FSO system's total outage probability $P_{out,oc}$ of all the W links is given by

$$P_{out,oc} = \prod_{w=1}^{W} P_{out,w} = \prod_{w=1}^{W} Pr(\gamma_w \leq \gamma_{th,w}) = \prod_{w=1}^{W} F_{\gamma_w}(\gamma_{th,w}) \tag{3.39}$$

Putting Eq. (3.11) in Eq. (3.39), the final closed form expression of outage probability with optimal combining is written as

$$P_{out,oc} = \prod_{w=1}^{W}\left[\frac{1}{\Gamma(a_w)} G_{1,3}^{2,1}\left(a_w\sqrt{\frac{\gamma_{th,w}}{\mu_w}}\,\middle|_{a_w,1,0}^{1}\right)\right] \tag{3.40}$$

3.5.2 Selection Combining

To derive outage probability expression using SC, consider the γ_{th} is the threshold value of the SNR. If there are W links then the probability at which the SNR of all the links are lower than the threshold γ_{th} is given by

$$P_{out,sc} = P(max\{\gamma_1, \gamma_2, \ldots \ldots, \gamma_w\}) \tag{3.41}$$

Now,

$$P_{out,sc} = P_r(\gamma \leq \gamma_{th,w}) = F_\gamma(\gamma_{th,w}) = \frac{1}{\Gamma(a_w)} G_{1,3}^{2,1}\left(a_w\sqrt{\frac{\gamma_{th,w}}{\mu_w}}\,\middle|_{a_w,1,0}^{1}\right) \tag{3.42}$$

Assuming P_{out} is independent for the different wavelength channels in the wavelength diversity based FSO system. Then, the total outage probability $P_{out,sc}$ of the FSO system which is taken into account will correspond to the outage probabilities of W independent links with different wavelength. Based on this, the outage probability with SC method is given as

$$P_{out,W}^{SC} = \left[\left[\frac{1}{\Gamma(a)} G_{1,3}^{2,1}\left(a\sqrt{\frac{\gamma_{th}}{\mu}}\,\middle|_{a,1,0}^{1}\right)\right]\quad\right]^{W} \tag{3.43}$$

3.5.3 Results and Discussions

The results of outage probability for FSO system with wavelength diversity considering OC and SC are reported in this section. Results are obtained for the distance of 2 km and 3 km. All the other parameters like wavelengths and receiver aperture size are kept same as in the case of average BER.

Fig. 3.7 demonstrates the outage probability vs. normalized average electrical SNR (μ/γ_{th}), of the FSO system with the wavelength diversity using SC method. This graph is plotted from Eq. (3.43). It is evident from the graph that as the wavelength diversity order increases the outage probability of FSO system decreases. A maximum improvement of 10 dB is observed in the outage probability at the SNR of 30 dB with diversity order of 2 compared to no diversity case at the distance of 2 km. However, increasing diversity order does not bring the improvement in the outage probability of FSO system under strong turbulence. The similar results are observed at the distance of 3 km.

The outage probability of FSO system with wavelength diversity using OC method is shown in Fig. 3.8. It is evident from the graph that the use of wavelength diversity makes outage probability of FSO smaller. The outage probability of FSO system is reduced by 10 dB at the distance of 3 km with diversity order 3 compared to diversity less scenario at SNR of 30 dB. The similar results are observed for the distance of 2 km. The detailed results are shown in Table 3.2.

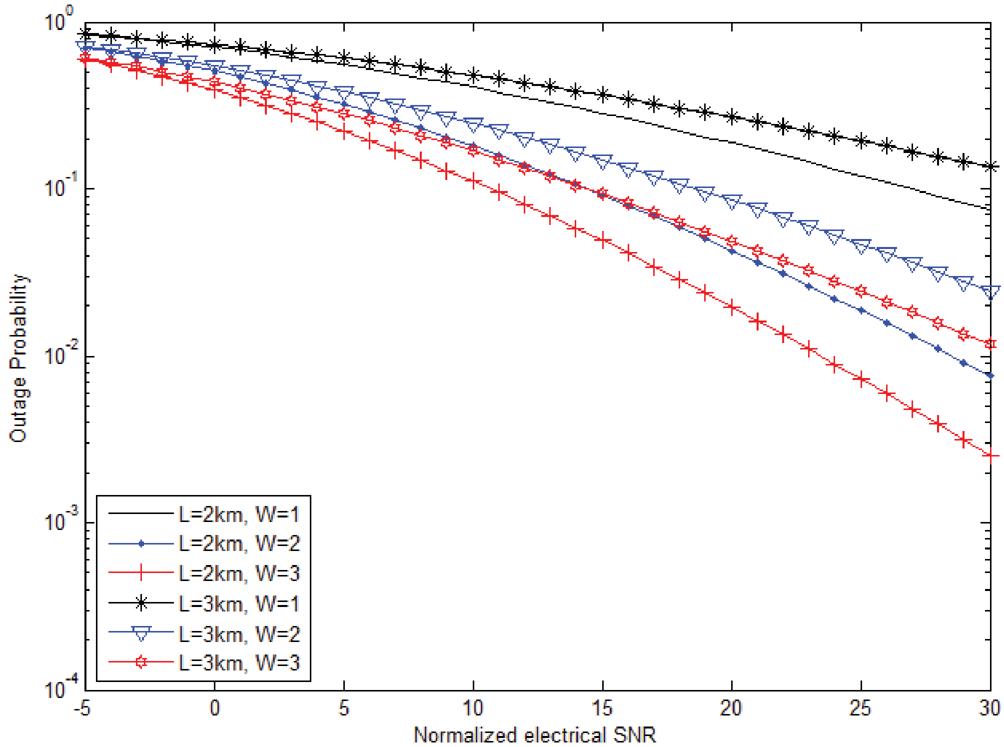

Fig. 3.7 Outage probability of FSO system using SC method

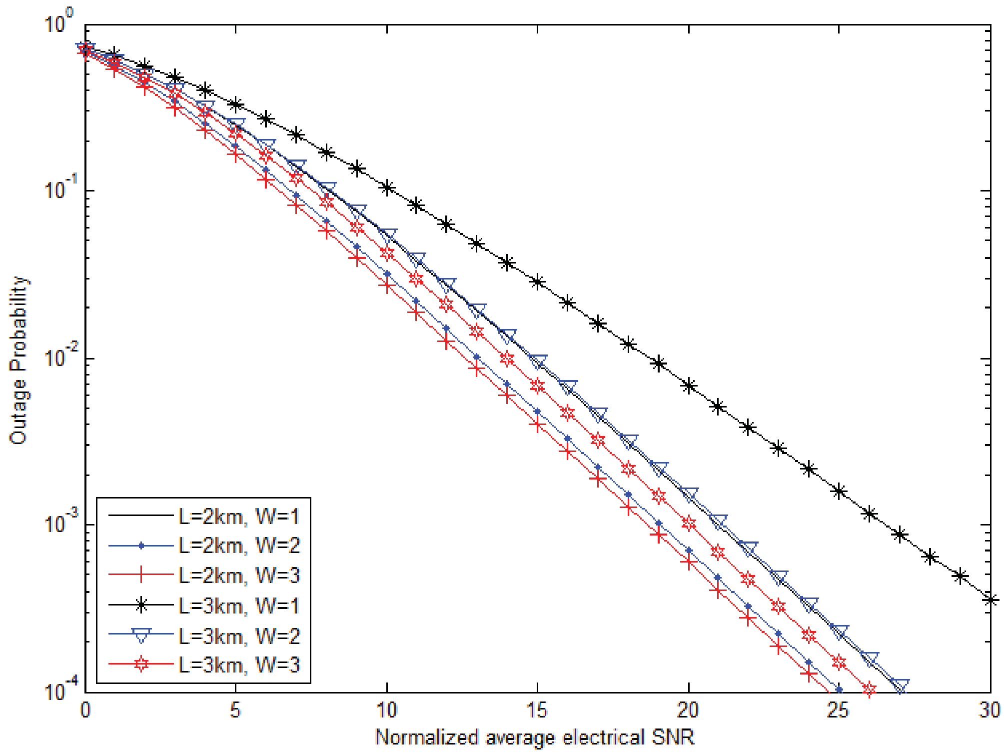

Fig. 3.8 Outage probability of FSO system using OC method

It is evident from Table 3.2 that wavelength diversity reduces the outage probability of FSO system. Both the combining methods, OC and SC have gained an equal improvement of 10 dB in the outage probability with the diversity order of 2 at both the distance compared to no diversity scenario. However, the performance of FSO system with OC method is still better than SC method. It also evident from the Table 3.2 that increase in diversity order from 2 to 3 has not gained significant improvement in the outage probability under strong turbulence scenario.

Table 3.2 Outage probability of FSO system at SNR of 30 dB

Diversity order	Combining Method			
	OC		SC	
	L = 2 km	L = 3 km	L = 2 km	L = 3 km
W=1	0.35×10^{-4}	3.50×10^{-4}	0.74×10^{-1}	1.35×10^{-1}
W=2	1.49×10^{-5}	3.51×10^{-5}	0.77×10^{-2}	2.44×10^{-2}
W=3	1.28×10^{-5}	2.71×10^{-5}	0.25×10^{-2}	1.17×10^{-2}

3.6 Performance Comparison of Wavelength Diversity with Spatial diversity

The performance of FSO system under strong turbulence with spatial and wavelength diversity is compared and discussed in this section. In (Tsiftsis, 2009), authors have applied spatial diversity to analyze the performance of FSO system under strong turbulence condition using K channel. The performance of FSO system is reported in terms of BER for MISO and SIMO structures. The presented FSO system model in this chapter resemble SIMO case. So, the performance comparison between spatial and wavelength diversity is presented for SIMO case considering OC method at the receiver end.

In (Tsiftsis, 2009), spatial diversity has been realized by transmitting information signal on a single wavelength of 1550nm towards multiple receivers and few centimeter spacing between receivers has been considered. For a fair comparison between two turbulence mitigation techniques, all the required parameters for performance evaluation is considered as reported in (Tsiftsis, 2009). The value of refractive index structure parameter C_n^2, for strong turbulence and receiver aperture size is kept as $2 * 10^{-13} m^{-2/3}$ and 10 mm, respectively. Fig. 3.9 shows the result of comparison between two diversity techniques. The result is presented for the diversity order of 2 and 3 for the distance of 2 km. The result of spatial diversity has been obtained from Eq. (20) of (Tsiftsis, 2009) and the result of wavelength diversity is plotted using Eq. (3.29).

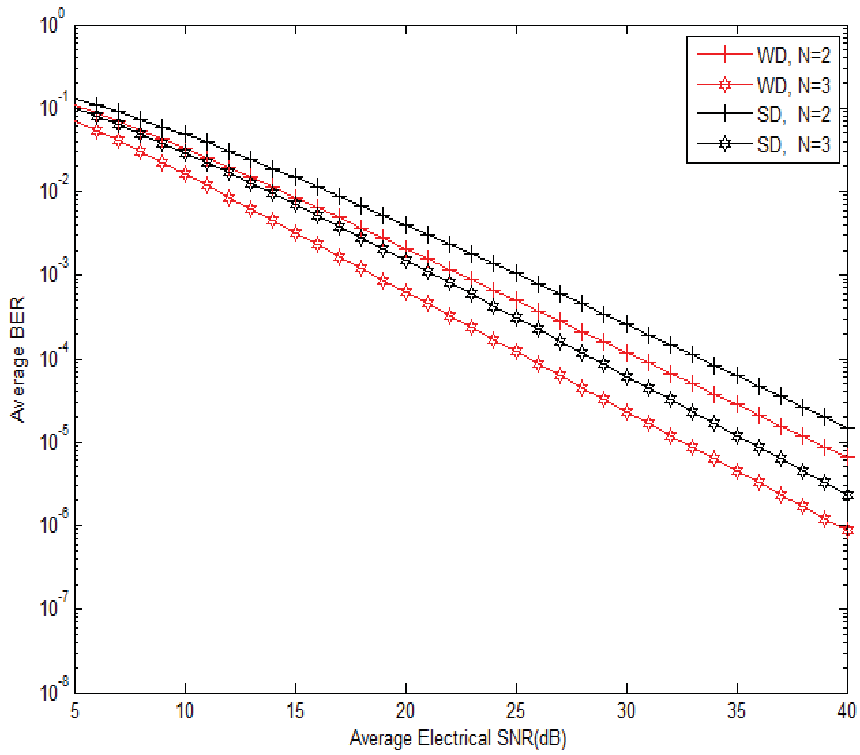

Fig. 3.9 Comparison of wavelength and spatial diversity using OC at 2 km distance

It is apparent from the Fig 3.9, that the performance of wavelength diversity is better compared to spatial diversity. The required SNR to obtain the BER of 10^{-5} is 41 dB and 38 dB for the spatial and wavelength diversity respectively, with two receivers. The similar performance difference is also observed with the diversity order of 3. This comparison shows that the wavelength diversity performs better than spatial diversity. Wavelength diversity requires 3 dB less SNR to achieve the targeted BER compared to spatial diversity technique.

3.7 Conclusion

The performance of the FSO link with wavelength diversity under strong turbulence is investigated and discussed in this chapter. The performance is found in terms of average BER and outage probability. In the case of average BER, mathematical expressions for the three different combining techniques namely OC, EGC and SC are derived. It is observed that diversity order of 3 decreases the SNR requirement by 13% and 25% for link length of 2 km and 3 km for the BER of 10^{-4}, respectively as compared to without wavelength diversity using OC method. The same is 25% and 27% in the case of SC. SC provides better improvement than OC at both the distances. However, OC requires 8 – 14 dB lesser SNR value than SC to achieve the targeted BER of 10^{-4}. It is also observed that the EGC performance is 2 to 3 dB lesser than OC. Overall, OC provides better results than other two combining methods i.e. EGC and SC.

The performance of proposed technique is also analyzed in terms of outage probability. An approximated closed-form expression of outage probability with SC and OC method is derived. OC method provides 30 dB more performance improvement compared to SC with different diversity levels at different distances. Numerical results once again show that the performance of OC is better than SC.

Finally, the performance comparison between spatial and wavelength diversity is presented for the SIMO case. It is found that the performance of wavelength diversity is better than spatial diversity.

Chapter 4

Performance of FSO Link with Wavelength Diversity over Exponentiated Weibull Channel

The performance of FSO link under strong turbulence condition using K channel is investigated and discussed in chapter 3. The obtained results show that required SNR is more than 30 dB to achieve BER of 10^{-4} with wavelength diversity of order of 3 with OC method. The BER in the range of 10^{-6} is the need of current communication systems which is operating at high data rates (Goldsmith, 2005). The further decrement in the BER with wavelength diversity using K channel is achieved by increasing SNR which is not a viable solution. So, this demands the further investigation on FSO link performance under strong turbulence condition using another channel model with wavelength diversity. EW channel model is another alternative to characterize strong turbulence condition. This chapter presents the performance analysis of FSO system under moderate and strong turbulence conditions using EW channel model with wavelength diversity. OC method is considered to combine different signals, as OC achieves better results than EGC and SC. The mathematical expressions have been derived to calculate outage probability and average BER using OC method. An appropriate wavelength diversity order to mitigate atmospheric turbulence effect is also a major concern. So, results are obtained for diversity order up to 6 at different link distances varying from 1 km to 3 km at a regular interval of 0.5 km under both turbulence conditions. The performance of this system is also analyzed with receiver aperture size as per commercial FSO system.

4.1 Exponentiated Weibull Channel Model

The EW channel model is enhanced version of Weibull channel model. The Weibull Channel model is widely used to model wind speed distribution (Seguro, 2000), particle size distribution (Fang, 1993) and for a specific type of clutter (Schleher, 1976) in the field of physics and engineering. It is also used in the field of wireless communication (Alouini, 2001), (Lupupa, 2009) to model channel. The PDF of Weibull distribution is written as.

$$f_I(I) = \frac{\beta}{\eta}\left(\frac{I}{\eta}\right)^{\beta-1} exp\left[-\left(\frac{I}{\eta}\right)^{\beta}\right] \tag{4.1}$$

where, $\beta > 0$ is a shape parameter and $\eta > 0$ represents scale parameter. η is dependent on β and it is related to the mean value of the irradiance. For the cases of β = 1and β = 2, Eq. (4.1) reduces to the Negative exponential and Rayleigh PDF, respectively.

The CDF of Weibull distribution is defined by

$$F_I(I) = \int_0^I f_I(I)dI = \int_0^I \frac{\beta}{\eta}\left(\frac{I}{\eta}\right)^{\beta-1} exp\left[-\left(\frac{I}{\eta}\right)^{\beta}\right] dI$$

$$= \frac{\beta}{\eta^\beta}\int_0^I (I)^{\beta-1} exp\left[-\left(\frac{I}{\eta}\right)^{\beta}\right] dI$$

Assume $\left(\frac{I}{\eta}\right)^{\beta} = t$ and $\beta\left(\frac{1}{\eta}\right)^{\beta}(I)^{\beta-1}dI = dt$ or, $\frac{\beta}{\eta^\beta}(I)^{\beta-1}dI = dt$, Now, $F_I(I) = \int_0^t e^{-t}dt = [-e^{-t}]_0^t + Constant = -e^{-t} - (-e^0)$. So, $F_I(I) = -e^{-t} - (-e^0)$

Finally, CDF of Weibull becomes,

$$F_I(I) = 1 - exp\left[-\left(\frac{I}{\eta}\right)^{\beta}\right] \tag{4.2}$$

This model is only applicable for stationary conditions, where channel statistic remains constant over the observation time period. Mudholkar and Srivastava (Mudholkar, 1993) have introduced an additional shape parameter to the Weibull distribution and proposed a new model as Exponentiated Weibull (EW) distribution. Barrios and Dios (Barrios, 2013) have used this EW distribution to model the distribution of the irradiance in FSO link. The CDF of a random variable I described by the EW distribution is given as (Barrios, 2013)

$$F_I(I) = \left\{1 - exp\left[-\left(\frac{I}{\eta}\right)^{\beta}\right]\right\}^{\propto} \tag{4.3}$$

The PDF of EW can be calculated by

$$f_I(I) = \frac{d}{dI}F_I(I) = \frac{d}{dI}\left\{1 - exp\left[-\left(\frac{I}{\eta}\right)^{\beta}\right]\right\}^{\alpha}$$

$$f_I(I) = \frac{\alpha\beta}{\eta}\left(\frac{I}{\eta}\right)^{\beta-1} exp\left[-\left(\frac{I}{\eta}\right)^{\beta}\right]\left\{1 - exp\left[-\left(\frac{I}{\eta}\right)^{\beta}\right]\right\}^{\alpha-1} \tag{4.4}$$

where, $\beta > 0$ and $\alpha > 0$ are shape parameters, and $\eta > 0$ is a scale parameter, which is related to the mean value of the irradiance. If ($\alpha = 1$), then Eq. (4.4) represents the Weibull distribution and for the cases of ($\alpha = 1$, $\beta = 2$), and ($\alpha = 1$, $\beta = 1$), Eq. (4.4) represents Rayleigh and the Negative exponential distribution, respectively. The equation to calculate the values of α, β and η is given in (Barrios, 2013).

4.2 System Model

The system model for FSO link with wavelength diversity is discussed in chapter 3. The same model is used in this chapter. In this system model, the atmospheric turbulence is modeled using an EW distribution. The PDF of EW distribution after applying Wavelength diversity is given as

$$f_{I_w}(I_w) = \frac{\alpha_w\beta_w}{\eta_w}\left(\frac{I_w}{\eta_w}\right)^{(\beta_w-1)} e^{\left[-\left(\frac{I_w}{\eta_w}\right)^{\beta_w}\right]} \times \left\{1 - e^{\left[-\left(\frac{I_w}{\eta_w}\right)^{\beta_w}\right]}\right\}^{\alpha_w-1} , I_w \geq 0 \tag{4.5}$$

where, $\alpha_w, \beta_w > 0$ are two shape parameters related to the scintillation index at the w_{th} wavelength, and $\eta_w > 0$ is a scale parameter related to the mean value of I_w for w_{th} wavelength channel. α_w gives more adaptability to the tail shape of the PDF. When data is visualized on a logarithmic scale, α_w controls the lower-tail steepness for the fixed values of the shape parameter β_w and the scale parameter η_w. This is an important property of the EW distribution, as lower tails expresses the error rate and fades probability (Parenti, 2005). The CDF of I_w can be easily derived by

$$F_{I_w}(I_w) = \int_0^{\infty} f_{I_w}(I_w) dI_w \quad (4.6)$$

OR,

$$F_{I_w}(I_w) = \left\{1 - exp.\left[-\left(\frac{I_w}{\eta_w}\right)^{\beta_w}\right]\right\}^{\alpha_w}, I_w \geq 0 \quad (4.7)$$

The expression of the shape parameter α_w for w_{th} wavelength in the case of wavelength diversity is written as

$$\alpha_w \approx 3.931\left(\frac{D}{\rho_{0,w}}\right)^{-0.519} \quad (4.8)$$

where, D is the receiving aperture diameter and $\rho_{0,w}$ is the atmospheric coherence radius at w_{th} wavelength which is calculated as

$$\rho_{0,w} = \left(1.46 C_n^2 {k_w}^2 L\right)^{-3/5} \quad (4.9)$$

here, $k_w = \frac{2\pi}{\lambda_w}$, is the wave number, λ_w is the operational wavelength of each of the W channels of the FSO system and L is the distance between the transmitter and receiver planes. The C_n^2 represents the refractive index structure parameter, depends on the altitude and the atmospheric conditions (Henniger, 2010).

The shape parameter β_w, which is related to the scintillation index σ_I^2 and it is expressed as

$$\beta_w \approx (\alpha_w \sigma_I^2)^{-6/11} \quad (4.10)$$

and the scale parameter η_w is written as

$$\eta_w = \frac{1}{\alpha_w \Gamma(1+1/\beta_w) g(\alpha_w, \beta_w)} \quad (4.11)$$

where, $g(\alpha_w, \beta_w)$ with w_{th} wavelength is calculated as

$$g(\alpha_w, \beta_w) = \sum_{i=0}^{\infty} \frac{(-1)^i (i+1)^{-(1+\beta_w)/\beta_w} \Gamma(\alpha_w)}{i! \Gamma(\alpha_w - i)} \quad (4.12)$$

where, $\Gamma(.)$ represents gamma function. For w_{th} wavelength, the instantaneous electrical SNR can be defined as $\gamma_m = \frac{(\xi_w I_w)^2}{N_0}$ and the average electrical SNR is defined as $\mu_m = \frac{(\xi_w E[I_w])^2}{N_0}$. Here, $E[I_w] = 1$ since I_w is normalized. After a power transformation of the random variable I_w, the PDF of the instantaneous electrical SNR, γ_w with w_{th} wavelength is derived as

$$f_{\gamma_w}(\gamma_w) = \frac{\alpha_w \beta_w}{\eta_w}\left(\frac{1}{\eta_w}\sqrt{\frac{\gamma_m}{\mu_m}}\right)^{(\beta_w - 1)} e^{\left[-\left(\frac{1}{\eta_w}\sqrt{\frac{\gamma_w}{\mu_w}}\right)^{\beta_w}\right]} \times \left\{1 e^{\left[-\left(\frac{1}{\eta_w}\sqrt{\frac{\gamma_w}{\mu_w}}\right)^{\beta_w}\right]}\right\}^{\alpha_w - 1}, \gamma_w > 0 \tag{4.13}$$

and the corresponding CDF of the instantaneous electrical SNR γ_w is

$$F_{\gamma_w}(\gamma_w) = \left\{1 - e^{\left[-\left(\frac{1}{\eta_w}\sqrt{\frac{\gamma_w}{\mu_w}}\right)^{\beta_w}\right]}\right\}^{\alpha_w}, \gamma_w > 0 \tag{4.14}$$

Thus, from Eq. (4.13) and Eq. (4.14), it is clear that both PDF and CDF of the instantaneous electrical SNR of EW channel strongly depend on the atmospheric conditions.

4.3 Outage Probability

The outage probability is a vital parameter for the reliability of diversity systems operating in the fading environments. Considering this concept and CDF of the EW channel, the closed form expressions for the outage probability using OC for the FSO system with the wavelength diversity is derived. The outage probability P_{out} of the FSO system for a single channel (i.e., W = 1) is calculated as

$$P_{out} = P_r(\gamma \leq \gamma_{th}) = F_\gamma(\gamma_{th}) \tag{4.15}$$

using Eq. (4.14), the Eq. (4.15) is modified as

$$P_{out} = \left\{1 - exp\left[-\left(\frac{1}{\eta}\sqrt{\frac{\gamma_{th}}{\mu}}\right)^{\beta}\right]\right\}^{\alpha} \tag{4.16}$$

For the multiple wavelength channel W, assuming that the outage probability for each of the channel is different. As each of the channel is working on different wavelength, the total outage probability $P_{out,w}$ of the considered FSO systems corresponds to the probability of outage of all the W links, i.e.,

$$P_{out,W} = \prod_{w=1}^{W} P_{out,w} = \prod_{w=1}^{W} Pr(\gamma_w \le \gamma_{th,w}) = \prod_{w=1}^{W} F_{\gamma_w}(\gamma_{th,w}) \tag{4.17}$$

OR,

$$P_{out,W} = \prod_{w=1}^{W} \left[\left\{ 1 - exp\left[-\left(\frac{1}{\eta_w} \sqrt{\frac{\gamma_{th,w}}{\mu_w}} \right)^{\beta_w} \right] \right\}^{\alpha_w} \right] \tag{4.18}$$

4.4 Average BER of the System

The average BER of FSO system with SISO is discussed in chapter 3. Following the same concept, the average BER of EW channel for SISO link of the FSO system is obtained by averaging over I, i.e.

$$P_{av} = \int_0^{+\infty} P_e(I) f_I(I) dI = \int_0^{+\infty} Q\left(\frac{\xi I}{\sqrt{2\pi}} \right) f_I(I) dI \tag{4.19}$$

In this scenario, average BER is computed from the CDF $F_I(I)$, as follows

$$P_{av} = -\int_0^{+\infty} P_e'(I) F_I(I) dI \tag{4.20}$$

where, $P_e'(I)$ in Eq. (4.20) is the first order derivative of the conditional BER $P_e(I)$. It is derived as

$$P_e'(I) = -\frac{1}{\sqrt{\pi}} exp.\left(\frac{-\xi^2 I^2}{4N_0} \right) = -\frac{1}{\sqrt{\pi}} exp.\left(\frac{-\gamma}{4} \right) \tag{4.21}$$

Substituting Eq. (4.7) and Eq. (4.21) into Eq. (4.20), average BER is expressed as

$$P_{av} = \frac{1}{\sqrt{\pi}} \int_0^{+\infty} exp.\left(\frac{-\xi^2 I^2}{4N_0} \right) \left\{ 1 - exp.\left[-\left(\frac{I}{\eta} \right)^{\beta} \right] \right\}^{\alpha} dI \tag{4.22}$$

A closed-form solution for the integral Eq. (4.22) is not available. On the other hand, putting the variable $x^2 = \frac{\xi^2 I^2}{4N_0} = \frac{\sqrt{\gamma}}{2}$, Eq. (4.22) becomes

$$P_{av} = \frac{2\sqrt{N_0}}{R\sqrt{\pi}} \int_{-\infty}^{+\infty} exp.(-x^2) \left\{1 - exp.\left[-\left(\frac{2\sqrt{N_0}}{\xi\eta} x\right)^{\beta}\right]\right\}^{\alpha} dx \tag{4.23}$$

here, Eq. (4.23) is in the form of $\int_{-\infty}^{+\infty} g(x)\, e^{-x^2}$, where $g(x) = \left\{1 - exp.\left[-\left(\frac{2\sqrt{N_0}}{\xi\eta} x\right)^{\beta}\right]\right\}^{\alpha}$, and it can be approximated by using Gauss–Hermite quadrature rule. The Gauss–Hermite quadrature approximation is defined as (Abramowitz, 1972)

$$\int_{-\infty}^{+\infty} g(x)\, e^{-x^2} \approx \sum_{i=1}^{n} m_i g(x_i) \tag{4.24}$$

where, n is the number of sample point used. x_i is the roots of the Hermite Polynomials $H_n(i)$ $(i = 1, 2, \dots, n)$ and the associated weight m_i are given as

$$m_i = \frac{2^{(n-1)} n! \sqrt{\pi}}{n^2 [H_{n-1}(x_i)]^2} \tag{4.25}$$

Using Eq. (4.24) and Eq. (4.25), Eq. (4.23) is written as

$$P_{av} \approx \frac{2\sqrt{N_0}}{\xi\sqrt{\pi}} \sum_{i=1}^{n} m_i \left\{1 - exp.\left[-\left(\frac{2\sqrt{N_0}}{\xi\eta} x_i\right)^{\beta}\right]\right\}^{\alpha} \tag{4.26}$$

In terms of the average electrical SNR of the SISO system, μ, (4.26) is expressed as

$$P_{av} \approx \frac{2}{\sqrt{\pi\mu}} \sum_{i=1}^{n} m_i \left\{1 - exp.\left[-\left(\frac{2}{\eta\sqrt{\mu}} x_i\right)^{\beta}\right]\right\}^{\alpha} \tag{4.27}$$

If wavelength diversity is to be used, its average BER will be derived by considering the channel model presented in chapter 3, i.e. one transmitter and W receivers. This case can be compared to a single input multiple output (SIMO) scheme. Considering above case, the optimum decision metric for OOK is written as

$$P(\vec{y}|off, I_w) \underset{on}{\overset{off}{\lessgtr}} P(\vec{y}|on, I_w) \tag{4.28}$$

where, vector signal $\vec{y} = (y_1, y_2, \dots, y_w)$ is received at different receiver. In this respect, the expressions for the average BER for wavelength diversity FSO system with W different channels at receiver has been derived. At receiver side, OC method is being considered. The average BER of the FSO system with the W different wavelength channels considering OC method can be achieved as follows

$$P_{W,OC} = \int_{\vec{I}} f_{\vec{I}}(\vec{I})\, Q\left(\frac{1}{\sqrt{2WN_0}}\sqrt{\sum_{w=1}^{W} {\xi_w}^2 {I_w}^2}\right) d\vec{I} \tag{4.29}$$

In terms of CDF, $F_{I_w}(I_w)$, the average BER for W_{th} channel is written as

$$P_{W,OC} = \prod_{w=1}^{W} \frac{1}{\sqrt{\pi}} \int_0^{+\infty} e^{\left(\frac{-{\xi_w}^2 {I_w}^2}{4N_0}\right)} \left\{1 - e^{\left[-\left(\frac{I_w}{\eta_w}\right)^{\beta_w}\right]}\right\}^{\alpha_w} dI_w \tag{4.30}$$

where, $\vec{I} = (I_1, I_2, \ldots, I_w)$ is the vector of the normalized irradiances for each of the W receivers. Applying Gauss-Hermite quadrature rule on Eq. (4.30), the average BER expression with wavelength diversity is obtained as

$$P_{W,OC} \approx \prod_{w=1}^{W} \frac{2\sqrt{N_0}}{\xi_w\sqrt{\pi}} \sum_{i=1}^{n} m_i \left\{1 - exp\left[-\left(\frac{2\sqrt{N_0}}{\xi_w \eta_w} x_i\right)^{\beta_w}\right]\right\}^{\alpha_w} \tag{4.31}$$

In the form of average electrical SNR, μ_w, the final average BER expression for OC method is expressed as

$$P_{W,OC} \approx \prod_{w=1}^{W} \frac{2\sqrt{W}}{\sqrt{\pi \mu_w}} \sum_{i=1}^{n} m_i \left\{1 - exp\left[-\left(\frac{2\sqrt{W}}{\eta_w \sqrt{\mu_w}} x_i\right)^{\beta_w}\right]\right\}^{\alpha_w} \tag{4.32}$$

where, μ_w defines the average electrical SNR for the w_{th} wavelength channel.

4.5 Results and Discussion

The numerical results obtained for the outage probability and average BER are discussed in this section. The optimal combining scheme is applied at the receiver end to combine all the signals. Results are obtained for the different turbulence conditions at different link distances. The link performance is analyzed and presented for the moderate ($C_n^2 = 6 \times 10^{-14} m^{-2/3}$) and strong turbulence ($C_n^2 = 2 \times 10^{-13} m^{-2/3}$) conditions with different size (10 mm and 60 mm) of receiver aperture. All the available literature on wavelength diversity has considered receiver aperture diameter of 10 mm. However, a commercially available FSO has receiver aperture diameter more than 10 mm (fSONA, 2016). So, the aperture diameter of 60 mm is also considered to realize the results for practical applications under possible worst case scenario. Three different wavelengths of 1550 nm, 1310nm and 850 nm is chosen to realized the wavelength diversity. A few centimeter spacing between the receivers is sufficient to make the receiver diversity effective (Peppas, 2012). Considering this, the independent channel fading is considered for all the receivers. The EW channel parameters α_w, β_w and η_w are obtained from the Eq. (4.8), (4.10) and (4.11), respectively. For the wavelength diversity scheme, same average electrical SNR and sensitivity limits are considered for all the W receivers. The obtained results are also compared with no diversity case. In the presented results, W =1 represents diversity less scenario, while W =2 and W =3 represent the wavelength diversity order of 2 and 3, respectively. For the diversity less scenario, the signal is transmitted using 1.55 μm wavelength. The signal is transmitted at 1550 nm and 1310 nm in the case of W =2. For the diversity order of 3, the signal is transmitted on 1550 nm, 1310 nm and 850 nm. To identify adequate diversity order, results are also plotted with higher diversity order up to 6. The other three wavelengths are 1500 nm, 1300 nm and 800 nm. The signal is transmitted over 1550 nm, 1310 nm, 850 nm and 1500 nm for diversity order 4. In the case of order 5, signal is transmitted on 1300 nm apart from the other wavelengths which are used for the order 4. Finally, signal is transmitted on all the six wavelengths for the diversity order of 6. Selection of wavelengths is done considering the availability of the components at these wavelengths.

4.5.1 Outage probability with wavelength diversity

The outage probability, P_{out} versus normalized average electrical SNR, μ/γ_{th} using OC (from Eq. (4.18)) is plotted in Fig. 4.1 and Fig. 4.2 for moderate and strong turbulence conditions with propagation link length $L_1 = 1.5\ km$ and $L_2 = 2.5\ km$ respectively. Each graph is plotted to take into the consideration of absence and presence of wavelength diversity. The observed improvement in outage probability at SNR of 20 dB under moderate turbulence is of the order of 50dB at distance of 1.5km with a diversity order of 3 compared to no wavelength diversity and the same for strong turbulence is 40 dB. The similar values for the distance of 2.5 km are 40 and 30 dB, respectively. The results are also obtained for the distance of 1 km, 2 km and 3 km which is given in Table 4.1.

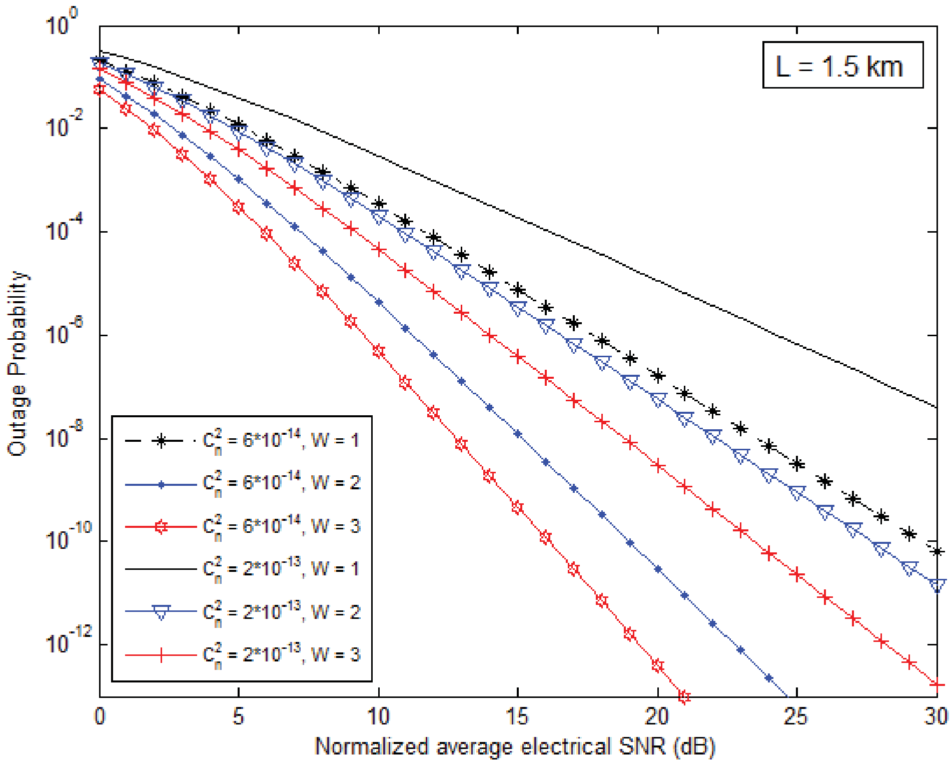

Fig. 4.1 Outage probability versus normalized average electrical SNR at 1.5 km

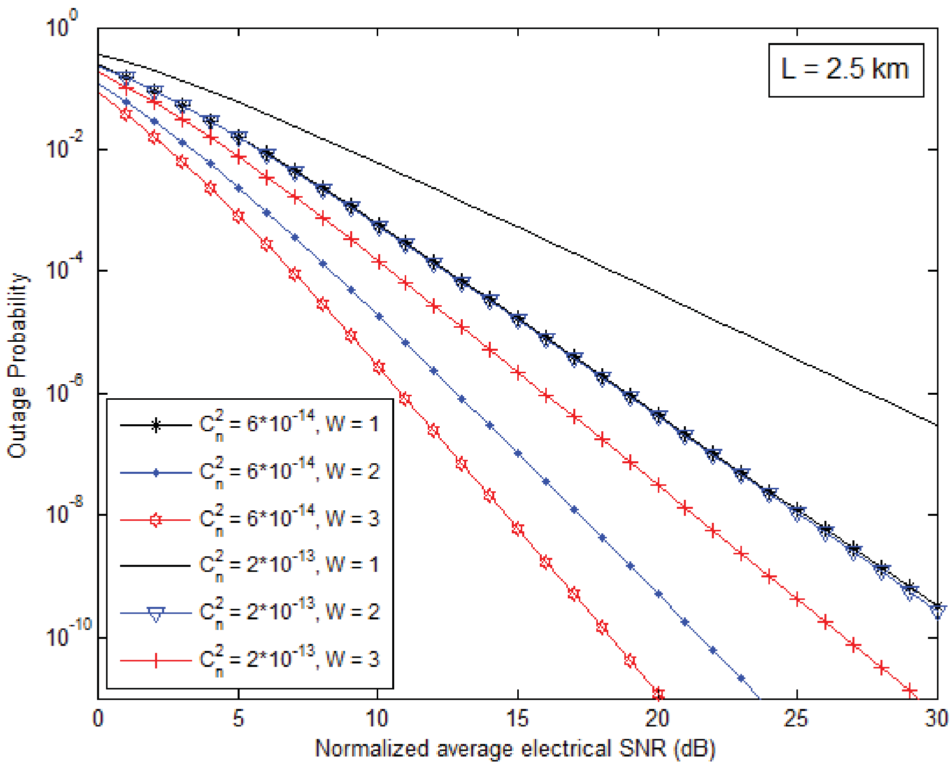

Fig. 4.2 Outage probability versus normalized average electrical SNR at 2.5 km

The results of outage probability with higher diversity order (up to w = 6) is plotted in Fig. 4.3 and Fig. 4.4 for the distance of 1.5 km with different turbulence conditions. Fig. 4.3 shows the plot of outage probability under a moderate turbulence condition with different diversity levels at the distance of 1.5 km between transmitter and receiver. The similar results are plotted for strong turbulence conditions in Fig. 4.4. From both these figures, it is observed that the outage probability is in order of 10^{-8} to 10^{-5} if no diversity is applied. It is apparent that the application of wavelength diversity improves the outage probability. The improvement is almost 10 dB with each level of wavelength diversity. Diversity level of 2 provides the outage of around 10^{-8} to 10^{-11} for various turbulence conditions. The improvement of around 40 dB with W=3 is observed compared to the no diversity case. An incremental improvement of about 20 dB is observed for both turbulence scenario with diversity level of 4 and 5. The further 10 dB improvement in the outage is observed with the diversity order of 6.

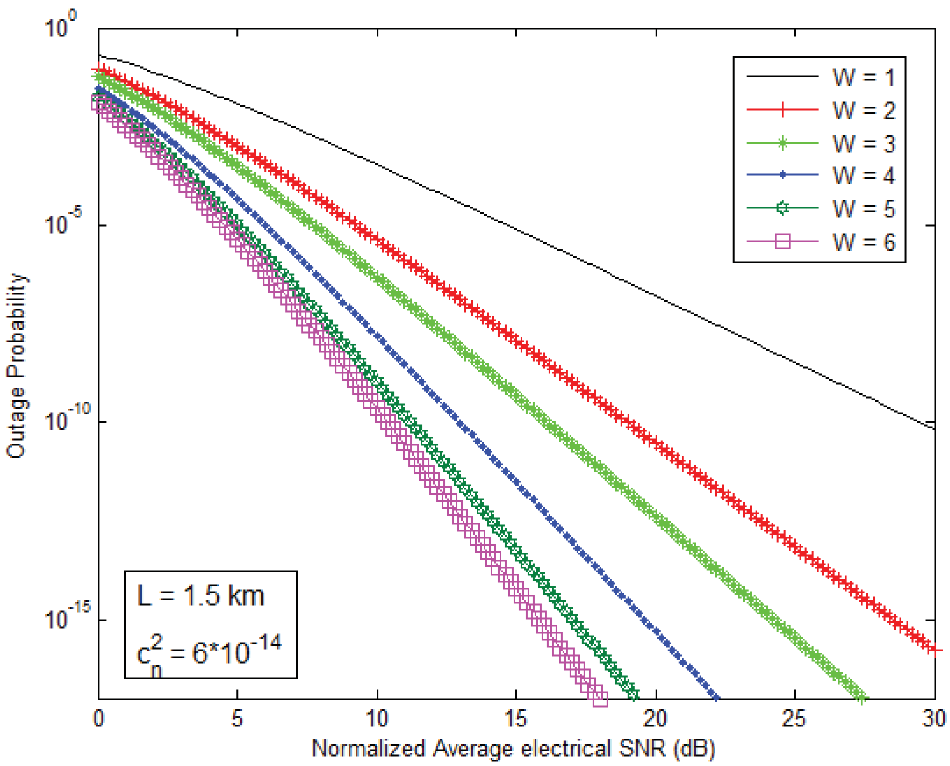

Fig. 4.3 Outage probability with different diversity order under moderate turbulence

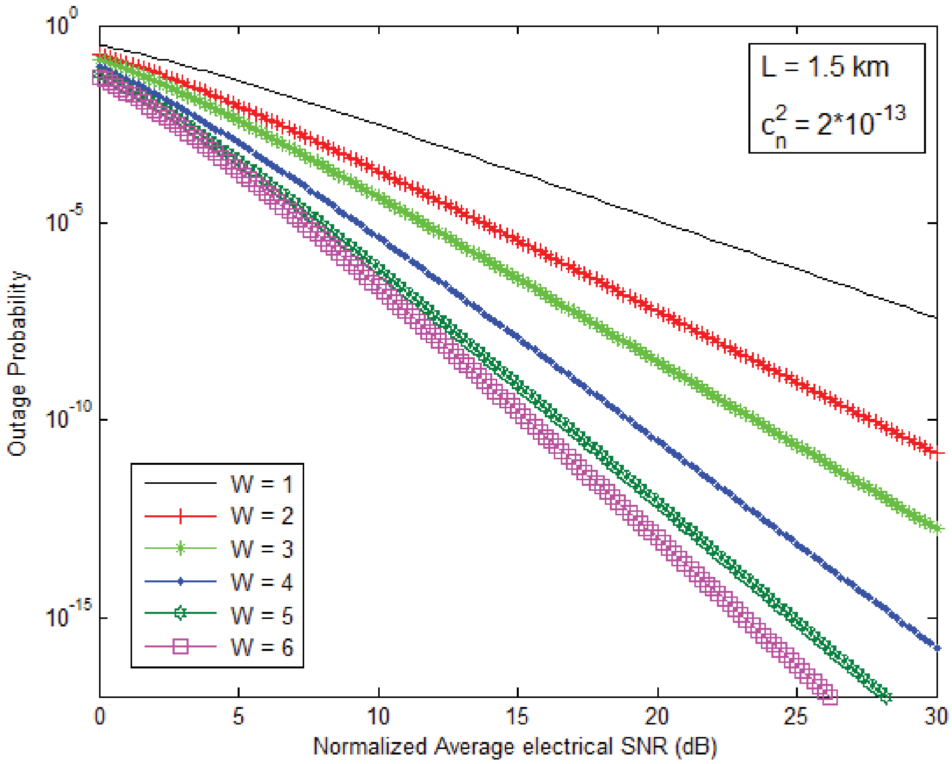

Fig. 4.4 Outage probability with different diversity order under strong turbulence

The plot of outage probability against SNR for the distance of 2.5 km is shown in Fig. 4.5 and Fig. 4.6 for moderate and strong turbulence conditions, respectively. As it can be seen from the figures, the outage probability is in the range of 10^{-5} for strong turbulence and 10^{-7} for moderate turbulence condition when no diversity is applied. With the diversity level of 2, the outage probability observed for moderate turbulence condition is in order of 10^{-10}, which is 30dB higher than what is achieved without application of diversity. The outage probability of 10^{-7} is achieved with diversity level of 2 for strong turbulence, which shows an improvement of 20 dB compared to no diversity case. For the diversity level of 3, the outage probability is in order of 10^{-11} and 10^{-8} for moderate and strong turbulence conditions, which is 10 dB higher than the achievable outage of diversity level 2 case. The overall improvement in an outage is almost 30 dB in both moderate and strong turbulence condition is achieved with the diversity of level 3 compared to the no diversity case. Further incremental improvement of 20 dB under moderate turbulence condition and 10 dB under strong turbulence can be achieved by increase in the diversity level of 4, 5 or 6, but at a higher

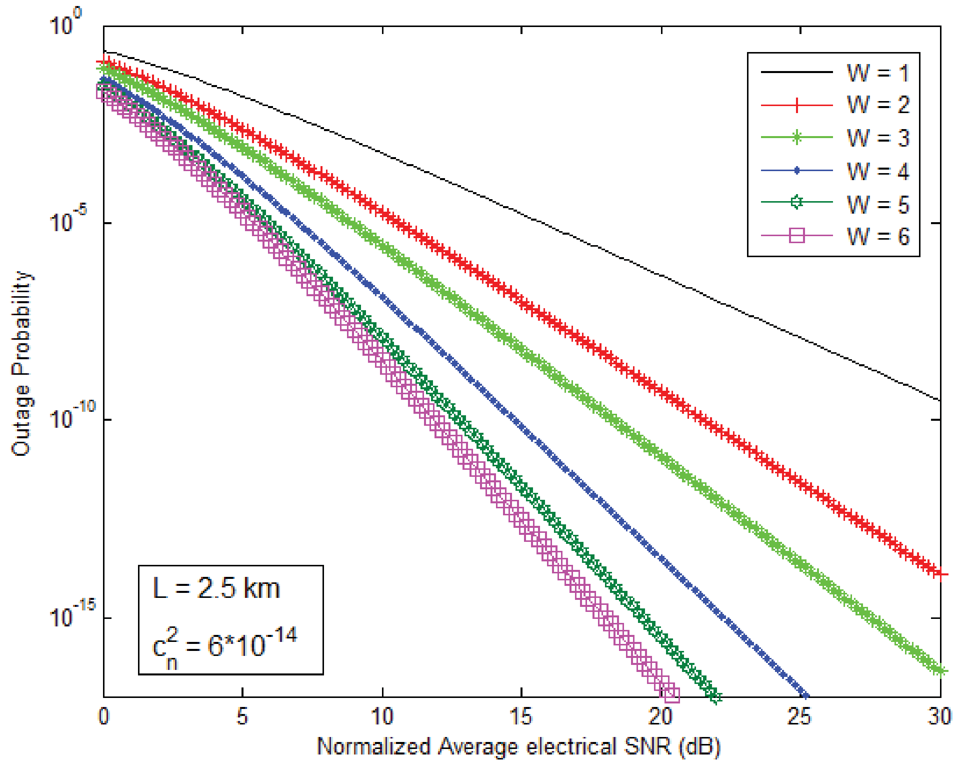

Fig. 4.5 Outage probability with different diversity order under moderate turbulence

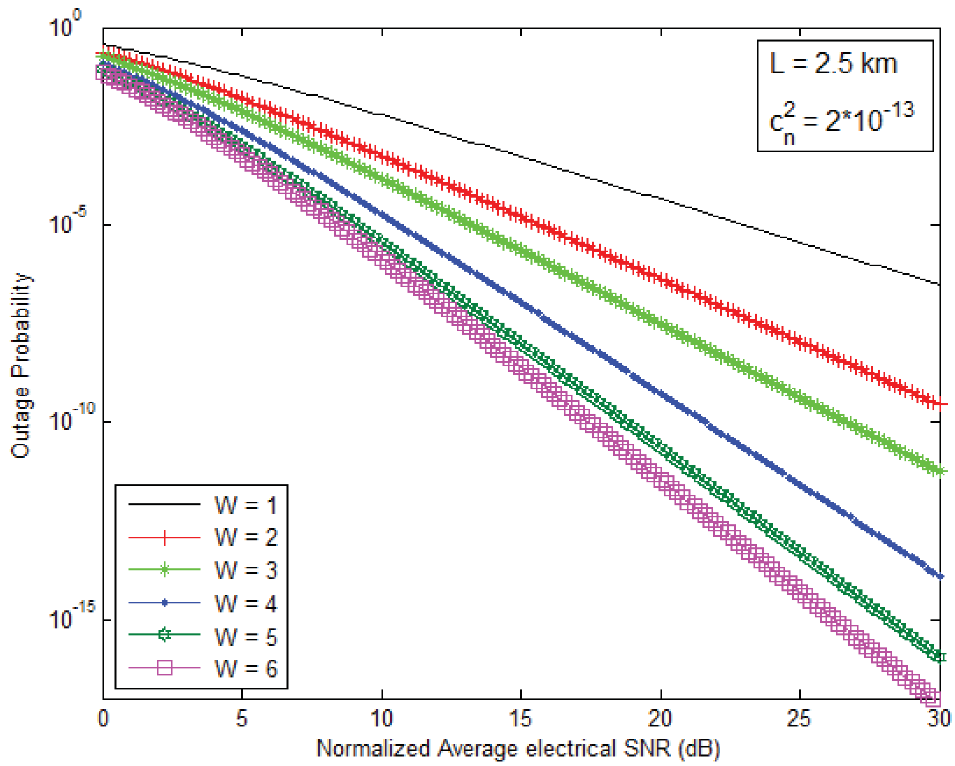

Fig. 4.6 Outage probability with different diversity order under strong turbulence

cost of the system and more complex design. The detailed result with different distance at different diversity order is presented in Table 4.1.

Table 4.1 Outage probability of FSO system at SNR of 20 dB

Diversity Order	Turbu-lence	D = 10 mm and SNR = 20 dB				
		L= 1 km	L=1.5 km	L= 2 km	L= 2.5 km	L= 3 km
W=1	M	1.36×10^{-8}	6.41×10^{-8}	1.70×10^{-7}	4.57×10^{-7}	9.06×10^{-7}
	S	3.91×10^{-6}	1.14×10^{-5}	2.45×10^{-5}	4.39×10^{-5}	7.04×10^{-5}
W=2	M	2.99×10^{-12}	2.92×10^{-11}	1.48×10^{-10}	5.19×10^{-10}	1.42×10^{-9}
	S	1.23×10^{-8}	5.74×10^{-8}	1.55×10^{-7}	4.15×10^{-7}	8.30×10^{-7}
W=3	M	2.83×10^{-14}	4.06×10^{-13}	2.80×10^{-12}	1.20×10^{-11}	3.94×10^{-11}
	S	3.89×10^{-10}	3.03×10^{-9}	1.12×10^{-8}	3.10×10^{-8}	7.06×10^{-8}
W=4	M	1.81×10^{-17}	4.95×10^{-16}	5.23×10^{-15}	3.24×10^{-14}	1.40×10^{-13}
	S	3.07×10^{-12}	3.02×10^{-11}	1.55×10^{-10}	1.16×10^{-9}	1.46×10^{-9}
W=5	M	5.88×10^{-20}	2.61×10^{-18}	3.83×10^{-17}	3.18×10^{-16}	1.71×10^{-15}
	S	6.11×10^{-14}	8.21×10^{-13}	6.14×10^{-12}	2.23×10^{-11}	7.09×10^{-11}
W=6	M	2.06×10^{-21}	1.26×10^{-19}	2.40×10^{-18}	2.20×10^{-17}	1.34×10^{-16}
	S	6.09×10^{-15}	1.02×10^{-13}	7.36×10^{-13}	3.55×10^{-12}	1.23×10^{-11}

M = Moderate turbulence and S = Strong turbulence

Table 4.1 shows results of the outage probability at different distances with different diversity order. The outage probability increases as distance increase. The value of outage probability for the distance of 1 km between the transmitter and receiver is 1.36 X 10^{-8} and 3.91 X 10^{-6} for moderate and strong turbulence conditions, respectively. The value of outage probability at the higher distance of 3 km is in order of 10^{-7} and 10^{-5} for moderate and strong turbulence conditions, respectively. The improvement in the outage probability is around 30 dB for the moderate turbulence condition for a distance of 1 km to 3 km while almost 20 dB improvement in outage probability is observed for strong turbulence conditions for the same distance if level 2 diversity is applied. It is also evident that the further improvement of 20 dB and 10 dB in outage probability can be achieved if the diversity level of 3 is applied under strong and moderate turbulence conditions, respectively. Further improvement in the outage probability is achieved with a diversity level of 4, 5 or 6, which increases the cost and complexity of the system.

4.5.2 Average BER with Wavelength diversity

Fig. 4.7 and Fig. 4.8 shows the variation of the average BER with respect to the average electrical SNR with and without wavelength diversity for moderate and strong turbulence conditions. These plots are achieved from Eq. (4.32). In both the cases, the wavelength diversity of the order of 2 and 3 is considered.

Fig. 4.7 shows the average BER of FSO system for link length of 1.5 km. The results are presented for the diversity order of 2 and 3. At the distance of 1.5 km, a maximum improvement of 30 dB and 20 dB in BER is obtained with a diversity order of 3 compared to no wavelength diversity under the moderate and strong turbulence regime, respectively. On the other hand, a consistent 10 dB improvement in BER is observed as the diversity order increases at the distance of 2.5 km under both turbulence scenario. The average BER results at distance of 2.5 km are shown in Fig. 4.8.

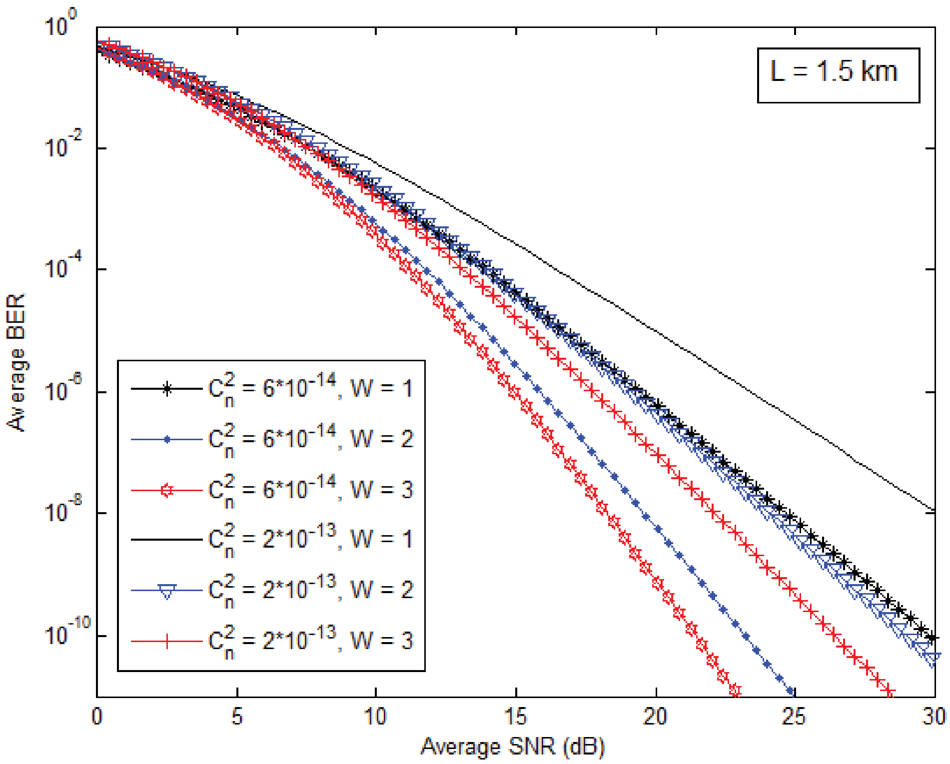

Fig. 4.7 Average electrical SNR versus average BER for link length of 1.5 km

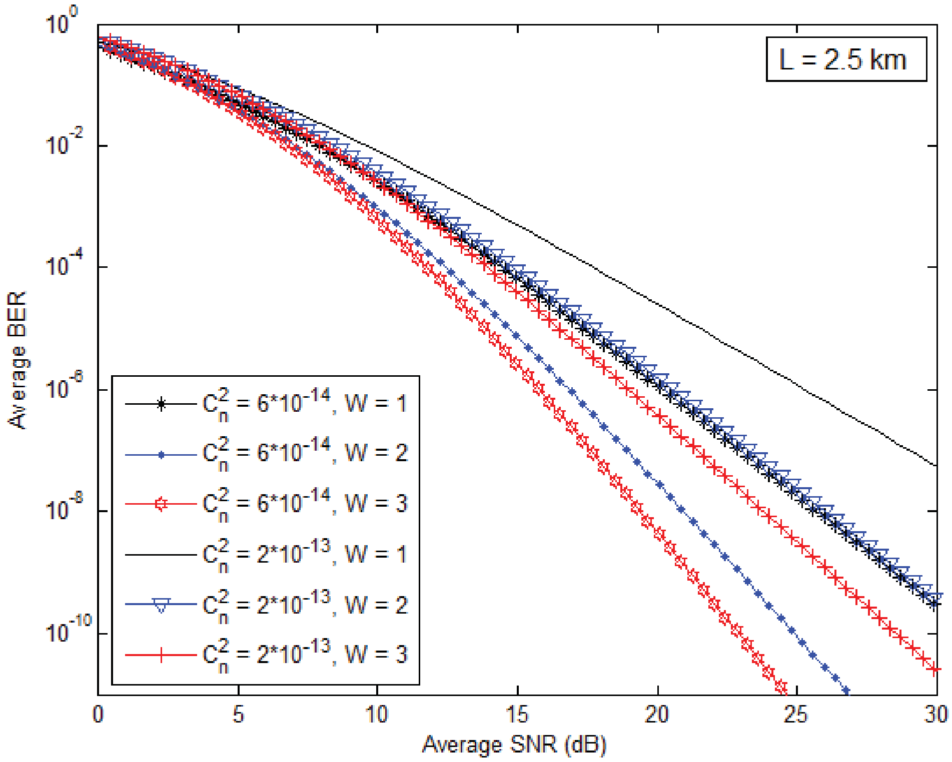

Fig. 4.8 Average electrical SNR versus average BER for link length of 2.5 km

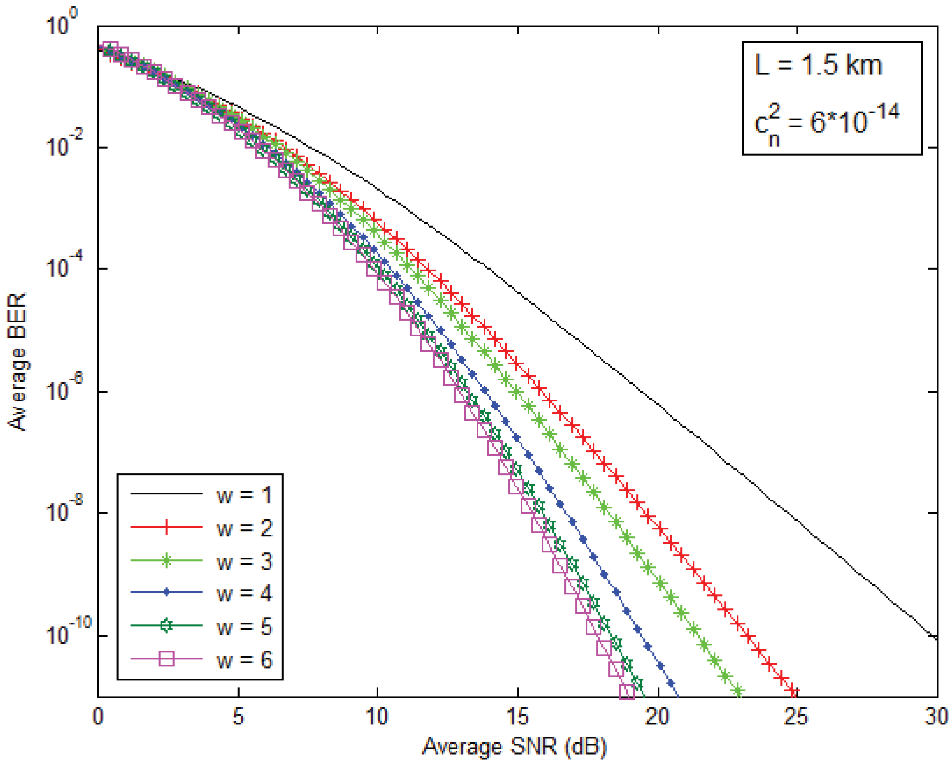

Fig. 4.9 Average BER with different diversity order under moderate turbulence

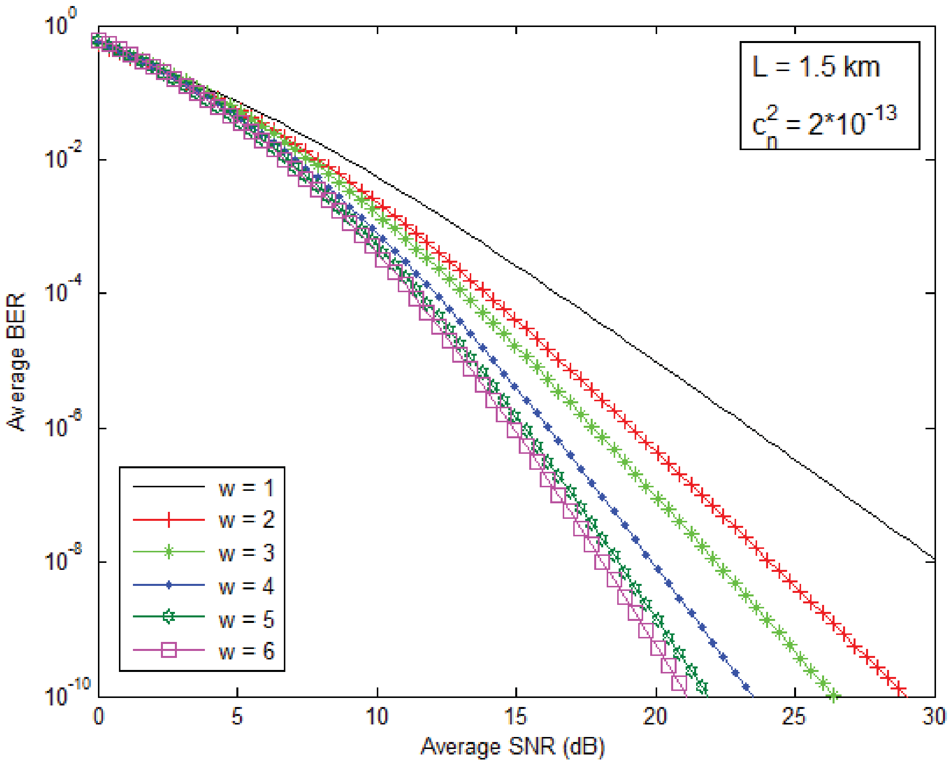

Fig. 4.10 Average BER with different diversity order under strong turbulence

Fig. 4.9 and Fig. 4.10 illustrates the average BER at 1.5 km distance with different diversity order for moderate and strong turbulence, respectively. A consistent improvement of 10 dB in BER is achievable with an increase in the diversity level. The BER of 10^{-7} is observed in the case of without diversity, which improves to 10^{-9}, 10^{-10} and 10^{-11} for the diversity level of w= 2, 3, and 4, respectively, at the distance of 1.5 km, for moderate turbulence condition. Similar results are obtained for strong turbulence condition as well. The higher improvement in the BER is achievable with the diversity level more than 3 but at higher channel implementation cost and complexity of system design. The BER obtained (in the range of 10^{-6}) with a diversity order of 2 with 10 mm receiver aperture diameter is sufficient to satisfy the need of modern communication channels (Goldsmith, 2005).

The results of BER vs SNR for the distance of 2.5 km with different diversity level under moderate and strong turbulence condition is plotted in the Fig. 4.11 and Fig. 4.12, respectively. The results resemble the results found in 1.5 km for both strong and

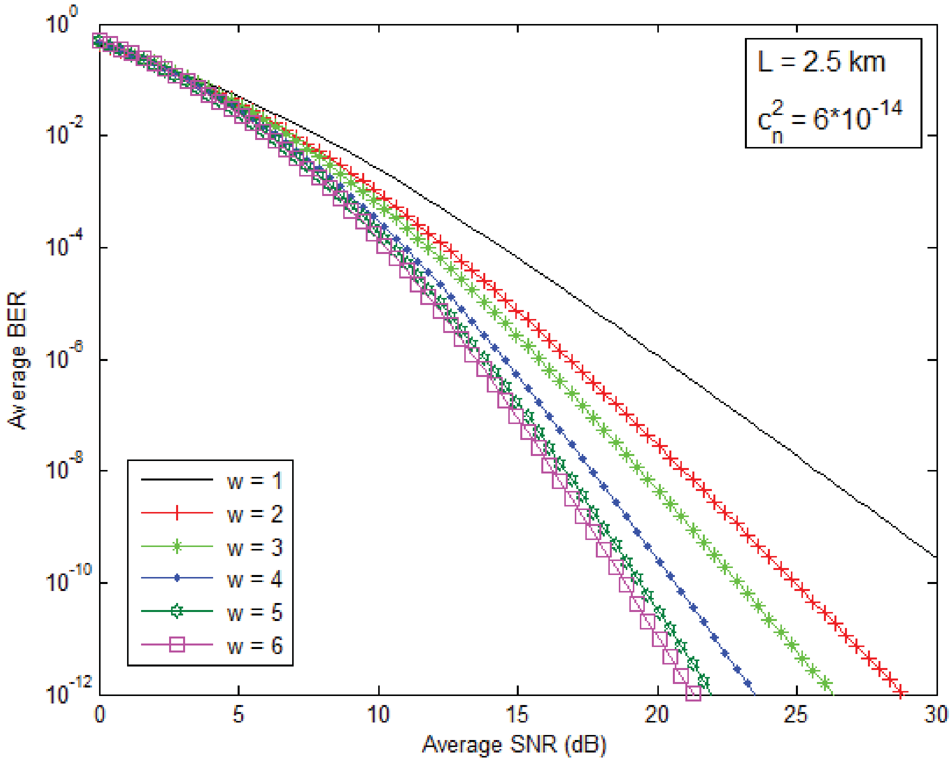

Fig. 4.11 Average BER at 2.5 km with different diversity order under strong turbulence

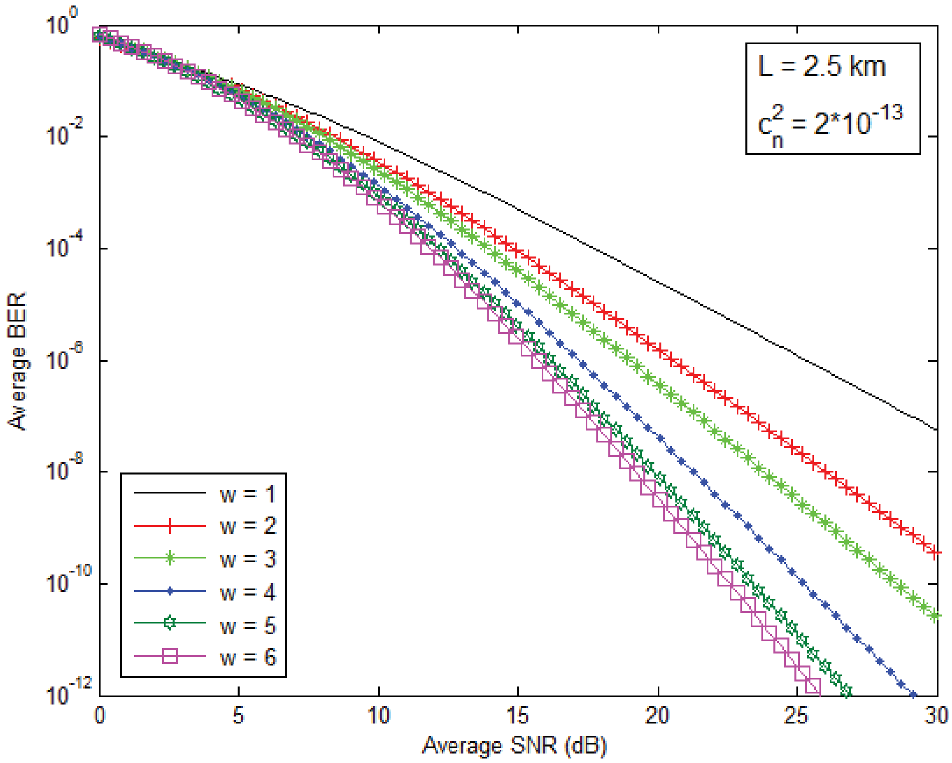

Fig. 4.12 Average BER at 2.5 km with different diversity order under strong turbulence

moderate turbulence conditions. As already stated earlier, the diversity level of 3 provides almost 20 dB and 10 dB improvement over diversity level of 2 and 1, respectively for even 2.5 km distance for both moderate and strong turbulence. Increase in the diversity improves the BER, but at a higher cost and complexity of design, which is not advisable to adopt for present communication needs. The detailed result of average BER with different diversity order at different distances is shown in Table 4.2.

As shown in Table 4.2, the BER increases as distance increases for with and without wavelength diversity. The BER improves with wavelength diversity for all distances in both moderate and strong atmospheric turbulence conditions. For the distance of 1 km between transmitter and receiver, the BER observed without application of wavelength diversity is in the order of 10^{-7} for moderate turbulence and in order of 10^{-6} for strong turbulence condition. For the same distance, the diversity of level 2 provides BER which is 100 times better than the BER achieved without the application of diversity. An additional 10 dB improvement in the BER is observed with diversity level of 3 under both turbulence conditions at the distance of 1 km. For the distance

Table 4.2 Average BER of FSO system with different diversity order at different distances

Diversity Order	Turbu-lence	D = 10 mm and SNR = 20 dB				
		L= 1 km	L=1.5 km	L= 2 km	L= 2.5 km	L= 3 km
W=1	M	1.25×10^{-7}	3.21×10^{-7}	6.41×10^{-7}	1.10×10^{-6}	1.72×10^{-6}
	S	4.50×10^{-6}	9.30×10^{-6}	1.57×10^{-5}	2.40×10^{-5}	3.38×10^{-5}
W=2	M	1.66×10^{-9}	5.52×10^{-9}	1.34×10^{-8}	2.68×10^{-8}	4.76×10^{-8}
	S	1.65×10^{-7}	4.25×10^{-7}	8.50×10^{-7}	1.10×10^{-6}	2.29×10^{-6}
W=3	M	1.93×10^{-10}	7.29×10^{-10}	1.94×10^{-9}	4.20×10^{-9}	7.96×10^{-9}
	S	3.16×10^{-8}	9.04×10^{-8}	1.95×10^{-7}	3.58×10^{-7}	5.91×10^{-7}
W=4	M	7.22×10^{-12}	3.27×10^{-11}	9.93×10^{-11}	2.40×10^{-10}	4.94×10^{-10}
	S	3.67×10^{-9}	7.96×10^{-9}	1.93×10^{-8}	3.86×10^{-8}	6.84×10^{-8}
W=5	M	6.71×10^{-13}	3.42×10^{-12}	1.13×10^{-11}	2.98×10^{-11}	6.53×10^{-11}
	S	3.65×10^{-10}	1.35×10^{-9}	3.81×10^{-9}	7.56×10^{-9}	1.41×10^{-8}
W=6	M	1.83×10^{-13}	1.01×10^{-12}	3.62×10^{-12}	9.66×10^{-12}	2.19×10^{-11}
	S	1.38×10^{-10}	5.17×10^{-10}	1.39×10^{-9}	3.14×10^{-9}	6.04×10^{-9}

M = Moderate turbulence and S = Strong turbulence

from 1.5 km to 3 km, the observed BER without wavelength diversity is in the range of 10^{-6} for moderate turbulence condition, while for strong turbulence conditions the value in the order of 10^{-5} is obtained. With the diversity of level 2, the improvement of around 10-20 dB is observed for both moderate and strong turbulence conditions. The interesting observation worth mentioning is that the BER further improves by almost 10 times (10 dB) with a diversity of level 3 compared to level 2 for both turbulence conditions. The improvement of almost 30dB is obtained with wavelength diversity w=3 compared to diversity less scenario. The BER, in order of 10^{-6} is adequate for proper reception of a signal for modern communication requirements. Diversity level of 2, suffices the requirement of the modern communication channel. The BER can further be improved by increasing the diversity level. There is an almost steady improvement of 10 dB is observed as diversity order increasing from 3 to 6. However, considering cost and complexity of implementation, diversity order of 3 is adequate enough to mitigate atmospheric turbulence effect under both the turbulence condition with acceptable BER for practical applications.

From the obtained results of outage probability and Average BER for both the turbulence condition, it is clear that diversity order of 2 is sufficient to improve the performance of wavelength diversity based FSO system with 10 mm receiver aperture size. However, commercial FSO system has more than 10 mm receiver aperture diameter (fSONA, 2016). To analyze the impact of wavelength diversity on practical FSO system, the results are obtained with 60 mm receiver aperture which is reported in the next section.

4.6 Performance of FSO system with 60 mm aperture size

The performance in terms of outage probability and average BER for wavelength diversity based FSO system with 60 mm receiver aperture size under moderate and strong turbulence condition is presented in this section.

4.6.1 Outage Probability at 60 mm receiver aperture

Fig. 4.13 and Fig. 4.14 shows the results of outage probability of FSO system with wavelength diversity under moderate and strong conditions at distance of 1.5 km and

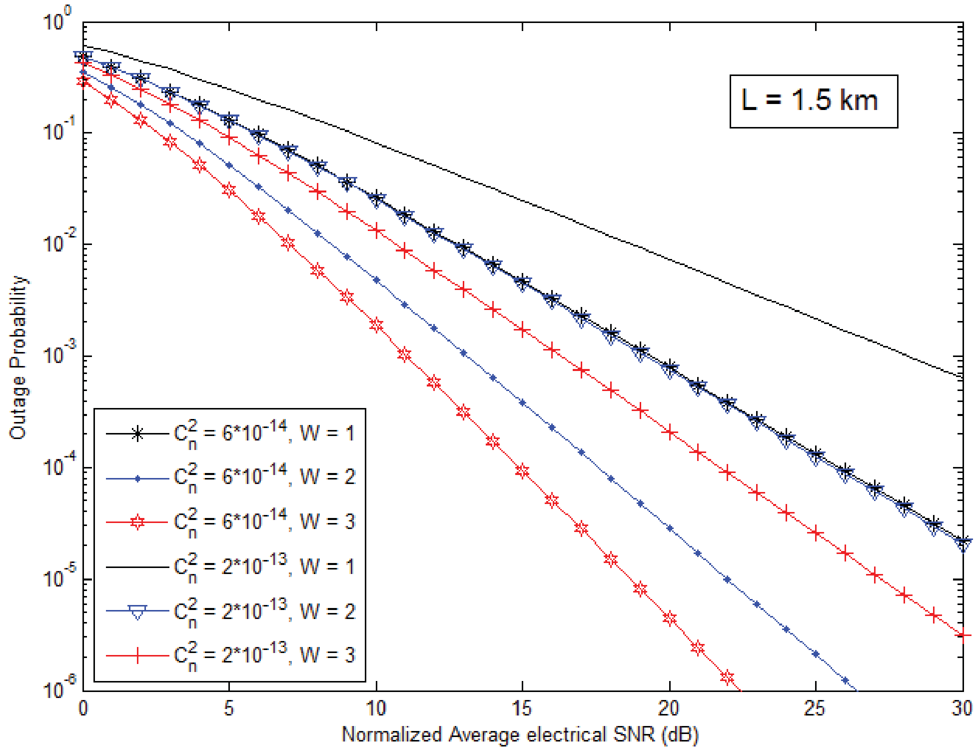

Fig. 4.13 Outage probability at the length of 1.5 km with 60 mm receiver aperture

2.5 km, respectively. It is evident from both the graphs that wavelength diversity improves the performance of FSO system even with an aperture of 60 mm. A maximum improvement of 20 dB is observed in the outage with a diversity order of 3 compared to no diversity scenario at SNR of 20 dB at both the distance under moderate turbulence condition. The same is of 10 dB and 20 dB at distance of 1.5 km and 2.5 km, respectively in the case of strong turbulence. Increasing diversity order further improves the performance of FSO system with wavelength diversity. The detailed results of outage probability with diversity order up to 6 at a different distance is presented in Table 4.3.

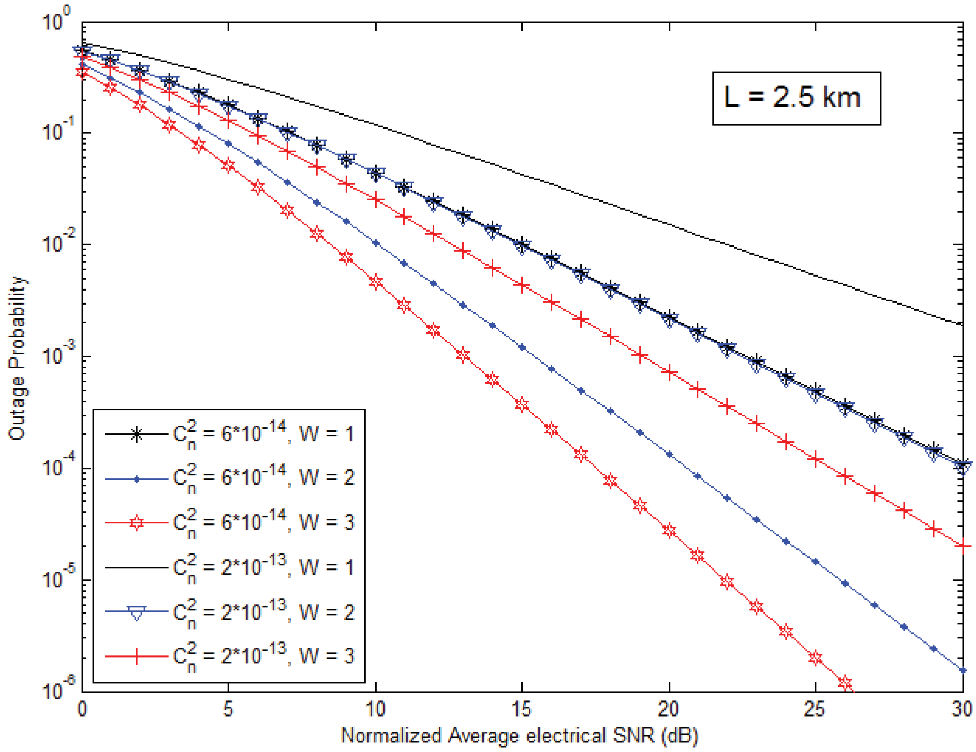

Fig. 4.14 Outage probability at the length of 2.5 km with 60 mm receiver aperture

Table 4.3 Outage probability of FSO system with 60 mm aperture at SNR of 20 dB

Diversity Order	Turbu-lence	D = 60 mm and SNR = 20 dB				
		L= 1 km	L=1.5 km	L= 2 km	L= 2.5 km	L= 3 km
W=1	M	3.01 X 10^{-4}	7.87 X 10^{-4}	1.45 X 10^{-3}	2.39 X 10^{-3}	3.05 X 10^{-3}
	S	3.80 X 10^{-3}	7.71 X 10^{-3}	1.12 X 10^{-2}	1.47 X 10^{-2}	1.88 X 10^{-2}
W=2	M	6.95 X 10^{-6}	2.83 X 10^{-5}	6.97 X 10^{-5}	1.44 X 10^{-5}	2.07 X 10^{-4}
	S	2.84 X 10^{-4}	8.04 X 10^{-4}	1.39 X 10^{-3}	2.10 X 10^{-3}	3.00 X 10^{-3}
W=3	M	8.56 X 10^{-7}	4.51 X 10^{-6}	1.30 X 10^{-5}	3.02 X 10^{-5}	4.72 X 10^{-5}
	S	6.78 X 10^{-5}	1.94 X 10^{-4}	4.37 X 10^{-4}	7.72 X 10^{-4}	1.08 X 10^{-3}
W=4	M	3.19 X 10^{-8}	2.87 X 10^{-7}	9.11 X 10^{-7}	2.82 X 10^{-6}	3.69 X 10^{-6}
	S	7.04 X 10^{-6}	2.87 X 10^{-5}	7.05 X 10^{-5}	1.24 X 10^{-4}	2.16 X 10^{-4}
W=5	M	2.45 X 10^{-9}	3.07 X 10^{-8}	1.54 X 10^{-7}	3.13 X 10^{-7}	7.30 X 10^{-7}
	S	1.21 X 10^{-6}	6.08 X 10^{-6}	1.70 X 10^{-5}	3.41 X 10^{-5}	6.24 X 10^{-5}
W=6	M	5.48 X 10^{-10}	6.83 X 10^{-9}	3.44 X 10^{-8}	1.01 X 10^{-7}	2.40 X 10^{-7}
	S	4.32 X 10^{-7}	2.45 X 10^{-6}	7.41 X 10^{-6}	1.48 X 10^{-5}	2.99 X 10^{-5}

M = Moderate turbulence and S = Strong turbulence

Table 4.3 shows the results of outage probability with diversity order from 1 to 6 at different distances. It can be clearly depicted from the results that increasing the propagation distance between transmitter and receiver decreases the outage probability. For the distance of 1 km between transmitter and receiver, the outage probability of 3.01 x 10^{-4} and 3.8 x 10^{-3} is obtained for the moderate and strong turbulence conditions, respectively. The improvement of almost 20 dB is achievable for the moderate condition if the diversity of level 2 is applied. For the same distance, the improvement of further 10 dB is observed with the diversity level of 3. Similar results can be obtained in the case of strong turbulence. A consistent improvement of 10 dB is obtained in the outage probability for the diversity level of 2 and 3 for the distance of 1 km between transmitter and receiver. Further increase in diversity level can still improve the outage probability by 6 to 10 dB but with the compromise in system cost and complexity. If the distance of 3 km between transmitter and receiver is considered then the outage probability of 3.05 x 10^{-3} and 1.88 x 10^{-2} is achieved for moderate and strong turbulence condition respectively. An improvement of 10 dB is observed in both the turbulence conditions with the diversity level of 2.

Table 4.4 Outage probability of FSO system at SNR of 30 dB

Diversity Order	Turbu-lence	D = 60 mm and SNR = 30 dB				
		L= 1 km	L=1.5 km	L= 2 km	L= 2.5 km	L= 3 km
W=1	M	4.89 X 10^{-6}	2.23 X 10^{-5}	5.23 X 10^{-5}	1.01 X 10^{-4}	1.68 X 10^{-4}
	S	2.36 X 10^{-4}	6.36 X 10^{-4}	1.19 X 10^{-3}	1.88 X 10^{-3}	2.65 X 10^{-3}
W=2	M	1.86 X 10^{-8}	1.54 X 10^{-7}	5.90 X 10^{-7}	1.55 X 10^{-6}	3.24 X 10^{-6}
	S	4.88 X 10^{-6}	1.94 X 10^{-5}	5.23 X 10^{-5}	1.01 X 10^{-4}	1.68 X 10^{-4}
W=3	M	8.10 X 10^{-10}	9.80 X 10^{-9}	4.71 X 10^{-8}	1.47 X 10^{-7}	3.49 X 10^{-7}
	S	5.63 X 10^{-7}	3.13 X 10^{-5}	9.21 X 10^{-6}	2.02 X 10^{-5}	3.64 X 10^{-5}
W=4	M	5.86 X10^{-12}	1.46 X10^{-10}	1.09X10^{-9}	3.60 X10^{-9}	7.90 X10^{-9}
	S	1.90 X10^{-8}	1.72 X10^{-7}	6.93 X10^{-7}	1.51 X10^{-6}	3.23 X10^{-6}
W=5	M	1.26 X10^{-13}	3.97 X10^{-12}	4.62 X10^{-11}	2.00 X10^{-10}	7.07 X10^{-10}
	S	1.36 X10^{-9}	1.48 X10^{-8}	7.15 X10^{-8}	2.19 X10^{-7}	5.52 X10^{-7}
W=6	M	1.33 X10^{-14}	5.00 X10^{-13}	6.55 X10^{-12}	3.70 X10^{-11}	1.58 X10^{-10}
	S	2.89 X10^{-10}	4.44 X10^{-9}	2.06 X10^{-8}	6.30 X10^{-8}	1.69 X10^{-7}

M = Moderate turbulence and S = Strong turbulence

Almost 20 dB improvement in outage probability is obtained with diversity level of 3 over the case without diversity in both the turbulence conditions. The improvement in an outage with the increase in diversity level is observed even after the diversity level 3, but the marginal improvement is achievable at a cost of system complexity. As it can be seen from Table 4.3, the similar improvement with different level of diversity is observed for different distance and turbulence conditions. Further improvement in the outage probability is obtained by increasing SNR by 10 dB. The achieved results of outage probability at 30 dB SNR is shown in Table 4.4.

4.6.2 Average BER at 60 mm receiver aperture

The average BER of FSO system with wavelength diversity under moderate and strong turbulence condition with 60 mm aperture at distance of 1.5 km and 2.5 km is shown in Fig. 4.15 and Fig. 4.16, respectively.

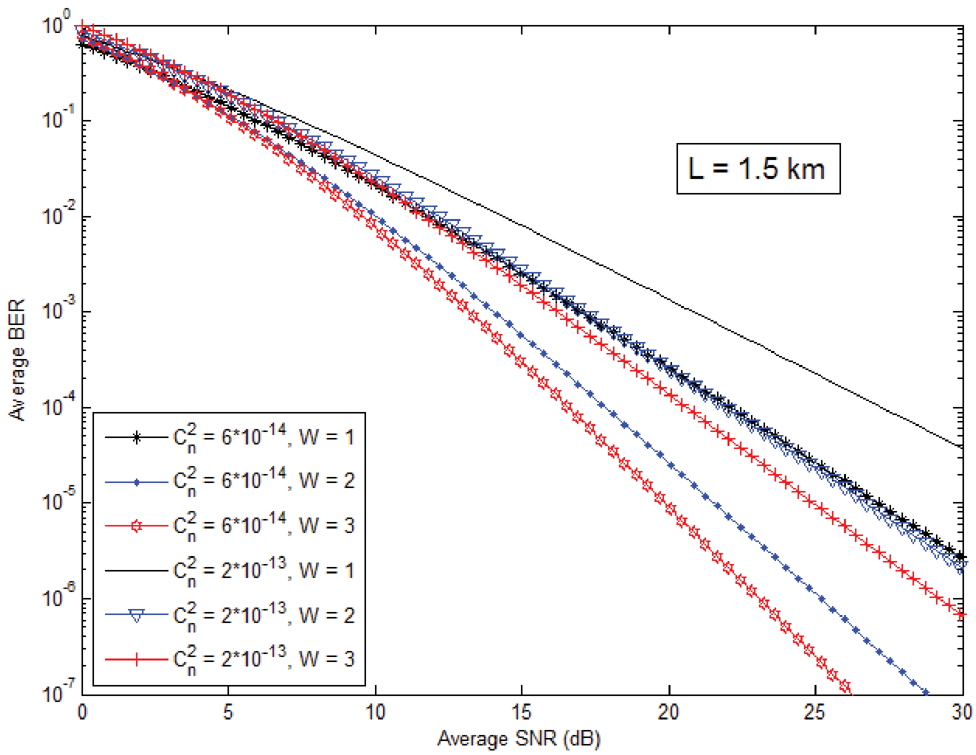

Fig. 4.15 Average BER for link length of 1.5 km with 60 mm aperture size

The observed BER at 1.5 km without diversity is in the range of 10^{-4} and 10^{-3} at 20 dB SNR under moderate and strong turbulence condition, respectively. Applying diversity order of 2 improves the BER performance by 10 dB under both turbulence condition.

Further improvement of 10 dB is obtained with a diversity order of 3 at the same distance as shown in Fig. 4.15. The BER performance of FSO system with wavelength diversity at a distance of 2.5 km is shown in Fig. 4.16. The BER performance improvement obtained at SNR 20 dB with a diversity order of 2 is 10 dB compared to no diversity case at the distance of 2.5 km under both turbulence conditions. An additional improvement of 4.5 dB and 3 dB in the BER is observed with diversity order 3 under moderate and strong turbulence condition, respectively. Increasing diversity order further improves BER performance which is presented in Table 4.5.

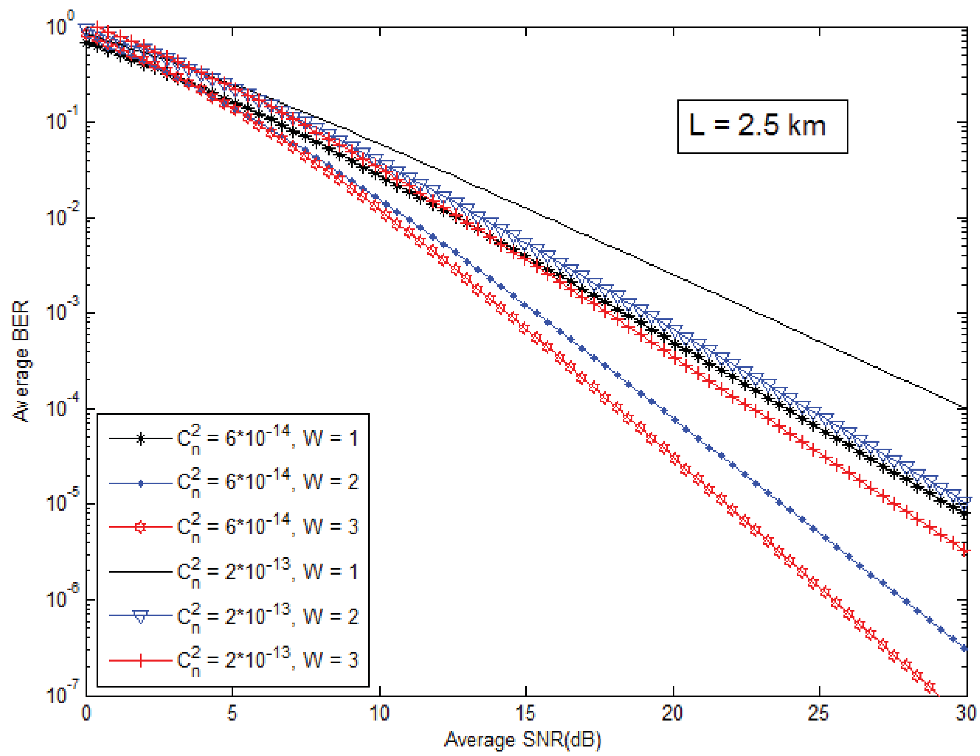

Fig. 4.16 Average BER for link length of 2.5 km with 60 mm aperture size

Table 4.5 shows the BER performance of FSO system with different diversity order (W = 1 to W = 6) at different distances varying from 1 km to 3 km at an interval of every 0.5 km. The BER of 9.94 X 10^{-5} is observed for moderate and 7.47 X 10^{-4} is observed for strong turbulence condition for the distance of 1 km between transmitter and receiver as shown in Table 4.4. BER is improved by almost 10 dB and 20 dB with diversity level of 2 and 3 respectively over the case when no diversity is applied for the distance of 1 km and moderate turbulence condition. For the strong turbulence condition, the improvement in BER of around 8 dB for diversity level 2 and further 10 dB with diversity level of 3 is observed. The BER is improved by around 5dB and further 8 dB with the application of a diversity of level 2 and 3 respectively compared to no diversity for moderate turbulence condition when the transmitter and receiver are 3 km apart. For the same distance and strong turbulence conditions, the BER is improved by around 10 dB and 6 dB for level 2 and 3 diversity respectively. A common observation can be drawn that the improvement in BER of almost 4 to 6 dB can be achieved with an increase in diversity for different distances with both moderate and strong turbulence conditions. The higher the level of diversity, higher will be the cost and complexity of the system.

For a standard high rate communication, the BER of 10^{-6} is necessary (Goldsmith, 2005). Looking at Table 4.5, it is obvious that for the standard BER requirements are not fulfilled even at the diversity level of 6 if the 60 mm receiver aperture is used with 20 dB SNR. This demands high SNR for better results. Table 4.6 reveals the results obtained with the SNR of 30 dB for the 60 mm receiver aperture.

Table 4.5 Average BER with 60 mm aperture at SNR of 20 dB

Diversity Order	Turbu-lence	D = 60 mm and SNR = 20 dB				
		L= 1 km	L=1.5 km	L= 2 km	L= 2.5 km	L= 3 km
W=1	M	9.94×10^{-5}	2.09×10^{-4}	3.40×10^{-4}	4.86×10^{-4}	6.39×10^{-4}
	S	7.47×10^{-4}	1.31×10^{-3}	1.85×10^{-3}	2.46×10^{-3}	3.04×10^{-3}
W=2	M	9.38×10^{-6}	2.49×10^{-5}	4.74×10^{-5}	7.52×10^{-5}	1.09×10^{-4}
	S	1.34×10^{-4}	2.84×10^{-4}	4.64×10^{-4}	6.67×10^{-4}	8.69×10^{-4}
W=3	M	2.85×10^{-6}	8.57×10^{-6}	1.76×10^{-5}	2.96×10^{-5}	4.54×10^{-5}
	S	5.68×10^{-5}	1.32×10^{-4}	2.29×10^{-4}	3.37×10^{-4}	4.67×10^{-4}
W=4	M	4.20×10^{-7}	1.49×10^{-6}	3.43×10^{-6}	6.23×10^{-6}	9.22×10^{-6}
	S	1.34×10^{-5}	3.53×10^{-5}	6.77×10^{-5}	1.06×10^{-4}	1.55×10^{-4}
W=5	M	1.03×10^{-7}	4.13×10^{-7}	1.03×10^{-6}	2.04×10^{-6}	3.48×10^{-6}
	S	4.61×10^{-6}	1.35×10^{-5}	2.75×10^{-5}	4.66×10^{-5}	6.93×10^{-5}
W=6	M	4.80×10^{-8}	2.05×10^{-7}	5.39×10^{-7}	1.08×10^{-6}	1.87×10^{-6}
	S	2.59×10^{-6}	8.02×10^{-6}	1.69×10^{-5}	2.84×10^{-5}	4.47×10^{-5}

M = Moderate turbulence and S = Strong turbulence

Table 4.6 Average BER of FSO system with 60mm aperture diameter at 30 dB SNR

Diversity Order	Turbu-lence	D = 60 mm and SNR = 30 dB				
		L= 1 km	L=1.5 km	L= 2 km	L= 2.5 km	L= 3 km
W=1	M	$5.37 X 10^{-7}$	$2.76 X 10^{-6}$	$5.05 X 10^{-6}$	$7.96 X 10^{-6}$	$1.41 X 10^{-5}$
	S	$1.58 X 10^{-5}$	$3.82 X 10^{-5}$	$6.78 X 10^{-5}$	$1.02 X 10^{-4}$	$1.41 X 10^{-4}$
W=2	M	$9.36 X 10^{-9}$	$4.91 X 10^{-8}$	$1.90 X 10^{-7}$	$3.15 X 10^{-7}$	$5.78 X 10^{-7}$
	S	$8.10 X 10^{-7}$	$2.73 X 10^{-6}$	$6.01 X 10^{-6}$	$1.06 X 10^{-5}$	$1.66 X 10^{-5}$
W=3	M	$1.04 X 10^{-9}$	$6.90 X 10^{-9}$	$2.36 X 10^{-8}$	$4.49 X 10^{-8}$	$9.09 X 10^{-7}$
	S	$1.70 X 10^{-7}$	$6.84 X 10^{-7}$	$1.68 X 10^{-6}$	$2.69 X 10^{-6}$	$5.40 X 10^{-6}$
W=4	M	$3.22X10^{-11}$	$2.90 X10^{-10}$	$1.29X10^{-9}$	$3.62X10^{-9}$	$1.66 X 10^{-8}$
	S	$1.35X10^{-8}$	$6.98 X10^{-8}$	$2.07X10^{-7}$	$4.38X10^{-7}$	$8.17 X10^{-7}$
W=5	M	$2.28X10^{-12}$	$2.80 X10^{-11}$	$1.43X10^{-10}$	$4.78X10^{-10}$	$1.20 X10^{-9}$
	S	$1.98X10^{-9}$	$1.24 X10^{-8}$	$4.23X10^{-8}$	$1.03X10^{-7}$	$1.99 X10^{-7}$
W=6	M	$3.20 X10^{-13}$	$7.42 X10^{-12}$	$4.19X10^{-11}$	$1.46X10^{-10}$	$3.85 X10^{-10}$
	S	$6.79 X10^{-10}$	$4.90 X10^{-9}$	$2.31X10^{-8}$	$3.23 X10^{-8}$	$9.03 X10^{-8}$

M = Moderate turbulence and S = Strong turbulence

From Table 4.6, it is evident that increment of 10 dB SNR achieves significant improvement in the performance with lower diversity order for all distances in both moderate and strong atmospheric turbulence conditions. For the distance of 1 km between transmitter and receiver, the BER observed without application of wavelength diversity is in the order of 10^{-7} for moderate turbulence and in order of 10^{-5} in strong turbulence condition. For the same distance, the diversity of level 2 provides BER which is 100 times better than the BER achieved without the application of diversity. Similar results are obtained using the diversity level of 3, which does not result in further improvement in BER for the distance of 1 km. For the distance from 1.5 km to 3 km, the BER observed without wavelength diversity is 10^{-6} for moderate turbulence condition, while for strong turbulence conditions the value in the order of 10^{-5} is obtained. With the diversity of level 2, the improvement of around 10 dB is observed for both moderate and strong turbulence conditions. The interesting observation worth mentioning is that the BER further improves by almost 10 times (10 dB) with a diversity of level 3 compared to level 2 for both turbulence conditions. The improvement of almost 20dB is obtained with wavelength diversity w=3 compared to diversity less scenario. The required BER for the modern communication (in order of

10^{-6}) is obtained with diversity level of 3 for all the distance under both turbulence condition. The BER can further be improved with an increase in the diversity level. There is an almost steady improvement of 10 dB is observed as diversity order increases from 3 to 6. However, considering cost and complexity of implementation, diversity order of 3 is adequate enough to mitigate atmospheric turbulence effect under both the turbulence conditions with acceptable BER for practical applications with an aperture size of 60 mm.

From the obtained results of outage probability and average BER of FSO system with wavelength diversity at 60 mm receiver aperture, it is clear that diversity order of 3 is sufficient to achieve reliable communication under both the turbulence scenario for distance up to 3 km. Further, it is also clear that increasing aperture size requires SNR of 30 dB to meet the requirement of the modern communication channel.

4.7 Conclusion

In this chapter, the performance of an FSO communication system over the EW channel model with wavelength diversity schemes is investigated. The mathematical expressions for the average BER and the outage probability have been derived. The results are obtained with an ideal (10 mm) and practical (60 mm) receiver aperture size. A performance enhancement as high as 10^5 in the outage probability and 10^3 in the BER is achieved in the case of moderate turbulence with diversity order 3 compared to no diversity with 10 mm aperture size. In the strong turbulence scenario, a consistent 20 dB and 10 dB improvement is achieved in the outage probability and average BER, respectively as the diversity order increases at 10 mm receiver aperture. The working of FSO system with practical receiver aperture size is examined with wavelength diversity. This technique is found effective for all turbulence conditions with practical receiver aperture size (60 mm). However, it is noteworthy to mention that FSO system with practical aperture size requires additional 10 dB SNR compared to ideal receiver aperture size to obtain average BER in the range of 10^{-6} for effective results under different turbulence conditions. Increasing aperture size decreases the performance improvement of FSO system. Results are also obtained with higher diversity order with both aperture sizes. It reveals that diversity order of 3 is adequate for the performance enhancement of FSO link under all turbulence conditions.

Chapter 5

Comparative Analysis of BER performance of FSO system with wavelength diversity under different turbulence conditions

Wavelength diversity technique has shown significant improvement in the performance of FSO system under different turbulence conditions with different channel models. The performance enhancement of system under moderate and strong turbulence condition using EW channel with this technique is seen in chapter 4. Use of wavelength diversity to improve the results of FSO system under weak turbulence using Lognormal channel is already explored and discussed in chapter 2. The performance enhancement of system with wavelength diversity under different turbulence conditions represented with single-channel model is still to be identified. In this chapter, the improvement in the BER of FSO system with wavelength diversity under weak turbulence using EW channel is explored. A comparative analysis of BER performance of wavelength diversity based FSO system under different turbulence conditions is carried out. In this work, BER results achieved using EW channel for different turbulence conditions is compared with the published results in the literature for different turbulence conditions using different channel models. Receiver aperture size of 10 mm and OC method at the receiver side is considered as adopted in the published articles in the literature.

5.1 Performance comparison of LN and EW

The Lognormal (LN) channel model is well accepted to characterize FSO channel under weak turbulence condition. In literature (Hassan Moradi, 2010), (Zhu, 2002), (Zhu, 2003), (2.25, 5.1-5.5) and (A. Viswanath, 2014), authors have opted this model to investigate the performance of FSO system under weak turbulence. The concept of wavelength diversity with this model is first time presented by Xarcha (V.Xarcha, 2012) to calculate the average BER of FSO system. The PDF of LN channel (Eq. 2.14) with wavelength diversity is written as

$$f_{I_w}(I_w) = \frac{1}{\sqrt{2\pi\sigma_w^2 I_w}} \exp\left[-\frac{(\ln(I_w)+\sigma_w^2/2)^2}{2\sigma_w^2}\right] \tag{5.1}$$

Using Eq. (5.1), authors (V.Xarcha, 2012) have derived a mathematical expression of BER considering OC method at receiver and presented numerical results for weak and moderate turbulence conditions at the link distance of 1 km and 1. 5 km with receiver aperture of 10 mm. Three wavelengths of 1550 nm, 850nm and 1310 nm have been chosen to apply wavelength diversity. The value of refractive index structure parameter C_n^2 is kept as $1 \times 10^{-14} m^{-2/3}$ and $5 \times 10^{-14} m^{-2/3}$ for weak and moderate turbulence, respectively. Same parameters has been chosen and applied in the Eq. (4.32) to obtain the BER performance of wavelength diversity based FSO system under weak to moderate condition using EW channel model. The comparison is presented in Fig. 5.1 to Fig. 5.4. In these results, the BER results of LN channel is plotted from ((V.Xarcha, 2012), Eq. 20).

Fig. 5.1 and Fig. 5.2 shows the BER performance comparison of wavelength diversity-based system under weak turbulence condition at a distance of 1 km and 1.5 km, respectively. It is clearly evident that performance of FSO system with wavelength diversity improves with both the channel model. In the case of LN model, the performance improvement of 70 dB observed at SNR of 20 dB with the diversity order of 3 compared to no diversity case at 1 km distance under weak turbulence. The same was of 40 dB with EW channel model. At the distance of 1.5 km, both channel model

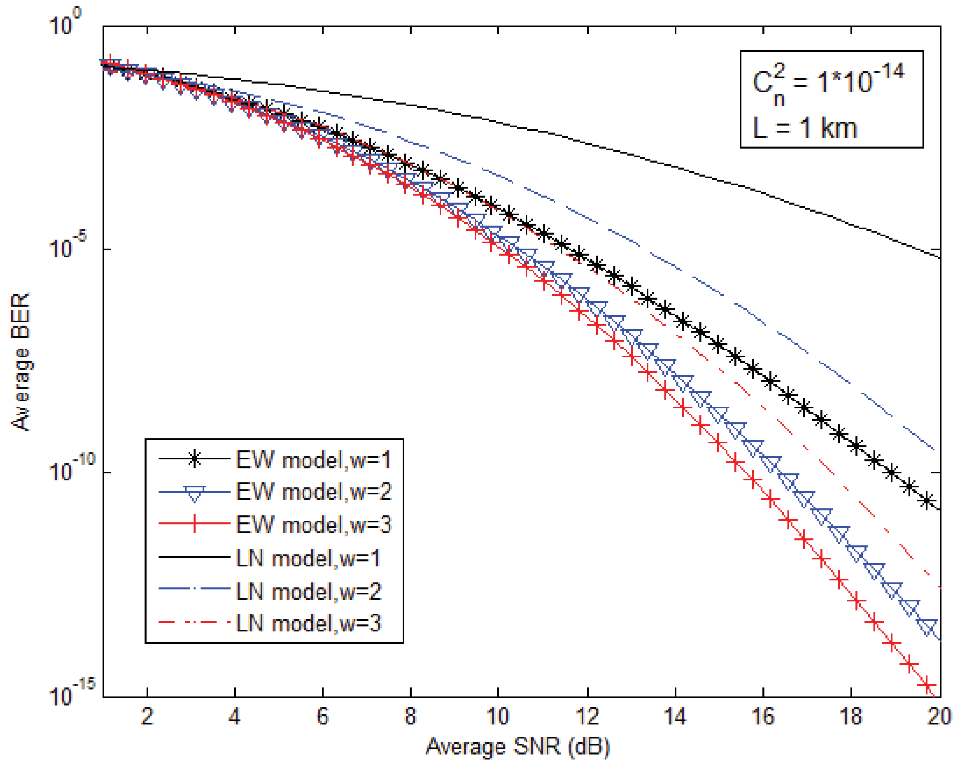

Fig. 5.1 BER Performance comparison of LN and EW with wavelength diversity

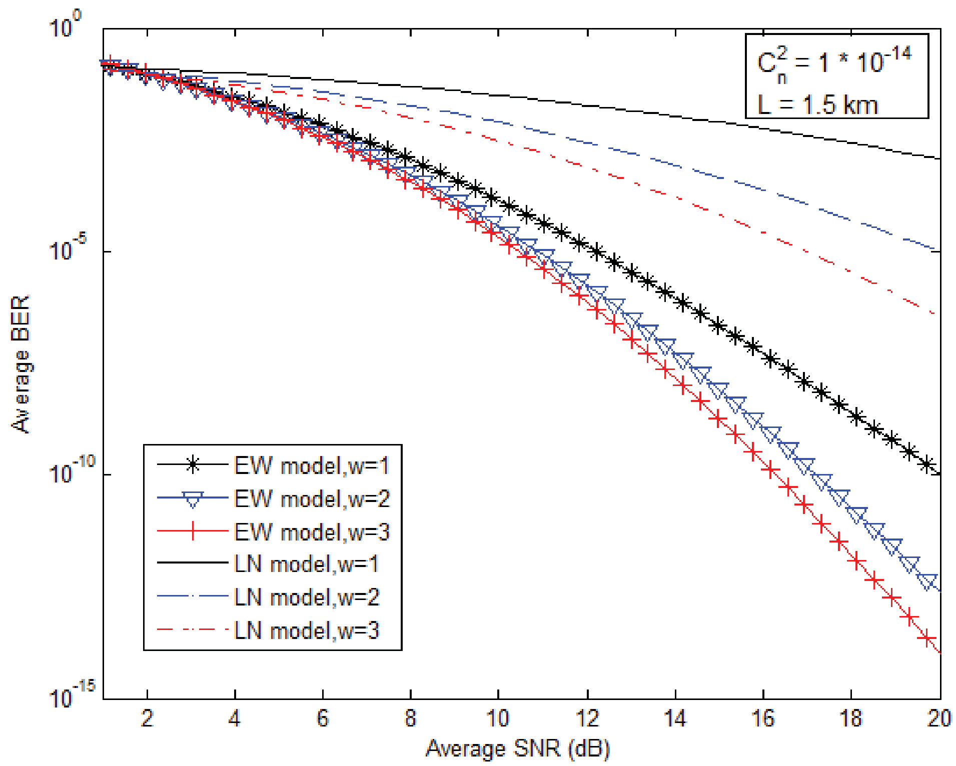

Fig. 5.2 BER Performance comparison of LN and EW under weak turbulence

with a diversity order of 3 give an equal improvement of 40 dB compared to no diversity case. However, the performance obtained with EW channel is 70 dB higher than that obtained with LN channel for all diversity level at the distance of 1.5 km. The similar trend is observed at the distance of 1 km. The detailed results are presented in Table 5.1.

Table 5.1 BER performance comparison between LN and EW under weak turbulence

Diversity order	D = 10 mm , SNR = 20 dB , $Cn^2 = 1 \times 10^{-14}$			
	L = 1 km		L = 1.5 km	
	Lognormal	EW	Lognormal	EW
W=1	6.28×10^{-6}	2.41×10^{-11}	1.16×10^{-3}	1.70×10^{-10}
W=2	2.51×10^{-10}	3.88×10^{-14}	9.74×10^{-6}	4.66×10^{-13}
W=3	2.69×10^{-13}	1.73×10^{-15}	3.45×10^{-7}	2.35×10^{-14}

It is apparent from Table 5.1 that BER performance obtained with EW channel with different diversity order is much higher compared to LN channel at both the distance under weak turbulence condition. The improvement in BER with EW channel is 50 dB, 40 dB and 20 dB higher than LN channel at diversity level of 1, 2 and 3, respectively at 1 km distance. This difference in the performance of both channels is further increases at a higher distance. At 1.5 km, performance improvement with EW is 70 dB higher at all diversity level compared to LN channel. Apparently, weak turbulence scenario characterized by EW channel does not require wavelength diversity to meet standard BER requirement of 10^{-6} (Goldsmith, 2005) at both the distance. Whereas, LN channel demands wavelength diversity to improve performance at distance of 1.5 km.

The BER results comparison between LN and EW under moderate turbulence is presented in Fig. 5.3 and Fig. 5.4 for the distance of 1 and 1.5 km, respectively. The BER performance achieved with EW channel is about 60 dB higher than that achieved with LN at 20 dB SNR for all diversity level at 1 km as shown in Fig. 5.3. This difference is further increased by 10 dB at distance of 1.5 km. The detailed results are presented in Table 5.2.

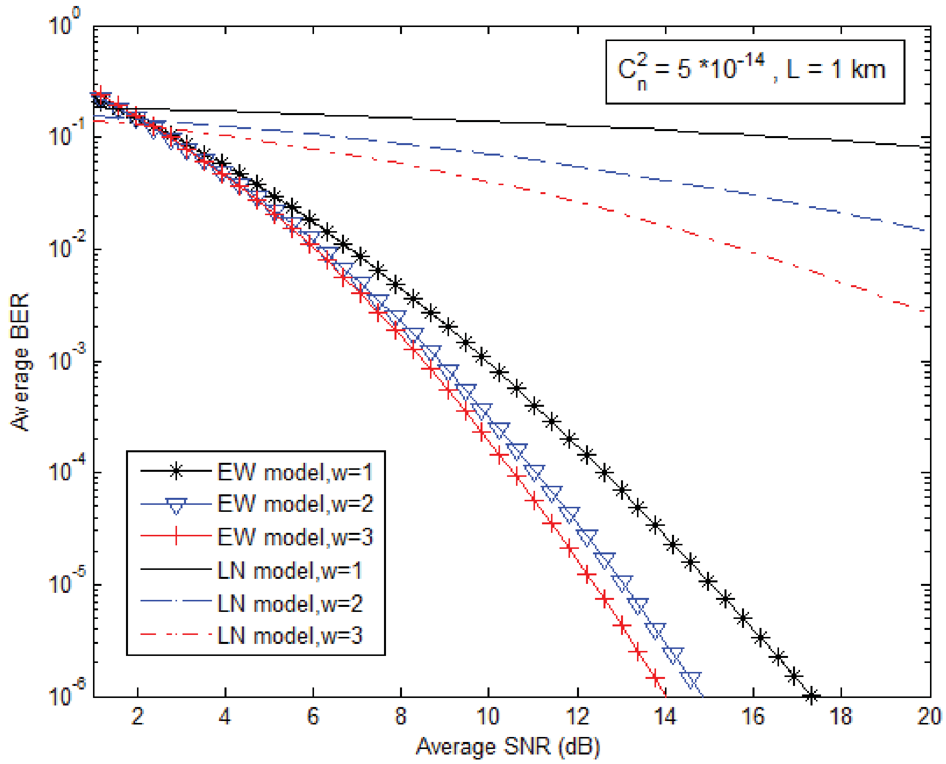

Fig. 5.3 Performance comparison of LN and EW under moderate turbulence

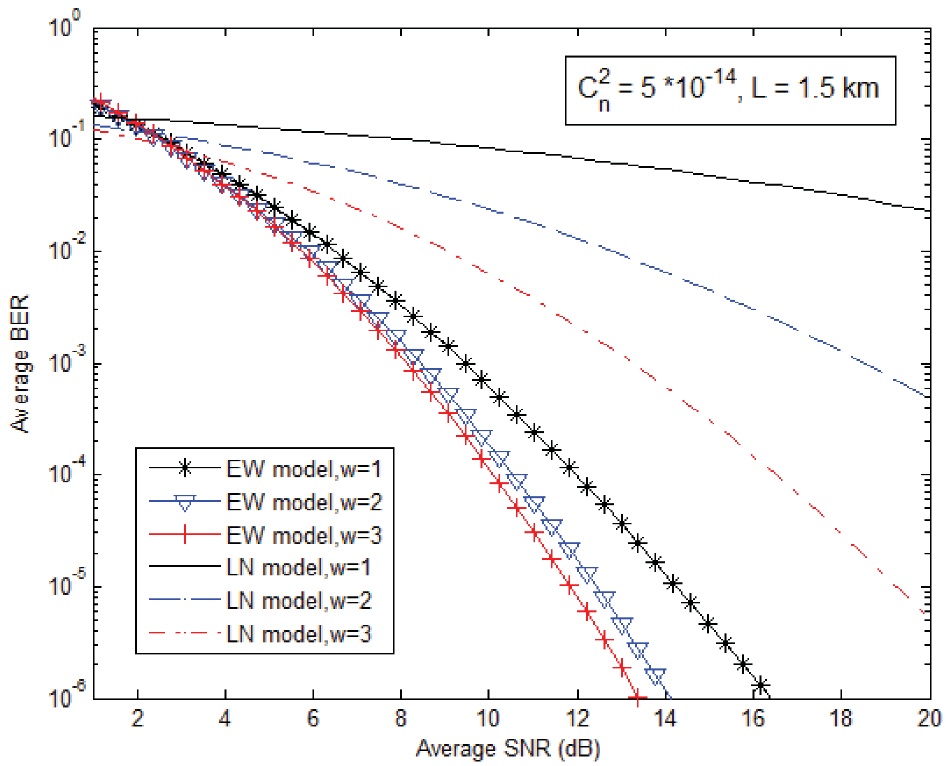

Fig. 5.4 Performance comparison of LN and EW under moderate turbulence

It is evident from the Table 5.2 that use of LN for moderate turbulence condition requires diversity order of 3 and more at the distance of 1 and 1.5 km, respectively to satisfy standard BER requirement of the modern communication channel. Whereas, use of EW channel fulfils it without using diversity for the same distances. So, use of EW channel is more suitable than LN channel while obtaining performance of FSO system under moderate turbulence condition.

Table 5.2 BER performance comparison between LN and EW under moderate turbulence

Diversity order	D = 10 mm ,	SNR = 20 dB ,		Cn^2= 5 X 10^{-14}
	L = 1 km		L = 1.5 km	
	Lognormal	EW	Lognormal	EW
W=1	2.28 X 10^{-2}	2.41 X 10^{-8}	8.20 X 10^{-2}	9.09 X 10^{-8}
W=2	4.47 X 10^{-4}	2.16 X 10^{-10}	1.44 X 10^{-2}	1.29 X 10^{-9}
W=3	4.98 X 10^{-6}	2.10 X 10^{-11}	2.60 X 10^{-3}	1.40 X 10^{-10}

From the comparison between LN and EW for different turbulence condition at distance of 1 and 1.5 km, it is clear that use of EW model to describe weak and moderate turbulence conditions achieves better performance for FSO system with and without diversity.

5.2 Performance comparison of EW and Gamma-Gamma channel

Gamma-Gamma (GG) channel is found suitable to define moderate and strong turbulence condition in FSO system. This model is used in the literature (Uysal, 2006), (Al-Habash, 2001) and (Gappmair, 2009) to investigate the performance of FSO system under moderate and strong turbulence condition without wavelength diversity. Similarly, FSO system performance under moderate and strong condition using EW model is investigated in (Barrios Porras, 2013). The performance of FSO system with wavelength diversity using GG is reported in (Nistazakis, 2012). In this article, authors have presented result for 1 km and 2 km distance under moderate and strong turbulence scenario. In this section, the performance of FSO system with wavelength diversity using EW is investigated and compared with the results presented in (Nistazakis, 2012). For moderate and strong turbulence condition, the value of C_n^2 is kept 6 X 10^{-14} and 2 X 10^{-13}, respectively. The result of GG with wavelength diversity is plotted using ((Nistazakis, 2012), Eq. 16) and the result of EW channel with wavelength diversity is obtained using Eq. (4.32).

Fig. 5.5 and Fig. 5.6 show the comparison results at 1 km distance under moderate and strong turbulence, respectively. It is apparent from the plots that average BER decreases with increase in diversity order for both channel model. Moderate turbulence represented by Gamma-Gamma model has shown improvement of 20 dB with a diversity order of 3 compared to no diversity case. The same is observed 30 dB with EW channel model which is 10 dB higher than the achieved results using GG model. In strong turbulence scenario, 20 dB improvement in the performance is observed with a diversity order of 3 compared to no diversity case with both channel models.

The comparison at 2 km distance for moderate and strong turbulence scenario is presented in Fig. 5.7 and Fig. 5.8, respectively. At the distance of 2 km, the BER obtained with GG model is in the range of 10^{-2} under moderate turbulence for diversity less scenario at 20 dB SNR. The same was in the range of 10^{-7} with EW model. The performance improvement of 20 dB is observed with both the model at diversity order of 3 compared to no diversity case. Similar results have been observed under strong turbulence condition at 2 km distance. Though the performance improvement achieved by both the channel models is similar under different turbulence condition, the use of EW channel achieves 50 dB and 30 dB higher performance compared to use of GG channel at moderate and strong turbulence scenario, respectively at 20 dB SNR. The detailed results are shown in Table 5.3.

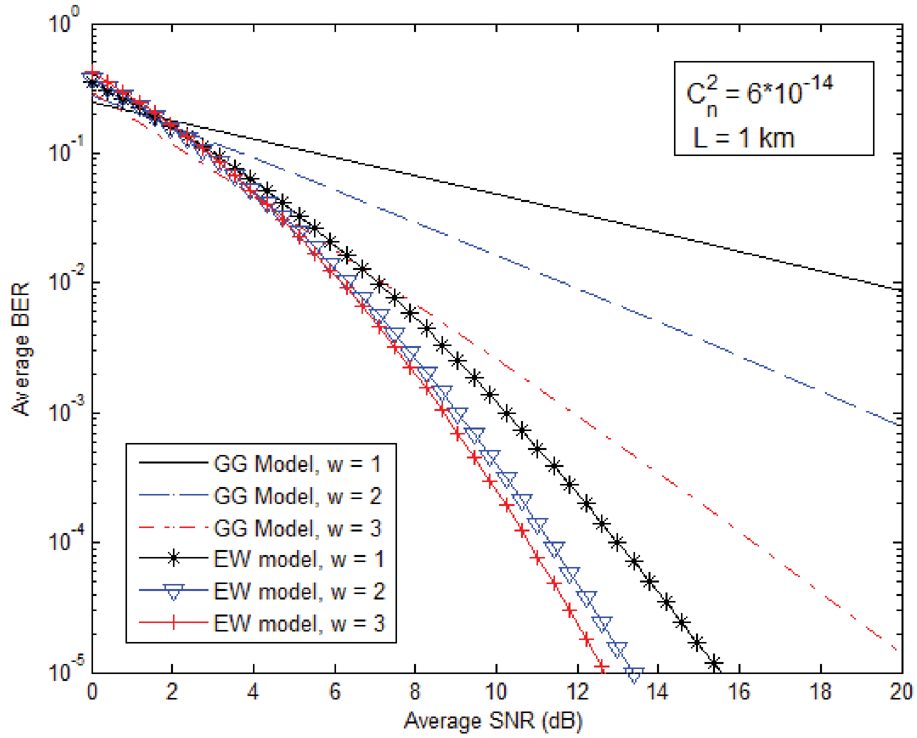

Fig. 5.5 Performance compassion of GG and EW for moderate turbulence condition

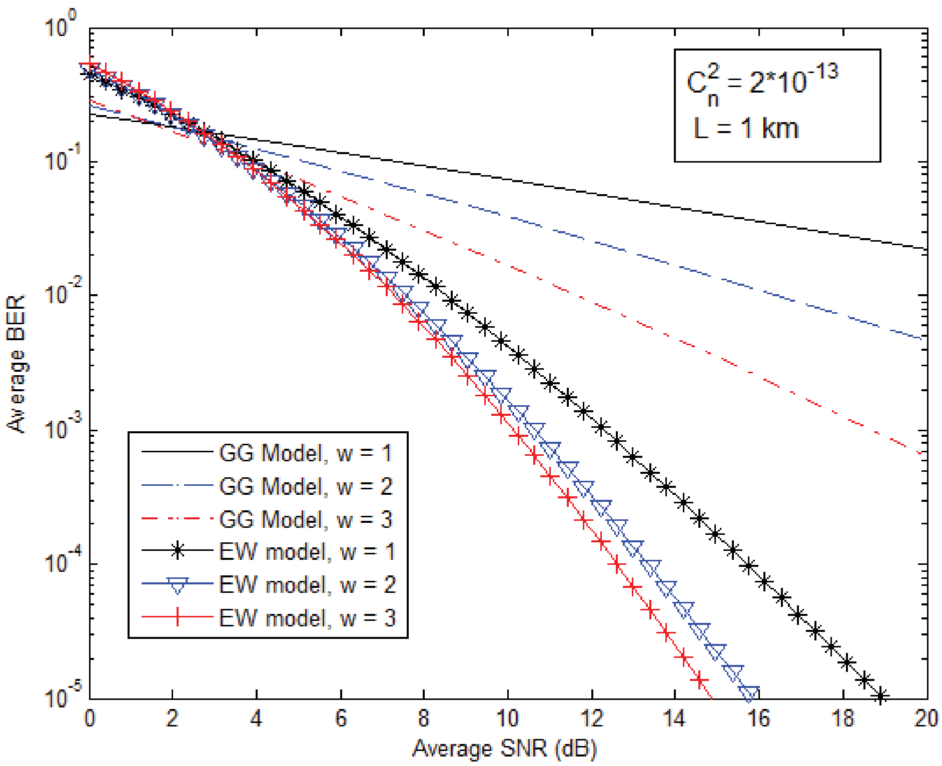

Fig. 5.6 Performance compassion of GG and EW for strong turbulence condition

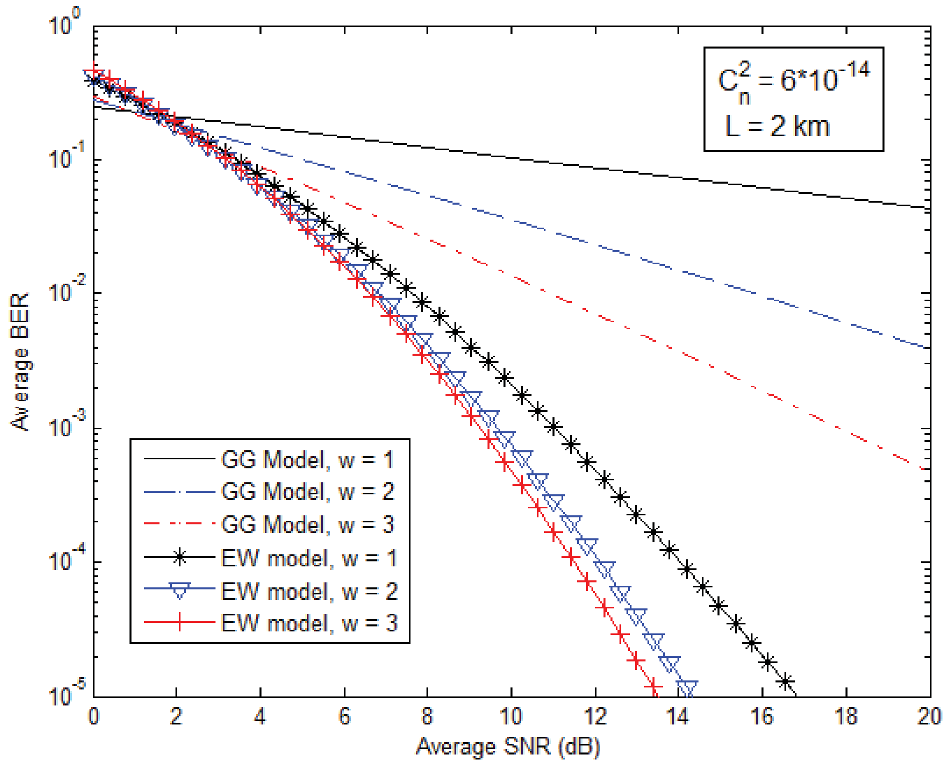

Fig. 5.7 Performance compassion at 2 km under moderate turbulence condition

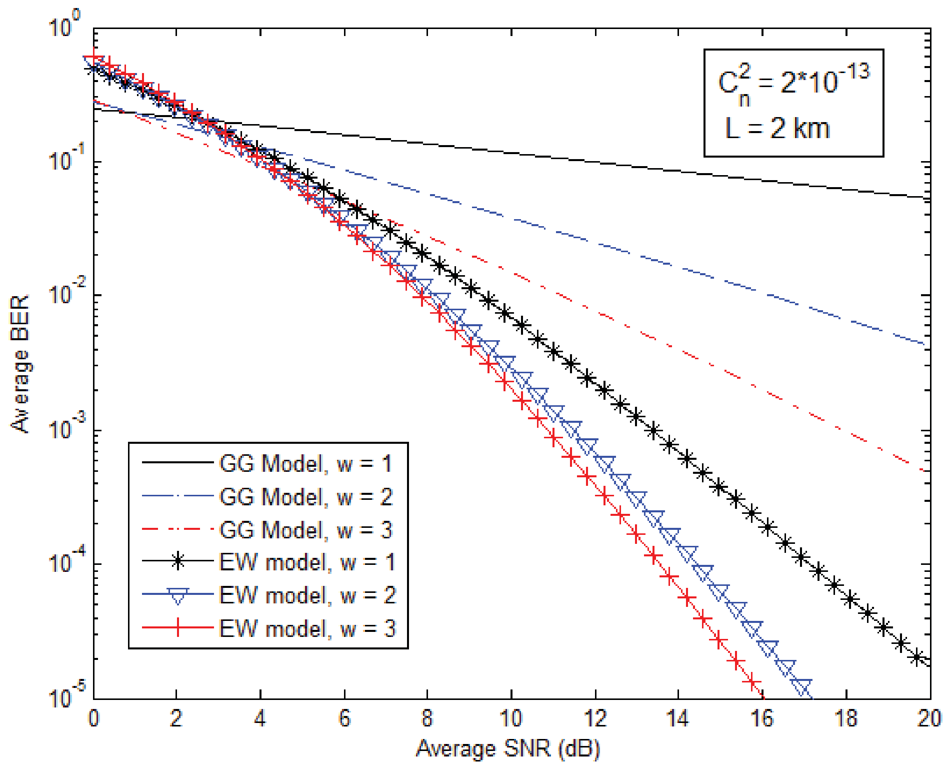

Fig. 5.8 Performance compassion at 2 km under strong turbulence condition

Table 5.3 Performance comparison between Gamma-Gamma and EW

Diversity order	Turbulence condition	D = 10 mm, SNR = 20dB			
		L = 1 km		L = 2km	
		GG	EW	GG	EW
W = 1	Moderate	8.50×10^{-3}	4.68×10^{-8}	4.23×10^{-2}	4.60×10^{-7}
	Strong	2.18×10^{-2}	2.46×10^{-6}	5.32×10^{-2}	1.21×10^{-5}
W = 2	Moderate	7.72×10^{-4}	4.68×10^{-10}	3.88×10^{-3}	9.10×10^{-9}
	Strong	4.59×10^{-3}	6.13×10^{-8}	4.20×10^{-3}	6.10×10^{-7}
W = 3	Moderate	1.39×10^{-5}	5.25×10^{-11}	4.69×10^{-4}	1.29×10^{-9}
	strong	6.39×10^{-4}	1.07×10^{-8}	4.61×10^{-4}	1.37×10^{-7}

As shown in Table 5.3, moderate and strong turbulence characterized by GG channel shows a consistent 10 dB improvement with higher diversity level at both the distances. The observed improvement is of about 25 dB with a diversity order of 3 compared to no diversity when turbulence condition is characterized by EW channel. Further, overall BER performance of FSO system using EW is much higher than that obtained with Gamma-Gamma under both the turbulence condition at a different distance. The channel characterized by EW has a maximum performance gain of about 60 dB and 40 dB over GG channel under moderate and strong turbulence condition, respectively. It is also apparent from Table 5.3 that moderate and strong turbulence characterized by EW channel does not require wavelength diversity at the distance of 1 km to meet standard BER (10^{-6}) requirement.

5.3 Performance comparison of EW and K channel

K channel is found suitable to represent strong turbulence condition (E.Jakeman, 1978) (Jakeman, 1980). Using this model, the performance of FSO channel under strong turbulence is investigated in (Kiasaleh, 2006) and (Uysal M., 2004). The performance improvement of FSO channel with wavelength diversity under strong turbulence using K channel is examined and reported in (Dhaval Shah, 2017). In this investigation, results are presented using 10 mm receiver aperture diameter for the distance of 2 and 3 km. This section presents the BER performance comparison of FSO system with wavelength diversity under strong turbulence using K and EW channel. Results are presented in Fig. 5.9 and Fig. 5.10 for the distance of 2 and 3 km, respectively considering OC method at receiver.

As shown in Fig. 5.9, the obtained BER at 30 dB SNR is in the range of 10^{-4} and 10^{-5} using K and EW channel, respectively in no diversity case at the distance of 2 km. Deployment of wavelength diversity improves the performance with both models. An improvement of around 4.5 dB is observed with a diversity order of 3 at same SNR compared to no diversity scenario when K channel is used to represent strong turbulence condition. The same was of around 20 dB with EW channel. It is clearly evident that performance of FSO with EW is much better with EW compared to K at the distance of 2 km. This trend continues even at a higher distance of 3 km. The BER performance comparison at 3 km distance is shown in Fig. 5.10. The BER performance of FSO system with wavelength diversity using K channel gives an improvement of about 10 dB with a diversity order of 3 compared to no diversity at 30 dB SNR. While the use of EW channel for the same system achieves an improvement of 20 dB with a diversity order of 3 compared to no diversity at same SNR. The detailed comparison is presented in Table 5.4.

Table 5.4 BER Performance comparison between K and EW

Diversity order	D = 10 mm , SNR = 30 dB , $Cn^2 = 2 \times 10^{-13}$			
	L = 2 km		L = 3 km	
	K	EW	K	EW
W=1	5.75×10^{-4}	1.57×10^{-5}	2.60×10^{-3}	3.38×10^{-5}
W=2	2.36×10^{-4}	8.50×10^{-7}	5.14×10^{-4}	2.29×10^{-6}
W=3	1.60×10^{-4}	1.95×10^{-7}	2.74×10^{-4}	5.91×10^{-7}

Table 5.4 reveals that performance of FSO system with wavelength diversity is much better when strong turbulence is categorized with EW channel. FSO system with EW channel obtains BER in the range of 10^{-7} at both the distance of 2 and 3 km at the diversity order of 3 which is 30 dB higher than the achieved with K channel. For a fair comparison, the result is also compared in the form of required SNR for the BER of 10^{-4} as reported in (Dhaval Shah, 2017) for OC method at receiver.

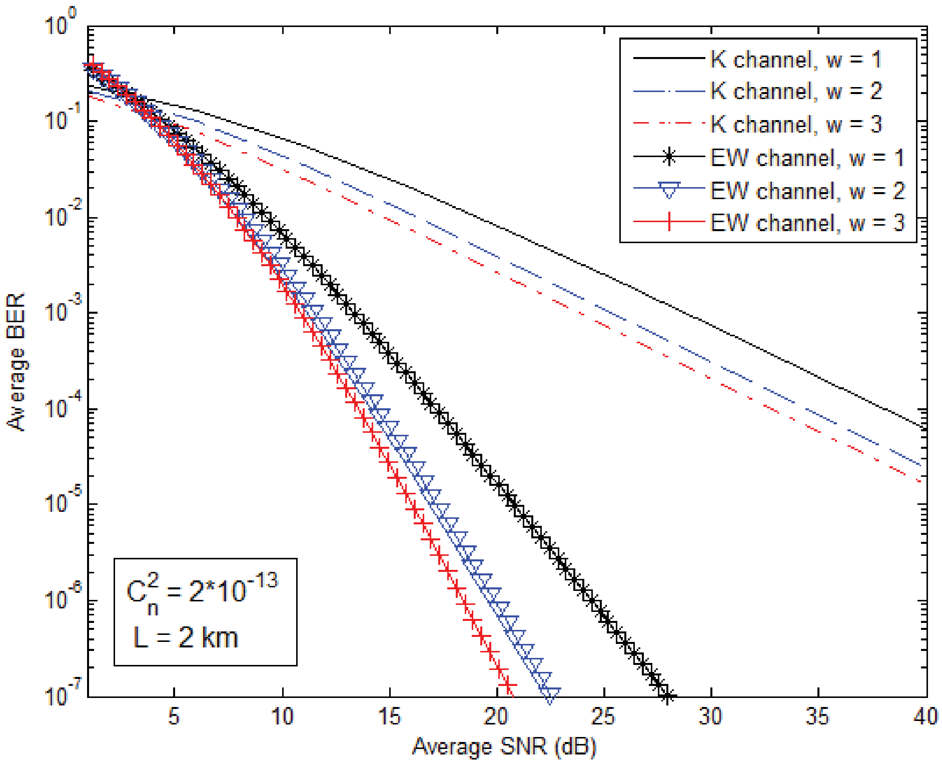

Fig. 5.9 Performance compassion using K and EW at 2 km

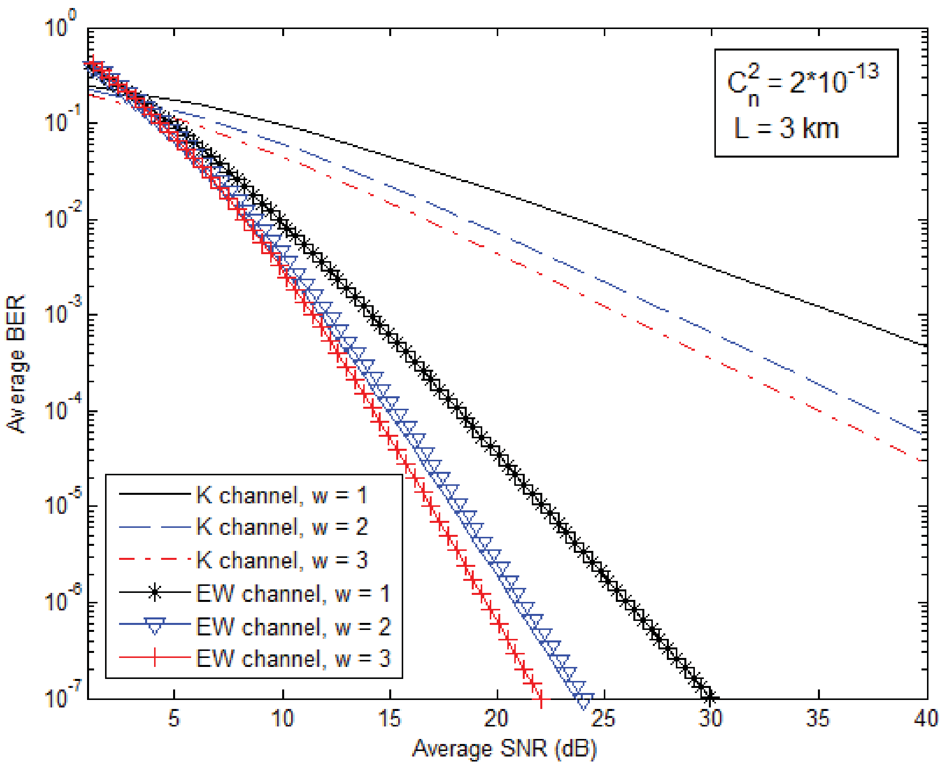

Fig. 5.10 Performance compassion using K and EW at 3 km

Table 5.5 Required SNR for the BER of 10^{-4}

Diversity order	L = 2 km		L = 3 km	
	K	EW	K	EW
W=1	38 dB	17 dB	47.5 dB	17.32
W=2	34 dB	14 dB	37.5 dB	14.96
W=3	33 dB	13 dB	35 dB	13.78

Table 5.5 shows the required SNR to obtain BER 10^{-4} with wavelength diversity using K and EW channel. Apparently, use of EW channel decreases the SNR requirement by 55% compared to K channel for the targeted BER in the case of without diversity at distance of 2 km. It decreases further by 5% with a diversity order of 3 at the same distance. The similar results are observed at distance of 3 km. Use of EW reduces the SNR requirement by 62% compared to K channel with a diversity order of 3 at the distance of 3 km for the targeted BER. From the table 5.4 and 5.5, it is clear that use of EW channel for strong turbulence condition is recommended to take maximum performance gain through wavelength diversity.

5.4 Conclusion

In this chapter, BER performance obtained using EW channel for different turbulence conditions is compared with the published results of the BER obtained by different channel models for different turbulence conditions using wavelength diversity. It is observed from the comparison that EW channel is more suitable to describe FSO channel under different turbulence conditions. Further, it is also revealed that use of EW to define different turbulence condition from weak to strong at the distance of 1 km does not require wavelength diversity to achieve standard BER requirement of 10^{-6}. FSO system with distance higher than 1 km, requires the wavelength diversity to improve the BER performance under strong turbulence condition. Use of EW channel to describe strong turbulence condition achieves 30 dB higher performance than classical K channel model with wavelength diversity order of 3.

Chapter 6

Conclusion and Future Scope

6.1 Conclusion

The performance improvement of FSO system under atmospheric turbulence condition using wavelength diversity technique is investigated and analyzed. This technique is applied for all types of turbulence condition vary from weak to strong. For strong turbulence condition, FSO channel is characterized by K channel model. Using this channel model, the performance improvement of FSO system with wavelength diversity under strong turbulence condition is evaluated. Average BER and outage probability have been considered as performance metrics. The results of average BER have been obtained by deriving a mathematical expression for all the three well-known signal combining techniques namely, OC, EGC and SC in the field of wireless communication. The results of average BER have shown that as diversity order increases the required SNR for the targeted BER decreases. The BER performance obtained by all three combining methods is also compared. For the average BER of 10^{-4}, the required SNR decreases by 25%, 13% and 5% with SC, OC and EGC method, respectively with the diversity order of 3 compared to no diversity case at the distance of 2 km. The same is 27%, 25% and 19% at the distance of 3 km respectively. Though SC achieves the maximum improvement, the required SNR values are 8-17 dB lesser in case of OC. It is also observed that EGC method requires 2-3 dB more SNR than OC method to achieve targeted BER. The performance of FSO system with wavelength diversity is also investigated in terms of outage probability. The results are obtained and presented for OC and SC methods. It is observed that outage probability is improved by 11 dB and 10 dB with OC and SC method, respectively with the diversity order of 3 compared to no diversity case. Use of OC method achieves 30 dB higher improvement in the outage probability than SC at different diversity levels. From the obtained results of average BER and outage probability, it is clear that wavelength diversity improves the performance of FSO system under strong turbulence condition. Further, the maximum performance improvement with wavelength diversity is observed using OC method at receiver. A comparison of the BER performance obtained with wavelength diversity and spatial diversity technique is also investigated. Wavelength diversity technique achieves 3 dB higher improvement than spatial diversity technique at diversity level of 2 under strong turbulence condition. This also validates the use of wavelength diversity technique to mitigate atmospheric turbulence effect.

The performance improvement of wavelength diversity based FSO system under moderate to strong turbulence condition using EW channel is investigated and reported. The performance is found by deriving a mathematical expression of average BER and outage probability considering OC method at the receiver. The effect of receiver aperture size on the performance is also investigated. Numerical results are obtained and presented for the diversity order up to 6 for the 10 mm and 60 mm receiver aperture size. At 10 mm receiver aperture, wavelength diversity increases the performance as high as 10^5 in the outage probability and 10^3 in the BER at the 20 dB SNR under moderate turbulence with diversity order 3 compared to no diversity. Whereas, a consistent improvement of 20 dB and 10 dB is observed in the outage probability and average BER, respectively at the same SNR as the diversity order increases. It is observed that as aperture size increases the performance of FSO decreases. The performance improvement observed with 60 mm aperture size at 20 dB SNR is less compared to 10 mm receiver aperture for both the turbulence conditions. The BER in the range of 10^{-6} is achieved with the diversity order of 6 under strong turbulence condition. Increasing SNR by 10 dB achieves the same BER range with the diversity order of 3 under strong turbulence condition. From the obtained results, it is clear that diversity order of 3 is sufficient with practical aperture size to meet the need of modern communication.

The BER performance of wavelength diversity based FSO system under different turbulence conditions characterizes by EW channel model is compared with the BER performance reported considering different classical models for different turbulence conditions. It is clear from this analysis that weak and moderate turbulence condition defined by EW channel for the distance up to 1 km does not require wavelength diversity to achieve the BER of 10^{-6}. At the higher distance, wavelength diversity significantly improve the performance if the turbulence condition is represented by EW channel. It is observed that strong turbulence condition represented by EW channel achieves 30 dB higher performance than classical K channel model with wavelength diversity order of 3.

From this work, it is established that wavelength diversity significantly improves the performance of FSO system under all turbulence conditions. Use of EW channel to characterize different turbulence conditions is strongly recommended to take maximum gain of wavelength diversity. It is also proven that wavelength diversity order of 3 is sufficient to meet modern communication need with practical FSO system.

6.2 Future scope of work

The work presented in this thesis has considered OOK scheme for modulation. Looking at the power efficiency provided by PPM scheme, the performance of FSO with wavelength diversity using PPM can also be investigated. Further, the approach presented in this thesis can be further expanded by hardware realization and prototype development. This also helps to determine cost and complexity of the wavelength diversity technique implementation which has not been considered in this work. The concept of cooperative communication can also be explored by putting a center hub between two terminals where direct LOS is not available.

References

Abramowitz, Milton, and Irene A. Stegun. "Handbook of mathematical functions: with formulas, graphs, and mathematical tables." 1972.

Al-Habash, M. A., Larry C. Andrews, and Ronald L. Phillips. "Mathematical model for the irradiance probability density function of a laser beam propagating through turbulent media." *Optical Engineering* 40.8 (2001): 1554-1562.

Alouini, M-S., and Marvin K. Simon. "Performance of generalized selection combining over Weibull fading channels." *IEEE Vehicular Technology Conference, VTC-2001*. IEEE, 2001. 1735-1739.

Alzubi, Jafar A., Omar A. Alzubi, and Thomas M. Chen. *Forward error correction based on algebraic-geometric theory*. Springer International Publishing, 2014, 2014.

Andrews, Larry C. "Aperture-averaging factor for optical scintillations of plane and spherical waves in the atmosphere." *Journal of Optical Society of America* 9.4 (1992): 597-600.

Andrews, Larry C., and Ronald L. Phillips. *Laser beam propagation through random media*. Vol. 152. Bellingham: SPIE press, 2005.

Andrews, Larry C., Ronald L. Phillips, and Cynthia Y. Hopen. *Laser beam scintillation with applications*. Vol. 99. SPIE press, 2001.

Andrews, Larry C., Ronald L. Phillips, and Cynthia Y. Hopen. "Aperture averaging of optical scintillations: power fluctuations and the temporal spectrum." *Waves in Random Media* 2000: 53-70.

Barrios Porras, Ricardo. "Exponentiated Weibull fading channel model in free-space optical communications under atmospheric turbulence." *Optics & Laser Technology* 45 (2013): 13-20.

Barrios, Ricardo, and Federico Dios. "Exponentiated Weibull model for the irradiance probability density function of a laser beam propagating through atmospheric turbulence." *Optics & Laser Technology 45*. 2013. 13-20.

Bemard L. Edwards, Stephen A. Townes, Abhijit Biswas, David R. Bold, Roy S. Bondurant, Don Boroson, Jamie W Bumside, David 0. Caplan, Alan E. DeCew, Ramon DePaula, Richard J. Fitzgerald, et.al. "The Mars Laser Communication Demonstration." 2004: 1-15.

Chan, Vincent WS. "Free-space optical communications." *Journal of Lightwave technology* 24.12 (2006): 4750-4762.

Cheng, Mingjian, Lixin Guo, and Yixin Zhang. "Scintillation and aperture averaging for Gaussian beams through non-Kolmogorov maritime atmospheric turbulence channels." *Optics express* 23.25 (2015): 32606-32621.

Churnside, James H. "Aperture averaging of optical scintillations in the turbulent atmosphere." *Applied Optics* 30.15 (1991): 1982-1994.

Crane, Robert K., and Paul C. Robinson. "ACTS propagation experiment: rain-rate distribution observations and prediction model comparisons." *Proceedings of the IEEE*. 1997. 946-958.

D. K. Kumar, Y. S. S. R. Murthy, and G. V. Rao. "Hybrid cluster based routing protocol for free-space optical mobile ad hoc networks (FSO/RF MANET)." *Proceedings of the International Conference on Frontiers of Intelligent Computing: Theory and Applications (FICTA)*. Berlin Heidelberg: Springer , 2013. 613-620.

D. Shah, D. Kothari. "BER performance of FSO link under strong turbulence condition with different coding techniques." *International Journal of Computer Science & Communication* 8.1 (2017): 4-9.

Derenick, Jason, Christopher Thorne, and John Spletzer. *Hybrid Free-space Optics/Radio Frequency (FSO/RF) networks for mobile robot teams*. Swarms to Intelligent Automata. Netherlands: Springer, 2005.

Dhaval Shah, Bhavin Nayak, and Dharmendra Jethawani. "Study of different atmospheric channel models." *International Journal of Electronics and Communication Engineering & Technology (IJECET)* 5.1 (2014): 105-112.

Dhaval Shah, Dilip Kumar Kothari, Anjan K. Ghosh,. "Bit error rate analysis of the K channel using wavelength diversity,." *Optical Engineering* 56.5 (2017): 056106 (1-6).

Dhaval Shah, Dilipkumar Kothari. "BER Performance of Lognormal Channel Model with Imperfect CSI for Free Space Optical Communication." *Trends in Opto-Electro & Optical Communications* 2.3 (2012): 1-7.

—. "Implementation of FSO Link for Full Duplex Short Range." *Journal of Electronic Design Technology* 7.2 (2016): 8-15.

—. "Mitigation of Fog and Rain Effects in Free-Space Optical Transmission Using Combined Diversity." *International Conference on Computer and Communication Technologies.* Hyderabad: Springer, 2015.

—. "Optimization of 2.5 Gbps WDM-FSO link range under different rain conditions in Ahmedabad." *11th IEEE India conferenc INDICON-2014*. Pune: IEEE, 2014.

E. S. Oh, J. C. Ricklin, G. C. Gilbreath, N. J. Vallestero, and F. D. "Optical turbulence model for laser propagation and imaging applications." *Free-Space Laser Communication and Active Laser Illumination III*. SPIE, 2004. 25-32.

E.Jakeman, P. N. Pusey. "A model for non-Rayleigh sea echo." *IEEE Transactions on antennas and propagation* 24 (1976): 806-814.

E.Jakeman, P. N. Pusey. "The Significance of K distributions in scattering experiments." *Physical Review Letters* 40 (1978): 546-550.

Eardley, P. L., and D. R. Wisely. "1 Gbit/s optical free space link operating over 40 m system and applications." *IEE Proceedings-Optoelectronics*. IEEE, 1996. 330-333.

F. Xu, M. A. Khalighi, P. Causse, and S. Bourennane. "Performance of coded time-diversity free-space optical links." *Biennial Symposium on Communications*. Kingston, ON, Canada: IEEE, 2008. 146-149.

Fang, Zhigang, Burton R. Patterson, and Malcolm E. Turner. "Modeling particle size distributions by the Weibull distribution function." *Materials characterization* 31.3 (1993): 177-182.

Fried, D. L. *Theoritical Analysis of Apreture Averaging* . CA: Optical Science Consultants, 1973.

fSONA, System. *Optical Wireless Products*. n.d. 2017. <http://www.fsona.com>.

G. Fletcher, T. Hicks and B. Laurent. "The SLIEX optical interorbit link experiment." 3 (1991): 273-279.

G. L. Bastin, L. C. Andrews, R. L. Phillips, R. A. Nelsond. "Measurements of aperture averaging on bit-error-rate." 2005.

Gagliardi, Robert M., and Sherman Karp. *Optical communications*. New York: Wiley-Interscience, 1976.

Gappmair, Wilfried, and Markus Flohberger. "Error performance of coded FSO links in turbulent atmosphere modeled by gamma-gamma distributions." *IEEE Transactions on wireless communications* 8.5 (2009): 2209-2213.

Giggenbach, D.,Wilkerson,B.,Henniger,H.,Perlot N. "Wavelength-diversity transmission for fading mitigation in the atmospheric optical communication channel." *SPIE OPTICS + PHOTONICS*. San Diego, California, United States: SPIE, 2006. 63041H-1.

Goldsmith, Andrea. *Wireless Communication* . Cambridge university press,, 2005.

Goodwin, F. E. "A review of operational laser communication systems." *IEEE proceedings*. IEEE, 1970. 1746-1752.

Grumman, Northop. *Adaptive Optical System*. n.d. 24 April 2017. <http://www.northropgrumman.com/BusinessVentures/AOAXinetics/IntelligentOptics/Technology/Pages/AdaptiveOpticalSystem.aspx>.

H. G. Sandalidis, T. A. Tsiftsis, K. Karagiannidis and M. Uysal. "BER performance of FSO links over strong atmospheric turbulence channels with pointing errors." *IEEE Communications Letters*. IEEE, 2008. 44-46.

H. Kaushal, V. Kumar, A. Dutta, H. Aennam, H. Aennam, V. Jain. "Experimental study on beam wander under varying atmospheric turbulence conditions." *IEEE photon Technology Letters* 23.22 (2011): 1691-1693.

H. Moradi, M. Falahpour, H. H. Refai, and P. G. LoPresti. "BER analysis of optical wireless signals through lognormal fading channels with perfect CSI." *17th International Conference on Telecommunications (ICT)*. IEEE , 2010. 493-497.

H. Moradi, M. Falahpour, H. H. Refai, P. G. LoPresti,M. Atiquzzaman. "On the capacity of hybrid FSO/RF links." *Global Telecommunications Conference (GLOBECOM 2010)*. Miami, FL, USA: IEEE, 2010.

Hagenauer, Joachim, and Erich Lutz. "Forward error correction coding for fading compensation in mobile satellite channels." *IEEE Journal on Selected Areas in Communications* 5.2 (1987): 215-225.

Hassan Moradi, Maryam Falahpour, Hazem H. Refai, Peter G. LoPresti. "BER analysis of optical wireless signals through lognormal fading channels with perfect CSI." *Telecommunications (ICT),IEEE 17th International Conference*. IEEE, 2010. 493-497.

Hemmati, H. "Deep space optical communications and naviation series." 2006.

Henniger, Hennes, and Otakar Wilfert. "An Introduction to Free-space Optical Communications." *Radioengineering* 19.2 (2010): 203-212.

Hilal A. Fadhil, Angela Amphawan, Hasrul A.B. Shamsuddin,Thanaa Hussein Abd, Hamza M.R. Al-Khafaji, S.A. Aljunid and Nasim Ahmed. "Optimization of free space optics parameters: An optimum solution for bad weather conditions." *Optik-International Journal for Light and Electron Optics* 124.19 (2013): 3969-3973.

Hranilovic, Steve, and David A. Johns. "A multilevel modulation scheme for high-speed wireless infrared communications." *IEEE International Symposium on Circuits and Systems,(ISCAS'99)*. IEEE, 1999. 338-341.

I. Gradshteyn, I. Ryzhik, , A. jeffrey and D. Zwillinger. *Table of integrals, series, and products*. New York: Academic press, 2007.

Ibrahim, M. M., and A. M. Ibrahim. "Performance analysis of optical receivers with space diversity reception." *IEE Proceedings-Communications*. IEEE, 1996. 369-372.

ITU. "Prediction methods required for the design of terrestrial free-space optical links." *ITU*. International Telecommunication Union. 2007.

J. A. Anguita, I. B. Djordjevic, M. A. Neifeld, and B. V. Vasic. "High-rate error-correction codes for the optical atmospheric channel." *Optics and Photonics 2005. International Society for Optics and Photonics*. SPIE, 2005. 58920V-1-58920V-7.

Jakeman, E. "On the statistics of K-distributed noise." *Journal of Physics A: Mathematical and General* 13 (1980): 31-48.

Juan C. Juarez, Anurag Dwivedi, A. Roger Hammons, Jr., Steven D. Jones, Vijitha Weerackody, and Robert A. Nichols. "Free-space optical communications for next-generation military networks." 2006: 46-51.

K. P. Peppas, F. Lazarakis, A. Alexandridis, and K. Dangakis. "Simple, accurate formula for the average bit error probability of multiple-input multiple-output free-space optical links over negative exponential turbulence channels." *Optics letters* 37.15 (2012): 3243-3245.

Kamugisha Kazaura, Kazunori Omae, Toshiji Suzuki, Mitsuji Matsumoto, Edward Mutafungwa, Timo O. Korhonen, Tadaaki Murakami, Koichi Takahashi, Hideki Matsumoto, Kazuhiko Wakamori, and Yoshinori Arimoto. "Enhancing performance of next generation FSO communication systems using soft computing based predictions." *Optics Express* 14.12 (2006).

Kaushal, Hemani, and Georges Kaddoum. "Optical communication in space: Challenges and mitigation techniques." IEEE Communications Surveys & Tutorials , 2017. 57-96.

Kiasaleh, Kamran. "Performance of coherent DPSK free-space optical communication systems in K-distributed turbulence." *IEEE transactions on communications* 54.4 (2006): 604-607.

Kiasaleh, Kamran. "Performance of APD-based, PPM free-space optical communication systems in atmospheric turbulence." *IEEE Transactions on Communications*. 2005. 1455-1461.

Killinger, D. "Free space optics for laser communication through the air." 13.10 (2002): 36-42.

Kim, Isaac I., and Eric Korevaar. "Availability of free space optics (FSO) and hybrid FSO/RF systems." *International Symposium on the convergence of IT and Communications*. Denver, CO, United States: SPIE., 2001. 84-95.

L. C. Andrew, R. L. Phillips, C. Y. Hopen and M. A. Al-habash. "Theory of optical scintillation." *Journal of Optical Society America* 16.6 (1999): 1417-1429.

Langer, R. M. "Effects of atmospheric water vapour on near infrared transmission at sea level." 1957.

Lightpointe. *How to design a reliable FSO system*. Lightpointe. Light pointe white paper series, 2009.

Long, Ronald K. "Atmospheric attenuation of ruby lasers." *Proceedings of the IEEE*. IEEE, 1963. 859-860.

Lupupa, Mzabalazo, and Mqhele E. Dlodlo. "Performance of MIMO system in Weibull fading channel-Channel capacity analysis." *IEEE EUROCON 2009*. IEEE, 2009. 1735-1739.

M.A. Khalighi, N. Aitamer, N. Schwartz, S. Bourennane. "Turbulence mitigation by aperture averaging in wireless optical systems." *10th International Conference on Telecommunications, ConTEL 2009.* . Zarbeg, Croatia: IEEE, 2009. 59-66.

M.Bass. *Atmospheric optics*. Vol. 5. McGraw-Hill, 2010.

Mahalati, Reza Nasiri, and Joseph M. Kahn. "Effect of fog on free-space optical links employing imaging receivers." *Optics express* 20.2 (2012): 1649-1661.

Majumdar, Arun K., and Jennifer C. Ricklin. *Free-space laser communications: principles and advances*. Springer Science & Business Media, 2008.

Moradi, H.,Falahpour,M.,Reafi,H.H.,LoPresti,P.G.,&Atiquzzaman,M. "Availability modeling of FSO/RF mesh networks through turbulence-induced fading channels." *INFOCOM IEEE Conference on Computer Communications Workshops*. San Diego, CA, USA,: IEEE, 2010. 1-5.

Mudholkar, Govind S., and Deo Kumar Srivastava. "Exponentiated Weibull family for analyzing bathtub failure-rate data." *IEEE Transactions on Reliability* 42.2 (1993): 299-302.

N. Perlot, D. Fritzsche. *Aperture-Averaging - Theory and Measurements* . Germany: German Aerospace Center (DLR), D-82234 Wessling, n.d.

Nistazakis, H. E., V. D. Assimakopoulos, and G. S. Tombras. "Performance estimation of free space optical links over negative exponential atmospheric turbulence channels." *OPTIK-International Journal for Light and Electron Optics* 122.24 (2011): 2191-2194.

Nistazakis, Hector E. "A time-diversity scheme for wireless optical links over exponentially modeled turbulence channels." *Optik-International Journal for Light and Electron Optics* 124.13 (2013): 1386-1391.

Nistazakis, Hector E., and George S. Tombras. "On the use of wavelength and time diversity in optical wireless communication systems over gamma–gamma turbulence channels." *Optics & Laser Technology* 44.7 (2012): 2088-2094.

P. Barbier, D. Rush, M. Plett, and P. Polak-Dingels. "Performance improvement of a laser communication link incorporating adaptive optics." *Proc. SPIE*. SPIE, 1998. 93-102.

Parenti, Ronald R., and Richard J. Sasiela. "Distribution models for optical scintillation due to atmospheric turbulence." 2005.

Parikh, Jolly, and V. K. Jain. "Study on statistical models of atmospheric channel for FSO communication link." *International Conference on Current Trends in Technology (NUiCONE-2011)*. Ahmedabd: IEEE, 2011. 1-7.

Peppas, Kostas P., et al. "Simple, accurate formula for the average bit error probability of multiple-input multiple-output free-space optical links over negative exponential turbulence channels." *Optics letters* (2012): 3243-3245.

Popoola, Wasiu O., Zabih Ghassemlooy, and Vahid Ahmadi. "Performance of sub-carrier modulated free-space optical communication link in negative exponential atmospheric turbulence environment." *International Journal of Autonomous and Adaptive Communications Systems.* 1.3 (2003): 342-355.

Prudnikov, Anatoliĭ Platonovich. *Integrals and series*. Vol. 3. Amsterdam: Gordon and Breach Science, 1988.

S. S. Muhammad, T. javornik, I. Jelovcan, E. Leitgeb, and O. Koudelka. "Reed solomon coded PPM for terrestrial FSO links." *International Conference on Electrical Engineering.* Lahore, Pakistan: IEEE, 2007. 1-5.

Schleher, D. C. "Radar detection in Weibull clutter." *IEEE Transactions on Aerospace and Electronic Systems* 12.6 (1976): 736-743.

Schuster, John. "Free space optics technology overview." 2002.

Schwartz, N.H.,Vedrenne ,N.,Michau,V.,Velluet,M.T.,& Chazallet,F. "Mitigation of atmospheric effects by adaptive optics for free-space optical communications." *SPIE LASE: Lasers and Applications in Science and Engineering. International Society for Optics and Photonics*. SPIE, 2009. 72000J-72000J.

Seguro, J. V., and T. W. Lambert. "Modern estimation of the parameters of the Weibull wind speed distribution for wind energy analysis." *Journal of Wind Engineering and Industrial Aerodynamics* 85.1 (2000): 75-84.

Shin, Etty J., and Vincent WS Chan. "Optical communication over the turbulent atmospheric channel using spatial diversity." *Global Telecommunications Conference*. Taipei, Taiwan: IEEE, 2002. 2055-2060.

Trisno, Sugianto. "Design and analysis of advanced free space optical communication systems." 2006.

Tsiftsis, T.A.,Sandalidi,H.G.,Karagiannidis,G.K.,Uysal M. "Optical wireless links with spatial diversity over strong atmospheric turbulence channels." *IEEE Transactions on Wireless Communications* 8.2 (2009): 951-957.

Uysal M., and Jing Li. "BER performance of coded free-space optical links over strong turbulence channels." *IEEE Vehicular Technology Conference, VTC 2004-Spring*. 2004. 168-172.

Uysal, Murat, Jing Li, and Meng Yu. "Error rate performance analysis of coded free-space optical links over gamma-gamma atmospheric turbulence channels." *IEEE Transactions on wireless communications* 5.6 (2006): 1229-1233.

V.Xarcha, A.N. Stassinakis,H.E. Nistazakis,G.P.Latsas,M.P.Hanias,G.S. Tombras. "Wavelength Diversity for Free Space Optical Systems: Performance Evaluation over Log Normal Turbulence Channels." *19th International Conference on Microwaves,Radar and wireless Communications (MIKON)*. Warsaw,Poland: IEEE, 2012. 678-683.

Vavoulas, Alexander, Harilaos G. Sandalidis, and Dimitris Varoutas. "Weather effects on FSO network connectivity." *Journal of Optical Communications and Networking* 4.10 (2012): 734-740.

Vorontsov, M. A., G. W. Carhart, and J. C. Ricklin. "Adaptive phase-distortion correction based on parallel gradient-descent optimization." *Optics letters* 22.12 (1997): 907-909.

W. Hameed, S. S. Muhammad and N. M. sheikh. "Integration scenarios for free space optics in next generation (4G) wirelss networks." *International symposium on Communication Systems Networks and Digital Signal Processing*. Newcastle upon Tyne, UK: IEEE, 2010. 571-575.

Wainright, Eric, Hazem H. Refai, and James J. Sluss Jr. "Wavelength diversity in free-space optics to alleviate fog effects." *Free-Space Laser Communication Technologies XVII*. Bellingham, WA,: SPIE, 2005. 110-118.

Wainright, Eric, Hazem H. Refai, and James J. Sluss Jr. "Wavelength diversity in free-space optics to alleviate fog effects." *Proc. of SPIE*. 2005. 111.

Wallace, John M., and Peter V. Hobbs. *Atmospheric science: an introductory survey*. Academic press, 1977.

Wasiczko, Linda M., and Christopher C. Davis. "Aperture averaging of optical scintillations in the atmosphere: experimental results." *Proceeding. of SPIE*. SPIE, 2005. 197-208.

Willebrand, Heinz, and Baksheesh S. Ghuman. *Free space optics: enabling optical connectivity in today's networks*. SAMS publishing, 2002.

Wolfram. *The Wolfram Function Site*. n.d. <http://www.functions.wolfram.com>.

Wu, Haiping, and Mohsen Kavehrad. "Availability evaluation of ground-to-air hybrid FSO/RF links." *International Journal of Wireless Information Networks 14.1* 14.1 (2007): 33-45.

Yuksel, Heba, Stuart Milner, and Christopher Davis. "Aperture averaging for optimizing receiver design and system performance on free-space optical communication links." *Journal of Optical Networking* 4.8 (2005): 462-475.

Zhu, Xiaoming, and Joseph M. Kahn. "Free-space optical communication through atmospheric turbulence channels." *IEEE Transactions on communications* 50.8 (2002): 1293-1300.

Zhu, Xiaoming, and Joseph M. Kahn. "Performance bounds for coded free-space optical communications through atmospheric turbulence channels." *IEEE Transactions on Communications* 51.8 (2003): 1233-1239.

Zuev, V. E. "Spectroscopy of atmospheric gases (spectral databases)." 2012.